

The effect of the extracellular environment on the composition and function of synapses

Dissertation

zur Erlangung des akademischen Grades

doctor rerum naturalium

(Dr. rer. nat.)

genehmigt durch die Fakultät für Naturwissenschaften
der Otto-von-Guericke-Universität Magdeburg

von Dr. Barbara Christina Schweitzer

geb. am 09. April 1986 in Krefeld

Gutachter: PD Dr. Constanze Seidenbecher

Prof. Dr. Jacqueline Trotter

Eingereicht am: 21. Juli 2015

Verteidigt am: 16. Dezember 2015

Summary

The balance between stability and plasticity has to be regulated to maintain proper functionality of the brain and to promote learning and memory processes. In the adult, the extracellular matrix (ECM) that is formed by glia cells and neurons enwraps and stabilizes synapses and neuronal networks. ECM molecules as well as transmembrane proteins are cleaved by extracellular proteases and subsequently yield new signaling molecules that are important mediators of synaptic plasticity. The huge variety of ECM and transmembrane proteins and extracellular proteases lead to many unanswered questions about their involvement in the precise regulation of synapses throughout development and plasticity processes. In this thesis, the involvement of the hyaluronan based ECM on the regulation of postsynaptic NMDA receptors was investigated. Further, the signaling mechanism of the extracellular cleaved cadherin superfamily member Calsyntenin (Cst) is investigated.

In late postsynaptic development when neuronal networks are established (roughly P70 in mice), a drop in structural plasticity can be observed. On the molecular level, neurotransmitter receptors are recruited and stabilized at synaptic contacts, which determine the mature properties of synaptic transmission. Key events are changes in the subunit composition of NMDA receptors from predominantly GluN1/GluN2B- to GluN1/GluN2A-NMDA receptors, which alters plasticity processes of the synapses. At the same time the hyaluronan-based ECM matures, stabilizes synaptic contacts and limits plasticity processes. Removal of the ECM induces an increased and juvenile form of plasticity. In this thesis I hypothesized a causal link between the two developmental changes, and thus an influence of the ECM on the characteristics of the GluN2B-NMDA receptors. Indeed I found that enzymatic digestion of the ECM by the glycosidase hyaluronidase (Hya) increased the surface expression and synaptic currents of GluN2B-NMDA receptors in mature cultured dissociated hippocampal neurons. This was due to an altered phosphorylation state of GluN2B upon ECM digestion which led to a lower endocytosis rate. Further experiments demonstrated that this effect was β 1-integrin dependent. Finally lateral mobility of surface GluN2B was more confined after prolonged ECM removal. Taken together, these results suggest that ECM molecules regulate surface abundance of GluN2B-NMDA receptors and an increased surface abundance of GluN2B-NMDA receptors may mimic juvenile states. This may be

one mechanism underlying the observed increased neuronal plasticity after ECM removal.

In the second part the cellular function and signaling of the postsynaptic, transmembrane protein Cst and especially of its shed ectodomain were investigated. In humans, the Cst gene is known to have strong influence on episodic memory. *C. elegans* lacking Cst show impaired associative learning, which can be rescued by application of the ectodomain of Cst. It was suggested that Cst-1 binds secreted frizzled related protein 1 (sFRP-1), a protein involved in wnt signaling (Leuthäuser et al., unpubl.). So far no effect of Cst-1 on canonical wnt signaling could be shown. Furthermore Cst-1 did not directly bind to Frizzled-1, which was tested due to the close homology between sFRP-1 and the extracellular domain of Frizzled-1. Wnt signaling affects presynaptic activity and therefore I tested whether Cst-1 has a potential influence in this context. Synaptotagmin antibody uptake experiments demonstrated that the ectodomain of Cst-1 increased neurotransmitter release in cortical neurons, which was prevented by either blocking wnt signaling or inhibiting $\alpha 7$ -nAChRs that were shown to be involved in wnt signaling-dependent effects on presynaptic activity. Taken together the results suggest that the ectodomain acts as a trans-synaptic messenger, whose exact function needs to be further clarified.

Zusammenfassung

Die Fähigkeit zu plastischen Veränderungen im Gehirn, sowohl struktureller als auch funktioneller Art, wandelt sich während der Entwicklung und wird als Reaktion auf Aktivitätsveränderungen oder Verletzungen angepasst. Die Balance zwischen Stabilität und Plastizität muss ein Leben lang reguliert werden, um die Gehirnfunktionen aufrecht zu erhalten, und Lern- und Gedächtnisprozesse zu ermöglichen. Im adulten Gehirn sind die Synapsen von einer extrazellulären Matrix (ECM) ummantelt und stabilisiert, die gemeinsam von Gliazellen und Neuronen produziert wird. Sowohl ECM-Moleküle, als auch transmembranale Proteine werden durch extrazelluläre Proteasen gespalten, was neue Signalmoleküle hervorbringt, die wichtige Mediatoren für plastische Prozesse an der Synapse sind. Die große Bandbreite an extrazellulären und transmembranalen Molekülen birgt viele offene Fragen über deren Einfluss in der präzisen Regulation von Synapsen während der Entwicklung und Plastizitätsprozessen im Gehirn.

Diese Arbeit behandelt die Funktionen von zwei Komponenten der ECM. Zum einen wurde der Einfluss der Hyaluronsäure-basierten ECM auf die Regulation von postsynaptischen NMDA Rezeptoren untersucht. Andererseits wurde das Spaltungsprodukt des transmembranalen Proteins Calsyntenin (Cst), das Mitglied der Cadherin Superfamilie ist, auf dessen Signalweg sowie mögliche Rezeptoren erforscht.

In der postnatalen Entwicklung, zu einem Zeitpunkt an dem neuronale Netzwerke gefestigt werden (in Mäusen ~P70), ist ein Abfall der strukturellen Plastizität zu beobachten. Auf molekularer Ebene werden Neurotransmitterrezeptoren an den Synapsen stabilisiert, die die adulten Eigenschaften einer Synapse mitbestimmen. Ein Rezeptor, dessen Zusammensetzung sich in juvenilen und adulten Synapsen unterscheidet, ist der NMDA Rezeptor. Postnatale Synapsen sind hauptsächlich von GluN2B-NMDA-Rezeptoren dominiert, während adulte Synapsen vornehmlich GluN2A-NMDA-Rezeptoren aufweisen. Ob ein NMDA-Rezeptor die GluN2A oder GluN2B Untereinheit enthält bestimmt maßgeblich dessen Eigenschaften und beeinflusst damit auch das Plastizitätspotential einer Synapse. Parallel zum Wechsel der NMDA-Rezeptorzusammensetzung bildet sich die adulte Form der ECM aus. Das Erscheinen dieser reifen ECM wird als Endpunkt für eine juvenile, hochplastische Phase im Gehirn betrachtet. Die ECM stabilisiert Synapsen und

verhindert bis zu einem gewissen Grad plastische Prozesse im Gehirn. Durch die Behandlung mit Enzymen, die die Struktur der Matrix zerstören, können juvenile, plastische Prozesse wieder induziert werden. Auf Grund der zeitlichen Überlappung dieser zwei beschriebenen, entwicklungsabhängigen Prozesse und des gemeinsamen Einwirkens auf die Plastizität neuronaler Netzwerke wurde ein möglicher Einfluss der ECM auf die Zusammensetzung von NMDA-Rezeptoren postuliert. Das Enzym Hyaluronidase (Hya) spaltet das Hyaluronsäure-Rückgrat der ECM und zerstört so ihre dichte, netzwerkartige Struktur. Die Behandlung reifer, neuronaler Zellkulturen mit Hya erhöhte die Oberflächenexpression von GluN2B-NMDA-Rezeptoren, was zu erhöhten synaptischen Strömen durch diese Rezeptoren führte. Dieser Effekt wurde verhindert, indem β 1-Integrine in ihrer Funktion inhibiert wurden. Die Gesamtmenge an GluN2B Proteinen war jedoch nicht verändert durch den ECM Verdau, was auf eine veränderte Endo- oder Exozytose hinweist. Durch den ECM Verdau wurde GluN2B vermehrt phosphoryliert, woraus eine verringerte Endozytose resultierte. Außerdem zeigte sich, dass GluN2B-NMDA-Rezeptoren nach der Hya Behandlung eine geringere laterale Mobilität in der Membran aufwiesen. Die erhöhte synaptische Oberflächenexpression von GluN2B-NMDA-Rezeptoren nach der Hya-Behandlung, was einer juvenilen Rezeptorzusammensetzung entspricht, könnte ein molekularer Baustein sein, der eine erhöhte Plastizität nach EZM-Verdau begründet.

Im zweiten Teil dieser Arbeit wurden die zelluläre Funktion und die zu Grunde liegenden Signalwege von Calsyntenin (Cst), einem transmembranalen Protein der Cadherin Superfamilie, untersucht. Das Protein wird von Proteasen geschnitten und dabei wird ein Proteinfsegment, die Ectodomäne, in das extrazelluläre Milieu freigegeben. Es ist bekannt, dass das Cst-Gen in Menschen Einfluss auf das episodische Gedächtnis hat. In *C. elegans* Mutanten, denen das Cst-1-Gen fehlt, wurde ein verändertes assoziatives Lernen nachgewiesen, dass durch Zugabe der Ectodomäne wieder normalisiert wurde. Es gibt Hinweise, dass auch die Regulation von AMPA-Rezeptoren in diesen Tieren beeinflusst ist, jedoch ist der genaue Signalweg unbekannt. Unveröffentlichte Daten aus dem Labor von Prof. Sonderegger zeigen, dass Cst-1 secreted frizzled related protein 1 (sFRP-1) bindet. sFRP-1 ist ein extrazelluläres Protein, das den Wnt-Signalweg inhibiert. Auf Grund dessen wurde in dieser Arbeit untersucht, ob Cst-1 einen Einfluss auf den „canonical“ Wnt-Signalweg hat. Dieser verändert die Genexpression und wird mit einem Reportersystem erforscht, in dem Luciferase

exprimiert wird, wenn der Wnt spezifische Promotor aktiviert ist. Cst-1 zeigte keinen Einfluss auf die Expression der Luciferase. Auf Grund struktureller Homologien von sFRP-1 und dem Frizzled-Rezeptor wurde postuliert, dass Cst-1 auch an Frizzled bindet; dies konnte aber nicht nachgewiesen werden. Es ist bekannt, dass der Wnt Signalweg präsynaptische Aktivität regulieren kann, weshalb die Wirkung von Cst-1 auf die Präsynapse untersucht wurde. Anhand der Aufnahme eines Synaptotagmin-Antikörpers konnte gezeigt werden, dass die Ectodomäne von Cst-1 die präsynaptische Aktivität erhöht. Dieser Effekt konnte verhindert werden, indem entweder der Wnt Signalweg oder die $\alpha 7$ -nACh Rezeptoren inhibiert wurden, von denen bekannt ist, dass sie in Wnt abhängige Prozesse in der Präsynapse involviert sind. Zusammenfassend zeigen die Daten, dass die Ectodomäne von Cst-1 als transsynaptisches Signalmolekül fungiert, dessen genauer Einfluss weiter zu erforschen ist.

Acknowledgements

First of all, I like to acknowledge my supervisors PD Dr. Constanze Seidenbecher and Dr. Renato Frischknecht for providing me the opportunity to work in their group and to become a member of the ECM family. Special thanks go to Renato for millions of helpful discussions and your daily support in the lab. You always kept me going on, you gave comfort, coffee, jokes and headache pills. What else do you need to survive a PhD!? I thank you for creating a good atmosphere in the lab and your open-door-office.

Many thanks go to Jeet Singh for your help with hippocampal slices, your expertise with Western Blots and your permanent smile. I also want to give thanks to all the other members of the Magdeburg ECM family and the Molecular physiology group for their help, discussions and inputs during our seminars and the daily work.

But without all the technicians of the department it not would have been possible. Thank you for providing weekly cell cultures. Thank you for helping wherever you can. Special thanks to Kathrin Hartung. You did not only provide enormous technical help (even on the weekends!!!) but also emotional support. Thanks for taking care of me and my office plants by providing “drinks” that we all survived the PhD.

Finally I want to thank Prof. Dr. Eckart Gundelfinger and Prof. Dr. Michael Naumann, for allowing me to be member of the GRK1167. Being part of the GRK gave me insight into the immunological field, which was completely new and fascinating for me. The GRK enriched my scientific knowledge and gave me the opportunity to get insights into the field of scientific management, by organizing meetings and inviting guest speakers. Many thanks for the financial support that allowed me to participate in several scientific meetings.

Contents

| | |
|--|-----------|
| Summary..... | 1 |
| Zusammenfassung..... | 3 |
| Acknowledgements..... | 6 |
| Contents..... | 7 |
| Figures and tables..... | 10 |
| Abbreviations..... | 12 |
| 1 Introduction..... | 14 |
| 1.1 The ECM of the brain | 15 |
| 1.1.1 Molecular composition of the ECM..... | 15 |
| 1.1.2 ECM in neuronal plasticity..... | 17 |
| 1.2 The NMDA receptor..... | 19 |
| 1.2.1 Functionality of the NMDA receptor..... | 19 |
| 1.2.2 Subunit composition, characteristics and trafficking of NMDA receptors | 20 |
| 1.2.3 The GluN2A/GluN2B ratio..... | 23 |
| 1.3 Integrins..... | 24 |
| 1.3.1 Subunit composition, ligand binding and intracellular signaling..... | 24 |
| 1.3.2 Integrins in synaptic plasticity | 25 |
| 1.3.3 Regulation of integrins by ECM molecules..... | 25 |
| 1.4 Calsyntenin | 26 |
| 1.4.1 Expression and structure of calyntenin | 27 |
| 1.4.2 Proteolytic cleavage of calyntenin..... | 27 |
| 1.4.3 Calsyntenin as an intracellular transport protein | 29 |
| 1.4.4 Cellular functions of the ectodomain of calyntenin | 30 |
| 1.5 Wnt signaling..... | 31 |
| 1.5.1 Canonical wnt signaling..... | 32 |
| 1.5.2 Function of sFRPs | 32 |
| 1.5.3 Wnt signaling at the mature neuronal synapse | 33 |
| 1.6 Aims..... | 34 |
| 2 Material and Methods..... | 36 |
| 2.1 Neuronal cell cultures | 36 |
| 2.1.1 Glia cells | 36 |
| 2.1.2 Preparation of glass coverslips..... | 37 |
| 2.1.3 Preparation of neuronal cultures | 37 |
| 2.2 Stable HEK293-T cell line cultures..... | 38 |

| | | |
|----------|--|-----------|
| 2.3 | Molecular Biology..... | 38 |
| 2.3.1 | DNA constructs (commercially available) | 38 |
| 2.3.2 | DNA constructs (custom-made) | 39 |
| 2.3.3 | Transfection of dissociated hippocampal neurons | 39 |
| 2.3.4 | Transfection of HEK293-T cells..... | 39 |
| 2.3.5 | PCR to amplify defined DNA fragments | 40 |
| 2.3.6 | DNA agarose gel electrophoresis..... | 41 |
| 2.3.7 | DNA digestion by restriction enzymes and ligation of DNA fragments | 41 |
| 2.3.8 | Transformation of E. coli XL10 Gold competent cells | 42 |
| 2.3.9 | Plasmid Isolation (Mini Preparation) | 42 |
| 2.4 | Antibodies | 43 |
| 2.5 | Immunocytochemistry | 44 |
| 2.5.1 | Immunostainings of dissociated neuronal cultures..... | 44 |
| 2.5.2 | Binding Assay | 45 |
| 2.5.3 | Microscopy and image analysis | 45 |
| 2.5.4 | Quantum Dot experiments..... | 46 |
| 2.6 | Biochemistry | 47 |
| 2.6.1 | Acute hippocampal slices..... | 47 |
| 2.6.2 | SDS-Page using Laemmli system..... | 47 |
| 2.6.3 | Western Blotting | 48 |
| 2.6.4 | Immunoblot detection | 48 |
| 2.6.5 | Purification of eukaryotic expressed fusion proteins | 48 |
| 2.7 | Electrophysiology | 51 |
| 2.7.1 | Miniature Excitatory Synaptic Currents (mEPSCs)..... | 51 |
| 2.7.2 | Spontaneous Excitatory Synaptic Currents (sEPSCs)..... | 51 |
| 2.8 | Wnt signaling reporter systems | 52 |
| 2.8.1 | Reportersystem based on GFP expression | 52 |
| 2.8.2 | Reporter system based on luciferase expression..... | 52 |
| 3 | Results..... | 54 |
| Part I: | The effect of the ECM on the expression and dynamics of | |
| | GluN2B-NMDA receptors..... | 54 |
| 3.1 | Electrophysiological recordings after ECM removal..... | 54 |
| 3.1.1 | Isolation of NMDA receptor-mediated synaptic currents in dissociated cultures..... | 55 |
| 3.1.2 | Increased NMDA receptor-mediated sEPSCs after ECM removal..... | 56 |
| 3.2 | Unaffected GluN2B protein level after ECM removal..... | 58 |
| 3.3 | GluN2B surface expression is increased after ECM removal in a β 1-integrin-dependent manner..... | 59 |
| 3.4 | ChABC treatment increases surface expression of GluN2B-NMDA receptors | 61 |

| | | |
|--|---|------------|
| 3.5 | Hya treatment does not alter GluN2B expression in DIV 11 neurons..... | 62 |
| 3.6 | ECM digestion increases phosphorylation of GluN2B and decreases its endocytosis..... | 63 |
| 3.7 | Mobility of GluN2B-NMDA receptors..... | 65 |
| Part II: Cellular effects of Calsyntenin-1's ectodomain..... | | 67 |
| 3.8 | Purification of proteins..... | 67 |
| 3.9 | Cst-1 in canonical wnt signaling: GFP reporter system | 69 |
| 3.10 | Cst-1 in canonical wnt signaling: luciferase reporter system..... | 71 |
| 3.11 | Binding assay: Cst1Clea and Frizzled-1 | 72 |
| 3.12 | Cst-1 in presynaptic activity..... | 73 |
| 4 | Discussion | 75 |
| 4.1 | Regulation of surface expression of GluN2B-NMDA receptors..... | 75 |
| 4.1.1 | Src and Fyn kinase phosphorylate GluN2B-NMDA receptors..... | 75 |
| 4.1.2 | Lateral mobility of GluN2B-NMDA receptors..... | 76 |
| 4.1.3 | Integrins regulate NMDA receptors..... | 78 |
| 4.2 | ECM influences cellular properties via integrin signaling..... | 79 |
| 4.2.1 | Reelin regulates NMDA receptor properties | 80 |
| 4.3 | Cellular consequences of an altered GluN2A/GluN2B ratio upon ECM remodeling.. | 81 |
| 4.3.1 | Tri-heteromeric NMDA receptors | 82 |
| 4.3.2 | Regulation of LTP by NMDA receptors and the ECM..... | 83 |
| 4.3.3 | Regulation of metaplasticity by NMDA receptors and the ECM | 86 |
| 4.3.4 | Regulation of structural plasticity by NMDA receptors and the ECM | 87 |
| 4.4 | <i>In vivo</i> application of ECM digestion..... | 89 |
| 4.4.1 | ECM removal in the visual cortex and the role of NMDA receptors | 89 |
| 4.4.2 | Homeostatic plasticity as a model involved in ocular dominance plasticity ... | 91 |
| 4.4.3 | ECM removal in memory processes..... | 93 |
| 4.5 | Cst-1 in wnt signaling..... | 94 |
| 4.5.1 | Does Cst-1 bind Frzl?..... | 95 |
| 4.5.2 | Does Cst-1 influence canonical wnt signaling?..... | 95 |
| 4.6 | Cst1 increases presynaptic activity..... | 96 |
| 5 | Declaration | 101 |
| 6 | Curriculum Vitae | 102 |
| 7 | Literature..... | 104 |

Figures and tables

Figures

| | | |
|------------|---|----|
| Figure 1: | Developmental switch of NMDA receptors | 22 |
| Figure 2: | Schematic illustration of Cst-1 and its proteolytic cleavage | 28 |
| Figure 3: | Plot of the UV absorption (A280 nm) during protein purification..... | 49 |
| Figure 4: | Isolation of NMDA receptor mediated currents..... | 55 |
| Figure 5: | ECM removal enhances GluN2B-NMDA receptor-mediated synaptic currents | 57 |
| Figure 6: | Total GluN2B protein level stays unaffected after ECM removal..... | 58 |
| Figure 7: | ECM removal increases surface expression of GluN2B in a β 1-integrin dependent manner | 60 |
| Figure 8: | ChABC shows the same effect as Hya | 62 |
| Figure 9: | Surface expression of GluN2B-NMDA receptors was unaffected by Hya treatment in DIV 11 neurons | 63 |
| Figure 10: | Hya increases phosphorylation of GluN2B and decreases its endocytosis | 64 |
| Figure 11: | Prolonged ECM digestion increased confinement of GluN2B-NMDA receptors | 66 |
| Figure 12: | Purification of fusion proteins | 68 |
| Figure 13: | GFP based reporter system to analyze the influence of Cst1 on canonical wnt signaling..... | 70 |
| Figure 14: | Cst-1 does not affect canonical wnt signaling / Tcf/Lef promotor activation .. | 71 |
| Figure 15: | Neither Cst1Clea nor Cst3Clea bind to Frzl-1 | 72 |
| Figure 16: | Cst1Clea increased presynaptic activity | 74 |
| Figure 17: | Schematic presentation of the putative signaling mechanism that increases GluN2B-NMDA receptor surface expression upon ECM removal..... | 80 |
| Figure 18: | Scheme of potential signaling mechanisms involved in the stimulating effect of Cst1Clea on presynapses | 99 |

Tables

| | | |
|-----------|---|----|
| Table 1: | Media and reagents for neuronal cell cultures | 36 |
| Table 2: | Media and reagents for stable HEK293-T cell line cultures..... | 38 |
| Table 3: | DNA constructs (custom made) | 39 |
| Table 4: | Buffer for transfection of HEK293-T cells | 39 |
| Table 5: | Quantities of buffers and DNA for transfection of HEK293-T cells..... | 39 |
| Table 6: | Primer sequences for Cst constructs..... | 40 |
| Table 7: | PCR protocol / Cycles..... | 40 |
| Table 8: | Buffers for PCR..... | 40 |
| Table 9: | Buffers for DNA gel electrophoresis | 41 |
| Table 10: | Buffers for DNA digestion by restriction enzymes | 41 |
| Table 11: | Items for bacteria transformation..... | 42 |
| Table 12: | Buffers for plasmid isolation..... | 42 |

| | | |
|-----------|--|----|
| Table 13: | List of primary antibodies, origin and working concentrations..... | 43 |
| Table 14: | List of enzymes and drugs..... | 44 |
| Table 15: | Buffers for immunocytochemistry | 44 |
| Table 16: | Buffers for biochemistry..... | 47 |
| Table 17: | Buffer for protein purification | 48 |
| Table 18: | Buffers and drugs for electrophysiology | 51 |

Abbreviations

| | |
|----------------------|--|
| ADAM | A disintegrin and metalloproteinase |
| ADAMTS | A disintegrin and metalloproteinase with thrombospondin motifs |
| AMPA | α -amino-3-hydroxy-5-methyl-4-isoxazolepropionic acid |
| AP-2 | Clathrin adapter protein 2 |
| APC | Adenomatous polyposis coli |
| APV | (2R)-amino-5-phosphonovaleric acid |
| α 7-nAChR | α 7 nicotinic acetylcholine receptor |
| BgTx | Bungarotoxin |
| CAD | Cadherin-like repeat |
| CaMKII | Ca ²⁺ /Calmodulin-dependent protein kinase II |
| CD29 | Function blocking β 1-integrin antibody |
| ChABC | Chondroitinase ABC |
| CK2 | Casein kinase 2 |
| CNQX | 6-cyano-7-nitroquinoxaline-2,3-dione |
| CNS | Central nervous system |
| CRD | Cysteine-rich domain |
| CREB | cAMP response element-binding protein |
| CSPGs | Chondroitin sulfate proteoglycans |
| Cst | Calsyntenin |
| Cst1Clea | Cst1Clea-myc/his |
| Cst1Cad | Cst1Cad-myc/his |
| Ctl | Control |
| D1 receptors | Dopamine 1 receptors |
| DAG | 1,2 diacylglycerol |
| DIC | Differential interference contrast |
| D _{inst} | Instantaneous diffusion coefficient |
| DIV | Days in vitro |
| Dkk-1 | Dickkopf-related protein 1 |
| DVL | Dishevelled protein |
| ECM | Extracellular matrix |
| FAK | Focal adhesion kinase |
| Frzl | Frizzled |
| GluN2B-NMDA receptor | GluN2B-containing NMDA receptor |
| GPCRs | G-protein-coupled receptors |
| GSK-3 β | Glycogen synthase kinase-3 β |
| HAPLNs | Hyaluronan and proteoglycan link proteins |
| HEK293-T cells | Human Embryonic Kidney Cells |
| Hya | Hyaluronidase |
| ICC | Immunocytochemistry |
| Ifen | Ifenprodil |
| IP3 | Inositol 1,4,5-triphosphate |
| JIP1 | JNK-interacting protein 1 |
| JNK | c-Jun N-terminal kinases |
| KBS | Kinesin binding motives |
| KCl | Potassium Chloride |
| KLC1 | Kinesin light chain1 |
| KO | Knock out |

| | |
|-------------|--|
| LamG | Laminin-G domain |
| LRP | Low-density lipoprotein receptor related protein |
| LTP | Long-term potentiation |
| MAGUK | Membrane-associated guanylate kinase |
| Map2 | Microtubule-associated protein 2 |
| mEPSCs | Miniature excitatory postsynaptic currents |
| MMP | Matrix metalloproteinase |
| MSD | Mean square displacement |
| mTOR | Mammalian target of rapamycin |
| NFAT | Nuclear factor of activated T cells |
| NMDA | N-Methyl-D-aspartic acid |
| PAC1Rs | Pituitary adenylate cyclase activating peptide 1 receptors |
| PCP pathway | Planar cell polarity pathway |
| PI3K | Phosphatidylinositol 3-kinase |
| PKA | Protein kinase A |
| PKC | Protein kinase C |
| PLC | Phospholipase C |
| PNN | Perineuronal net |
| PSD-95 | Postsynaptic density protein 95 |
| PTSD | Post-traumatic stress disorder |
| RT | Room temperature |
| SAP-102 | Synapse-associated protein 102 |
| SEP | Superecliptic pHluorin |
| sEPSCs | Spontaneous excitatory postsynaptic currents |
| SFK | Src family kinase |
| sFRP-1 | Secreted frizzled related protein 1 |
| TCF/LEF | T-cell factor/lymphoid enhancer factor-1 |
| TIMPs | Tissue inhibitors of metalloproteinases |
| TPR | Tetratricopeptide repeats |
| Unpubl. | Unpublished |
| WB | Western Blot |
| WIF | Wnt inhibitory factor |
| WT | Wild type |
| X11L | X11-like protein |

1 Introduction

The proper function of the brain involves the precise orchestration of single synapses. The strengthening and weakening of synapses is an important process in this context and needs to be strictly regulated. For this general purpose there is a huge variety of regulatory proteins within the cells, which have been studied extensively. During my PhD I focused on the regulatory function of extracellular molecules at the synapse. Synapses are no isolated structures build up by the pre- and postsynapse; they are enwrapped by glia cells and the extracellular matrix (ECM). This arrangement is described as the quadripartite synapse (Sykova and Nicholson, 2008). Glia cells secrete proteins into the extracellular space which influence synaptic functions and form major constituents of the ECM. Thrombospondin for instance is a large ECM molecule, secreted by glia cells, which was shown to influence synaptogenesis in the hippocampus (Xu et al., 2010). Proteolytic cleavage of extracellular molecules is another mechanism to affect synaptic properties, as it was demonstrated for the neurotrypsin-dependent cleavage of agrin, which leads to filopodia formation in the hippocampus (Matsumoto-Miyai et al., 2009). The variety of extracellular proteins and transmembrane proteins influencing synaptic transmission is huge, which leads to several open questions.

I divided my thesis into two parts, in which I investigated both the influence of the hyaluronan-based ECM on synaptic transmission and cellular effects of an extracellular cleaved protein.

In the first part I describe my work on the hyaluronan-based ECM of the brain, which is known to influence the development of the brain and synaptic plasticity. The plasticity of glutamatergic synapses is mainly determined by their amount of AMPA and NMDA receptors. Therefore I studied the influence of the ECM on the expression pattern of NMDA receptors and underlying signaling mechanisms.

The second part focus on a protein called calstentenin (Cst), which is member of the cadherin superfamily. Especially its poorly described ectodomain, which is shed after extracellular proteolytic cleavage and its influence on cellular functions, was in focus of my work. Interestingly, in humans, the Cst gene was linked to episodic memory. *C. elegans* lacking Cst-1 show impaired associative learning, which can be rescued by application of the ectodomain. However, the

precise molecular function of Cst is poorly understood as well as its cellular receptor. The aim of this part was to elucidate potential receptors and cellular function of the ectodomain of Cst-1.

1.1 The ECM of the brain

1.1.1 Molecular composition of the ECM

Neurons in the brain are surrounded by a complex, three dimensional hyaluronan-based ECM. Around most cells and in the neuropil the ECM has a diffuse appearance. Beside this, the it can form unique, dense netlike structures, called perineuronal nets (PNNs), which were first described by Camillo Golgi 1893 (reviewed in Celio and Blumcke, 1994). During the past years more evidences were obtained that the ECM has both passive and active functions, which are important for the development and functionality of the brain.

The basic constituents of the PNNs are hyaluronan, chondroitin sulfate proteoglycans (CSPGs), link proteins (HAPLNs) and tenascin-R (Dityatev et al., 2010). Hyaluronan is a linear polysaccharide and builds the backbone of the ECM. In the brain it has been suggested to be anchored to the cell membrane by hyaluronan synthase (Kwok et al., 2010). Proteoglycans bind to hyaluronan, other ECM or cell-surface molecules and by that serve as organizational scaffolds. Lecticans, including aggrecan, versican, neurocan and brevican, are the most prominent proteoglycans in the brain (Yamaguchi, 2000). HAPLNs stabilize the interaction of hyaluronan and lecticans. Tenascin-R is the most prominent glycoprotein of the tenascin protein family in the adult brain. It builds trimers that can bind three other lecticans to stabilize the integrity of the PNN structure. All these components build up the netlike structure of the PNNs as described by Golgi.

During development the ECM undergoes several changes. It develops during the first three postnatal weeks in rodents (Celio and Blumcke, 1994). The formation of PNNs is activity dependent and concurs with the closure of the critical period, in which neurons are highly input sensitive and plastic (Lander et al., 1997, Hensch, 2005). The individual components of the juvenile and adult matrix differ and the density of formed nets increases during the postnatal development (Milev et al., 1998, Rauch, 2004). In dissociated rat hippocampal cultures grown for 11 days *in vitro* (DIV 11) PNNs are only present at some single cells, mostly

inhibitory, parvalbumin positive interneurons (Frischknecht et al., 2009). After DIV 21 PNNs are visible on almost every cell but in different intensities. They reach their adult properties with the ending of synaptogenesis (Koppe et al., 1997, John et al., 2006). At this time the synapses are fully wrapped by the ECM, apparently only the synaptic cleft is free of it.

Although the three-dimensional meshwork of extracellular proteins seems to be a stable structure, it undergoes continuous rearrangements with regard to plasticity processes. There are three families of endogenous remodeling enzymes. One of those is the matrix metalloproteinases (MMPs) family (Puente et al., 2003). These proteins are zinc- and calcium-dependent endopeptidases that are mainly secreted into the extracellular space (Sbai et al., 2008). The other two families of ECM degrading proteases are the "A disintegrin and metalloproteases" (ADAM) and the "A disintegrin and metalloproteinase with thrombospondin motifs" (ADAMTS) families. The majority of ADAMs are type I transmembrane proteins, which allows juxtamembrane cleavage of other membrane-associated proteins (Edwards et al., 2008). In contrast ADAMTSs are secreted proteins (Porter et al., 2005). All these proteases need to be highly regulated in their synthesis and/or activity by posttranslational modifications or release as inactive pro-enzymes. Additionally endogenous inhibitors like tissue inhibitors of metalloproteinases (TIMPs) control their activity state (Yong, 2005).

However, not only proteases may modulate the ECM but also glycosidases, but their physiological role during plasticity processes in the brain remains elusive. They are mainly used as experimental tools to modulate the ECM. The most commonly used enzymes are Hyaluronidase (Hya) and Chondroitinase ABC (ChABC). Hya is an endogenous enzyme that cleaves predominantly hyaluronan but has an intrinsic chondroitinase function (Margolis et al., 1972, Stern and Jedrzejewski, 2006). ChABC is a bacterial enzyme (from *Proteus vulgaris*) that removes chondroitin sulfate glycosaminoglycan side chains from molecules (Yamagata et al., 1968, Bukalo et al., 2001). Both of these enzymes have been extensively used to degrade the ECM *in vitro* and *in vivo* (Bukalo et al., 2001, Pizzorusso et al., 2002, Frischknecht et al., 2009, Kochlamazashvili et al., 2010, de Vivo et al., 2013, Happel et al., 2014).

1.1.2 ECM in neuronal plasticity

The interconnection of the ECM with different kinds of plasticity processes in the brain is subject of plenty of studies. On one hand it was studied whether modulation of the ECM influences synaptic plasticity and on the other hand whether synaptic activity changes ECM integrity.

ECM in long-term potentiation

On a molecular level it was shown that enzymatic digestion of the ECM with Hya or ChABC increases lateral mobility of GluA1-AMPA receptors and by that the exchange of synaptic and extrasynaptic receptors in primary hippocampal cultures. That results in an enhancement of short term plasticity (Frischknecht et al., 2009). In hippocampal slices treated with Hya L-type voltage-dependent Ca^{2+} channel (L-VDCC)-driven currents were suppressed and an L-VDCC-mediated component of long-term potentiation (LTP) abolished (Kochlamazashvili et al., 2010). Further indications for an influence of the ECM on LTP were given by experiments showing that mice lacking the CSPGs neurocan or brevican have deficits in LTP maintenance (Zhou et al., 2001, Brakebusch et al., 2002). MMP-9 mutant mice show also impairments in the late phase of LTP (Nagy et al., 2006). Using the enzymatic digestion as ECM manipulation, ChABC treatment of hippocampal slices reduces LTP and long-term depression (LTD) (Bukalo et al., 2001). However, *in vivo* ChABC treatment in the visual cortex supports LTP (de Vivo et al., 2013). The most obvious difference between these two studies is the experimental setup (*in vitro* vs. *in vivo*), which could be one explanation for the discrepancy. Additionally, the studies differ in their duration of ECM digestion. This suggests diverse short- or long-term effects of the ECM degradation.

ECM in homeostatic plasticity

Homeostatic plasticity describes the adjustment of synaptic transmission upon prolonged activity changes of the network. For example lesion of the entorhinal cortex results in chronic denervation of the dentate gyrus, which leads to increased levels of brevican and ADAMTS4-mediated brevican cleavage product after 2 days (Mayer et al., 2005). However, the injection of kainite that induces epileptic seizures, also upregulates ADAMTS4 expression and leads to a remodeling of the ECM (Yuan et al., 2002). This implication of the ECM in homeostatic adaptations could also be shown in neuronal cell cultures. A prolonged inactivation of primary hippocampal cultures leads to homeostatic

plasticity which is paralleled by an increased cleavage of brevican by ADAMTS4 (Valenzuela et al., 2014).

ECM in structural plasticity

On a structural level it has been shown that after spinal cord injury a CSPG-rich glial scar is formed that inhibits axonal growth. This inhibition is due to CSPGs since ChABC treatment stimulates axon outgrowth and the formation of new contacts after CNS or spinal cord injury (McKeon et al., 1999, Niederost et al., 1999, Moon et al., 2001, Bradbury et al., 2002).

The role of ECM in structural plasticity has been highlighted in the rat visual cortex. The so called critical period is a time frame of high plasticity during which topographic representations of sensory inputs are established in the cortex. Monocular deprivation during this critical period leads to a shift of ocular dominance of cortical neurons toward the open eye and in a loss of visual acuity for the deprived eye. Those cortical areas that were innervated by the deprived eye are now innervated by the open eye (Fagiolini et al., 1994). The ocular dominance shift is not seen any more if monocular deprivation is induced after the closure of the critical period. It was demonstrated that the critical period starts with the end of third postnatal week, peaks around the fourth week and begins to decline at the end of the fifth week. In 2002 Pizzorusso et al. presented that the development of the ECM overlaps with the critical period (Pizzorusso et al., 2002). The abundance of an adult ECM marks the end of the critical period. Dark rearing of animals from birth prolongs not only the critical period but also the development of the ECM, in particular of perineuronal nets. One-week exposure to a normal light/dark cycle is enough to rapidly terminate ocular dominance plasticity and the formation of perineuronal nets. Enzymatic removal of the ECM in the visual cortex of adult rats can reactivate ocular dominance plasticity and therefore virtually rejuvenate the plasticity of the cortex (Pizzorusso et al., 2002). But the study does not provide any molecular mechanism. In addition it has been found that ECM digestion in the visual cortex *in vivo* increases structural and functional plasticity in terms of higher spine motility and higher responses to theta-burst stimulation (de Vivo et al., 2013). Thus, there seems to be a close relation between the ECM and the plasticity of the visual cortex.

Another study that shows the critical role of the ECM in brain plasticity *in vivo* deals with the ability of Mongolian gerbils to relearn an auditory discrimination

task. Hya injection before the beginning of a reversal learning task increases the performance significantly without erasing the previously learned task (Happel et al., 2014). That proposes the modulation of the ECM as a potential tool to reopen a window of opportunities for plasticity processes in established neuronal networks.

The precise molecular mechanisms are still not clear. Regarding neuronal plasticity on a molecular level the NMDA receptor is a prominent candidate to regulate those processes. Before going into details about the connection of NMDA receptors with plasticity and ECM some basal information about the NMDA receptor will be provided.

1.2 The NMDA receptor

At excitatory synapses of the vertebrate brain the most common neurotransmitter is glutamate. It is released from presynaptic terminals and activates glutamate receptors at the postsynapse. Ionotropic glutamate receptors are ligand-gated ion channels that depolarize the postsynaptic membrane by an influx of cations. Ionotropic glutamate receptors can be subdivided into three families: AMPA (α -amino-3-hydroxy-5-methyl-4-isoxazolepropionic acid receptor), kainite and NMDA (N-Methyl-D-aspartic acid) receptors. AMPA receptors account for the fast postsynaptic response, but NMDA receptors exhibit a specialized role. Due to their diverse subunit composition, expression and association with intracellular signaling molecules they are essential for brain plasticity. They are also thought to transfer activity patterns into long-term changes in synapse structure and function (Traynelis et al., 2010).

1.2.1 Functionality of the NMDA receptor

NMDA receptors have unique properties that give them their special position among the ionotropic glutamate receptors. First, they are highly permeable for Ca^{2+} ions, which can activate intracellular signaling cascades (Mayer et al., 1987); second, their opening mechanism is more complex than the one of AMPA receptors. During resting membrane potential their pore is blocked by an extracellular Mg^{2+} block and the binding of glutamate does not lead to channel opening. It needs a preceding depolarization which removes the Mg^{2+} block to allow glutamate to open the pore (Lynch et al., 1983, Mayer et al., 1984, Nowak et al., 1984). This gives the receptor its special role as a coincidence detector for

synchronized pre- and postsynaptic activity. Additionally a co-agonist, glycine or D-serine is needed to activate the receptor (Johnson and Ascher, 1987). Third, they exhibit much slower kinetics than AMPA receptors due to slower glutamate unbinding (Vicini et al., 1998). Fourth, NMDA receptors have long intracellular tails that are docking stations for several signaling molecules and substrates for posttranslational modifications, i.e. phosphorylation (Kohr and Seeburg, 1996, Krupp et al., 1998). Therefore the NMDA receptor is of special interest for neuronal differentiation, synaptogenesis and synaptic plasticity.

1.2.2 Subunit composition, characteristics and trafficking of NMDA receptors

There are three families of NMDA receptor subunits: GluN1, GluN2 A-D and GluN3 A-B (Law et al., 2003). Functional receptors consist of hetero-tetramers with two obligatory GluN1 subunits and two GluN2 subunits. In some cases there is one GluN2 and one GluN3 subunit found (Cull-Candy and Leszkiewicz, 2004). The two GluN2 subunits can be of the same isoform, called di-heteromeric receptors (i.e. GluN1/GluN2A or GluN1/GluN2B) or different isoforms, called tri-heteromeric receptors (i.e. GluN1/GluN2A/GluN2B) (Sheng et al., 1994). The abundance of tri-heteromeric receptors was shown in many regions of the brain, particularly in the hippocampus and cortex, varying between 15 – 50% (Rauner and Kohr, 2011).

NMDA receptors have slower kinetics than the fast responding AMPA receptors. The kinetics of the receptor are mainly determined by the GluN2 subunit (Dzubay and Jahr, 1996). GluN2B-containing NMDA receptors (GluN2B-NMDA receptors) have longer opening and closing constants than GluN2A-NMDA receptors (Monyer et al., 1994, Vicini et al., 1998, Erreger et al., 2005) (Figure 1, inset). Additionally, GluN2B-NMDA receptors have higher calcium permeability and provide more calcium per unit of current than GluN2A-NMDA receptors (Erreger et al., 2005, Sobczyk et al., 2005).

Another molecular difference between GluN2A- and GluN2B-NMDA receptors is the association of the cytoplasmic C-terminus with intracellular signaling molecules. The most prominent signaling molecule which is linked to NMDA receptor is the Ca²⁺/Calmodulin-dependent protein kinase II (CaMKII). CaMKII is highly abundant at synapses (Erondu and Kennedy, 1985, Peng et al., 2004) and is crucial to induce LTP (Malinow et al., 1989, Otmakhov et al., 1997). GluN2B subunits have a high affinity for CaMKII whereas GluN2A shows only low

affinity (Strack and Colbran, 1998). This distinct binding affinity for CaMKII is thought to differentially regulate synaptic plasticity, which will be discussed in detail in sections 1.2.3 and 4.3.

Interestingly the subunit composition of NMDA receptors undergoes a developmental switch (Figure 1). During embryonic and early postnatal periods there are predominantly GluN2B-NMDA receptors present throughout the brain. After the first three postnatal weeks the expression of GluN2A-NMDA receptors increases, whereas the expression of GluN2B-NMDA receptors declines (Monyer et al., 1994, Kirson and Yaari, 1996). That results in an increase of the synaptic GluN2A/GluN2B ratio (Sheng et al., 1994, Flint et al., 1997, Hoffmann et al., 2000). This process requires synaptic activity or sensory experience, exemplified in the visual cortex (Carmignoto and Vicini, 1992), however the precise molecular mechanisms leading to the subunit switch are still unknown.

The trafficking and synaptic localization of NMDA receptors are regulated via the cytoplasmic tail of GluN2A and GluN2B. Members of the membrane-associated guanylate kinase (MAGUK) family anchor NMDA receptors at the synapse (Kornau et al., 1995, Niethammer et al., 1996). Especially, the postsynaptic density protein 95 (PSD-95) and the synapse-associated protein 102 (SAP-102) bind with their PDZ domains the PDZ-binding motifs of NMDA receptors. It was shown that mice lacking PSD-95 have a deficit in the GluN2 switch (Beique et al., 2006). The binding efficacy and by that synaptic tethering is controlled via phosphorylation of the PDZ-binding motif of GluN2A or GluN2B. Casein kinase 2 (CK2) phosphorylates S1480 in the PDZ binding motif of GluN2B that inhibits further binding of MAGUKs and therefore destabilizes GluN2B-NMDA receptors at the synapse (Chung et al., 2004, Sanz-Clemente et al., 2010). CK2 activity is also required for the acute activity-induced GluN2 switch. Another binding motif (YEKL) in the C-terminus of GluN2B provides the binding site for the clathrin adaptor protein 2 (AP-2) which is essential for the clathrin-dependent endocytosis of the receptor. After phosphorylation of the tyrosine residue (Y1472) in the YEKL motif, AP-2 cannot bind the GluN2B-NMDA receptor anymore, which leads to receptor stabilization at the surface (Lavezzari et al., 2003). Sanz-Clemente et al. created a model in which the coordinated phosphorylation of these two residues of GluN2B regulates its trafficking: Early in development the association of GluN2B-NMDA receptors with MAGUKs (S1480 unphosphorylated) stabilizes the receptors at the membrane. This is supported by the phosphorylated Y1472 (no binding of AP-2). During the critical

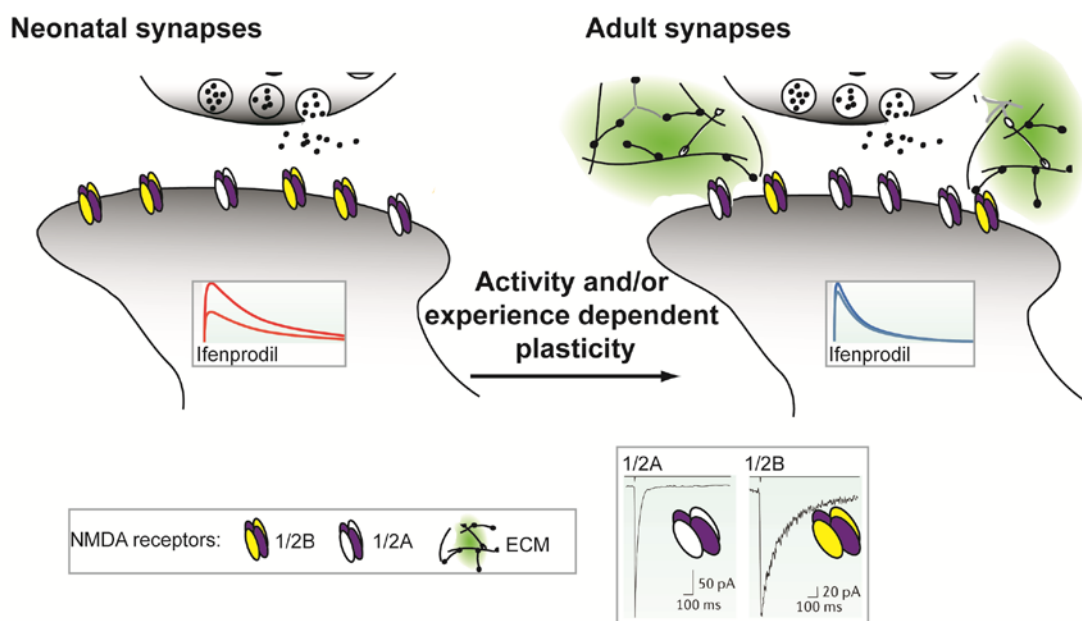


Figure 1: Developmental switch of NMDA receptors

Neonatal synapses throughout the brain contain mostly GluN2B-NMDA receptors, which are sensitive to the selective inhibitor Ifenprodil. The developmental switch in the subunit composition is dependent on activity and/or experience and coincides with the development of the ECM. In juvenile synapses GluN2B-NMDA receptors are more prominent. Those are sensitive to Ifenprodil (red current trace). In adult synapses GluN2A-NMDA receptors are dominating the synapse, which are not sensitive to Ifenprodil (blue current trace). The inset shows currents from either GluN2A- or GluN2B-NMDA receptors, demonstrating that GluN2B-NMDA receptors have much longer decay times which is an important feature for the coincidence detection of pre- and postsynaptic activity. This scheme is oversimplified as only diheteromeric receptors are presented, even though it is postulated that the majority of synaptic receptors is built by triheteromeric GluN2A/2B-NMDA receptors. Current traces are taken from Nature Review, Paoletto, Bellone and Zhou, 2013

period, NMDA receptor activation leads to phosphorylation of S1480 by CK2 (disruption of MAGUKs). This disruption of the NMDA receptor from MAGUKs triggers the de-phosphorylation of Y1472 (AP-2 binding), which results in promoted GluN2B-NMDA receptor endocytosis. It was also shown that metabotropic glutamate receptors and the release of intracellular calcium are required for the GluN2 switch (Bellone et al., 2011, Matta et al., 2011).

The subcellular localization of the different NMDA receptor subtypes is under ongoing debate. A simplified model suggests that in the adult forebrain di-heteromeric GluN1/GluN2A- and tri-heteromeric GluN1/GluN2A/GluN2B-NMDA receptors are found at synaptic sites with variable ratios due to plastic changes. Di-heteromeric GluN1/GluN2B-NMDA receptors are thought to be more prominent at extrasynaptic sites (Dalby and Mody, 2003, Townsend et al., 2003, Rauner and Kohr, 2011).

1.2.3 The GluN2A/GluN2B ratio

As mentioned before, the GluN2 subunit mainly determines kinetics and intracellular coupling of the receptor and therefore strongly influences the characteristics and plasticity of the synapse. The opening duration of NMDA receptors has critical influence on the coincidence detection of pre- and postsynaptic activity. The regulation of the GluN2A/GluN2B ratio contributes to define the threshold to induce synaptic plasticity. The change in the ability to induce subsequent synaptic plasticity was called metaplasticity in 1996 (Abraham and Bear, 1996).

Many studies describe GluN2B as the driving force to elicit LTP, since it targets CaMKII to the synapse and synapses with lower GluN2A/GluN2B ratio need lower stimulation for LTP induction (Barria and Malinow, 2005, Lee et al., 2010). Thus the GluN2A/GluN2B ratio is an important regulator in terms of metaplasticity. Controversial publications present GluN2A-NMDA receptors as more important for LTP (Yang et al., 2012). In summary the question which NMDA receptor elicits LTP or LTD cannot be answered easily and depends mainly on the experimental design (Paoletti et al., 2013). Results differ for example depending whether the isolation of NMDA receptor subtypes was achieved by pharmacology or genetic disruption. For further details see section 4.3.

The expression of GluN2B-NMDA receptors correlates with the developmental periods of enhanced plasticity *in vivo* (Kleinschmidt et al., 1987, Fox et al., 1989). In the model of ocular dominance plasticity in the visual cortex, it was shown that the GluN2A/GluN2B ratio increases during the critical period (Erisir and Harris, 2003). Additionally, dark rearing of animals, which prolongs ocular dominance plasticity into adulthood, increases the abundance of GluN2B subunits as well. Also visual deprivation in adult animals increases GluN2B expression (He et al., 2006). Interestingly, the developmental GluN2 subunit switch occurs within the same time window as the formation of the ECM. As mentioned before, removal of the ECM can reactivate juvenile plasticity in the visual cortex of adult mice, but the molecular mechanisms are still not fully understood. Since removal of the ECM rejuvenates cortex plasticity, it is tempting to speculate that it could also “rejuvenate”, i.e. decrease the GluN2A/GluN2B ratio.

Along this line it has been shown that the integrity of the ECM affects cell surface molecules like members of the integrin family are in their activity (Wu et al., 2002, Tan et al., 2011, Orlando et al., 2012). Integrins are coupled to intracellular signaling molecules and affect intracellular processes upon extracellular remodeling. As integrins are shown to affect NMDA receptor mediated synaptic currents (Lin et al., 2003, Bernard-Trifilo et al., 2005), they are prime candidates to be involved in ECM-dependent regulation of NMDA receptors.

1.3 Integrins

Integrins are transmembrane proteins that are responsible for cell-cell and cell-ECM interactions. They play critical roles in a variety of biological processes such as cell motility, adhesion, synaptogenesis, proliferation, apoptosis, neural development and inflammation but also in axon guidance, neurite extension, synaptic plasticity and axon regeneration (Lemons and Condic, 2008).

1.3.1 Subunit composition, ligand binding and intracellular signaling

Integrins are obligate heterodimers containing two distinct chains, called α and β subunits, which are non-covalently associated. 24 different integrins are formed by combinations out of 8 β and 18 α subunits (Hynes, 2002). They are expressed in nearly every cell type in the body and a subset is expressed in the brain. In particular $\alpha 3$, $\alpha 5$, $\alpha 8$, αV , $\beta 1$ and $\beta 3$ subunits are enriched in neurons (Bernard-Trifilo et al., 2005), whereas glia cells were shown to express $\alpha 1$, $\alpha 2$, $\alpha 3$, $\alpha 6$, αV and $\beta 1$ (Previtali et al., 1997). Both subunits span the plasma membrane and in general have short cytoplasmic but large extracellular domains, which recognize short peptides that contain a key constituent acidic amino acid. The ligand specificity is due to both subunits of the integrin heterodimer (Hynes, 2002). Integrin function is regulated by both intracellular (inside-out) and extracellular (outside-in) signals. The 'inside-out' signaling describes the change from a low ligand-binding affinity conformation (inactive) to a high affinity one (active) and is also termed 'integrin activation'. The 'outside-in' signaling depicts intracellular activation of signaling cascades upon integrin-ligand binding (Takagi et al., 2002, Mould and Humphries, 2004).

Many extracellular ligands like fibronectin, tenascins and thrombospondins contain an Arg-Gly-Asp (RGD) binding motif, originally identified as the sequence in fibronectin that binds to the $\alpha 5 \beta 1$ -integrin (Pierschbacher and

Ruoslahti, 1984). Synthetic RGD peptides are common tools to experimentally affect integrins.

With their short intracellular tail integrins are coupled to a multitude of signaling proteins like a variety of kinases i.e. Arg kinase, CaMKII, src family kinases (SFK) and focal adhesion kinase (FAK) (Yamaguchi, 2000, Bernard-Trifilo et al., 2005, Kwok et al., 2010). This broad spectrum of signaling cascades enables integrins to influence a wide range of cellular processes.

1.3.2 Integrins in synaptic plasticity

In my thesis I investigated putative plasticity changes after ECM removal the implementation of integrins in synaptic plasticity is of special interest. Several studies have shown that the blockage of integrins leads to impairments in LTP (Peng 1991; Staubli 1990). Theta burst stimulation in hippocampal slices regulates the activity pattern of β 1-integrins by increasing their trafficking to the plasma membrane (Kaeck and Banker, 2006). Further, genetic disruption of β 1-integrins in mature excitatory neurons impairs LTP (Chan et al., 2006). To clarify the role of integrins in plasticity processes, many studies address the influence of integrins on NMDA receptors due to their potential to elicit LTP. Activation of β 1-integrins affects the phosphorylation state of GluN2A and GluN2B subunits via increased SFK activity (Bernard-Trifilo et al., 2005). In line with that the application of the SFK inhibitor PP2 eliminated an RGD induced increase of NMDA receptor mediated currents (Lin et al., 2003).

β 3-integrins seem to be more important for the regulation of homeostatic plasticity, since this form of plasticity is abolished in β 3 knockout mice, whereas LTP or LTD are still inducible in those mice (Ueda et al., 1994). Moreover surface levels of β 3-integrins are increased after blockage of neuronal network activity and β 3-integrins regulate GluA2-AMPA receptor trafficking, which is a key mechanism for synaptic scaling (Hedstrom et al., 2007, Bikkavilli and Malbon, 2009). Collectively these data prove that integrins are involved in the regulation of synaptic plasticity.

1.3.3 Regulation of integrins by ECM molecules

How would ECM remodeling affect integrin signaling? The CSPGs aggrecan and versican interact with β 1-integrins and either decrease or increase Y397 phosphorylation of FAK, respectively (Wu et al., 2002, Tan et al., 2011).

Phosphorylation of FAK activates its kinase activity and subsequently further signaling cascades. As aggrecan and versican differ in their temporal and spatial expression (Yamaguchi, 2000, Popp et al., 2003) the opposed influence on β 1-integrins could be important in certain brain areas or developmental stages. Modulation of the ECM via proteases is also known to affect integrin signaling. MMPs cleave many ECM proteins which include integrin-ligands, such as laminin, N-cadherin, dystroglycans and proteoglycans (Lander et al., 1997). The application of purified MMP-9 leads to spine enlargement and increases postsynaptic currents, and both effects were dependent on β 1-integrin functionality (Wang et al., 2008). Further MMP-9 affects lateral mobility of NMDA but not AMPA receptors in a β 1-integrin-dependent manner (Michaluk et al., 2009). Degradation of the ECM in hippocampal slices by application of ChABC enhances β 1-integrin activation as well as pY397 FAK level, which leads to increased spine motility and the appearance of spine head protrusions (Orlando et al., 2012). In line with that, the inhibitory effect of aggrecan on laminin-mediated axon growth by impairing integrin signaling could be removed by application of ChABC (Tan et al., 2011). This underlines an inhibitory effect of chondroitin sulfates on integrin signaling.

Altogether, based on all these observations it is tempting to hypothesize that the ECM may regulate NMDA receptors in an integrin-dependent manner. This mechanism is a good candidate to transform the information about rearrangements of the ECM into intracellular, plasticity related signaling pathways.

1.4 Calsyntenin

Calsyntenin-1 (Cst-1) is the first identified member of a small protein family consisting of three members: Cst-1, -2, -3 (Vogt et al., 2001, Hintsch et al., 2002, Araki et al., 2003). They belong to the cadherin superfamily and are the only members showing sequence homology along the entire protein sequence in vertebrates and invertebrates. This indicates that the function of Cst is likely to be conserved throughout evolution. The protein was initially named calsyntenin due to its potential to bind synaptic Ca^{2+} (Vogt et al., 2001). Araki and colleagues termed this protein family alcadeins (Alzheimer-related cadherin-like protein) as they demonstrated a stabilizing function of alcadein for the amyloid precursor protein (APP) (Araki et al., 2003). In this thesis the term calsyntenin will be used.

1.4.1 Expression and structure of calsyntenin

The Csts are expressed in the whole brain as components of the postsynaptic membranes, predominantly in excitatory synapses (Vogt et al., 2001, Hintsch et al., 2002). But each of the three family members displays a distinct neuronal mRNA expression pattern, which was described in detail by Hintsch et al. Cst-1 is expressed in the majority of neurons with small variations in its expression level. In contrast to Cst-1, the expression of Cst-2 and Cst-3 is not uniform in neurons of the same neuronal subtypes. Pyramidal neurons of the CA2 and CA3 region of the hippocampus for example express high amounts of all three Csts whereas pyramidal neurons of the CA1 show a high level of Cst-1, but low levels of Cst-2 and Cst-3. Highest expression of Cst-2 and Cst-3 but a low level of Cst-1 is found in putative GABAergic neurons. Part of the cerebellar Purkinje cells express Cst-2 and Cst-3, but no Cst-1 (Hintsch et al., 2002). In summary, defined subpopulations of both excitatory and inhibitory neurons express different combinations of the three Csts.

Csts are type-1 transmembrane proteins with a large extracellular N-terminal part, a transmembrane segment and a short cytoplasmic C-terminal tail (Figure 1). The extracellular part contains two cadherin-like (CAD) repeats and a laminin-G domain (LamG). The intracellular part shows a conserved acidic region and kinesin light chain-binding motifs (Konecna et al., 2006). This part shows the largest sequence deviations between Cst-1, -2 and -3. The total number of acidic residues and the size of acidic clusters is the highest in Cst-1. Cst-2 is also rich in acidic residues however clusters are less abundant and smaller in comparison with Cst-1. The cytoplasmic segment of Cst-3 is markedly shorter, as it contains only one kinesin light chain-binding motif whereas Cst-1 and Cst-2 contain two of those motifs (Hintsch et al., 2002). In contrast the proximal part of the intracellular tail is highly conserved even through different species. This part contains binding sites for interaction partners, which will be described later.

1.4.2 Proteolytic cleavage of calsyntenin

Csts undergo proteolytic cleavage at the cell membrane. Primary cleavage by α -secretases (ADAM-10 and ADAM-17) takes place in the extracellular, juxtamembrane region. This cleavage releases the ectodomain (sCst) into the extracellular space. The release of an extracellular segment of a transmembrane protein is called 'shedding'. Therefore enzymes acting in this way are termed

shedases. α -secretase action triggers subsequent secondary cleavage in the transmembrane segment by a presenilin-dependent γ -secretase. A small peptide (p3-Cst) is released into the extracellular space (Araki et al., 2004, Hata et al., 2009). The transmembrane stump is internalized. Initially it was postulated that it accumulates in the spine apparatus (Vogt et al., 2001). In 2004 Araki et al. demonstrated that this cytoplasmic fragment of Cst-1 binds to the adapter protein FE65 and translocates into the nucleus. This interaction was shown to suppress FE65 dependent gene transactivation induced by AICD, the cytoplasmic fragment of APP which is also produced by γ -secretase cleavage. The cytoplasmic fragment of Cst-1 alone with FE65 does not affect gene transactivation (Araki et al., 2004).

Cst-1 has been proposed to compete as a substrate for cleavage with APP, which is a well-known substrate of α - and γ -secretase. Both Cst-1 and APP bind with

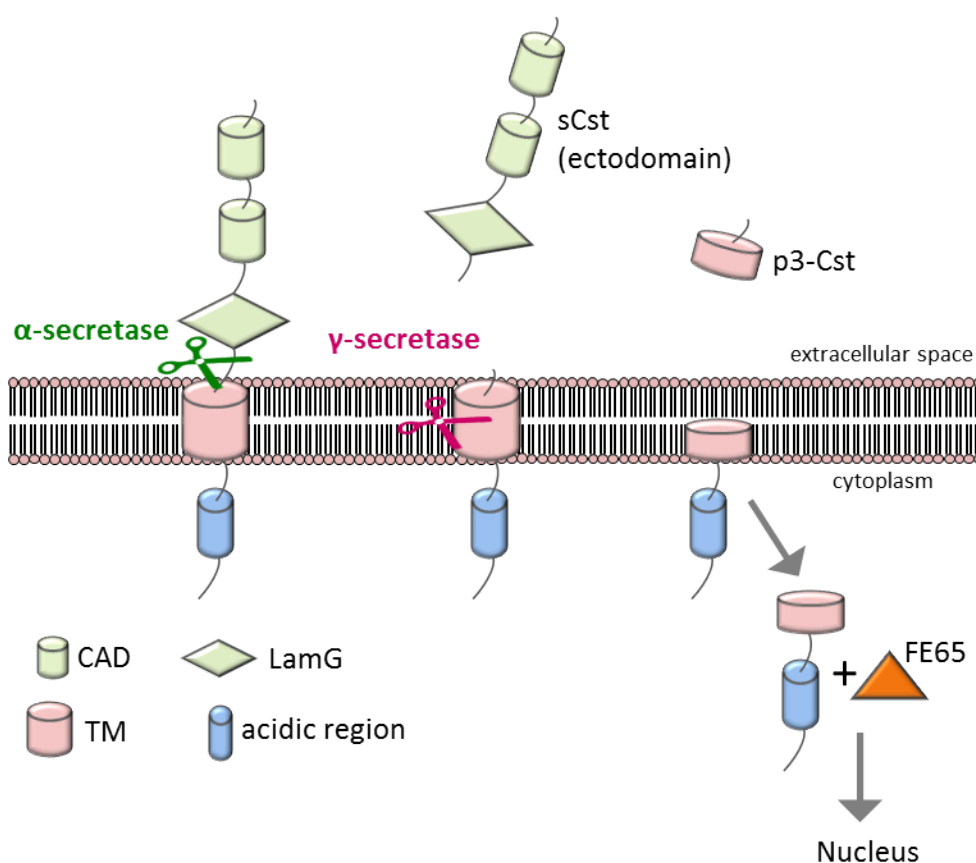


Figure 2: Schematic illustration of Cst-1 and its proteolytic cleavage

Csts undergo proteolytic cleavage by α - and γ -secretases, known from APP processing. The α -secretase cuts Cst within an extracellular, juxtamembrane region and releases the protein fragment sCst (corresponding to the soluble APP ectodomain sAPP) or ectodomain. This fragment was mainly investigated in this work. Subsequently the γ -secretase cleaves the protein within the transmembrane region and releases the small peptide p3-Cst (corresponding to the APP fragment, p3) into the extracellular milieu. The transmembrane stump is internalized and translocated to the nucleus by building a complex with FE65.

their intracellular segment to the same domain of X11-like Protein (X11L) (Araki et al., 2003). X11L is a neuron-specific adapter protein. Formation of this tripartite complex results in stabilization of APP's metabolism and enhances the X11L dependent suppression of A β production (Araki et al., 2003). This complex does not only protect APP but also Cst-1 from γ -secretase cleavage (Araki et al., 2004). This suggests, that APP processing and the formation of its potentially pathologic cleavage product A β are in close relation with Cst-1 processing. Deregulation of one of the proteins thus inevitably affects the processing and subsequently the signaling of the other protein (Araki et al., 2003, Araki et al., 2004).

1.4.3 Calsyntenin as an intracellular transport protein

As mentioned previously Cst-1 contains two kinesin light chain 1 (KLC1) binding motives (KBS) in the intracellular segment. Cst-1 binds with these two conserved motives, KBS-1 and -2, the tetratricopeptide repeats (TPR) of KLC1, which are known to be responsible for the interaction with cargo proteins (Verhey et al., 1998, Konecna et al., 2006, Araki et al., 2007). Kinesins are responsible for the fast anterograde axonal transport along microtubules. That awards Cst-1 a function in kinesin-dependent axonal vesicle transport as a cargo receptor protein. Hence it is plausible to assume that Cst-1 could have an impact on other proteins by influencing their transport dynamics. For instance the axonal transport of APP is influenced by Cst-1 as it mediates the *trans*-Golgi exit of APP in a kinesin dependent manner (Ludwig et al., 2009). By regulating the axonal transport of APP the production of A β is controlled as well (Araki et al., 2007, Steuble et al., 2012, Vagnoni et al., 2012). Cst-1 is present in the *trans*-Golgi network and Cst-1 positive vesicles are always found on plus end-directed trajectories, characteristic for vesicles that carry cargo intended for distal neuronal functions (Ludwig et al., 2009). Another cargo that is dependent on Cst-1 is the NMDA receptor. In juvenile Cst-1 KO mice the postsynaptic level of GluN2B-NMDA receptors is increased which leads to an increased GluN2B-NMDA receptor dependent LTP (Ster et al., 2014). Adult Cst1-KO mice do not show altered synaptic transmission or plasticity anymore. That implies that the developmental switch of predominantly GluN2B- to GluN2A-NMDA receptors is delayed in the mutant mice. It was demonstrated that Cst-1 vesicles are loaded with both GluN2A and GluN2B subunits and delivered to the *trans*-Golgi network without any preference. As the expression of Cst-1 peaks at postnatal day 7 (Konecna et al., 2006) they propose that Cst-1 drives the rapid implementation of the switch from

GluN2B to GluN2A subunits at synaptic level (Ster et al., 2014). When Cst-1 is absent the NMDA receptors still reach their destination in the postsynaptic membrane, even though delayed.

1.4.4 Cellular functions of the ectodomain of calyntenin

Two human studies about hippocampus-dependent memory resulted in the identification of CLSTN2 (encoding Cst-2) as a memory related human gene (Papassotiropoulos et al., 2006, Jacobsen et al., 2009, Preuschhof et al., 2010). Carrier of a single nucleotide polymorphism (T→C) within CLSTN2 show better episodic memory performance than TT genotype carriers. Preuschhof et al. could show that this positive effect of C allele carrier is not found in subjects being carrier of a C allele in the KIBRA gen, encoding a scaffolding protein. Further it has been shown that the Cst-1 orthologous CASY-1 is crucial for associative learning in *Caenorhabditis elegans* (*C. elegans*) (Ikeda et al., 2008, Hoerndli et al., 2009). Phenotypes of *casy-1* mutants are rescued by overexpressing the extracellular part, corresponding to the α -secretase cleavage product of CASY-1, suggesting a specific signaling function of this ectodomain. Additionally Hoerndli et.al showed that *C. elegans* lacking the AMPA-type glutamate receptor subunit GLR-1 (*glr-1* mutants) exhibit similar defects as the *casy-1* mutant. However, double loss-of-function mutants (*casy-1* + *glr-1* mutant) show no further reduction in learning performance. Further, increased levels of GLR-1 could rescue the phenotype of *casy-1* mutants. Thus CASY-1 very likely acts in a GLR-1 receptor-dependent pathway (Hoerndli et al., 2009). However, the cellular signaling mechanism and the receptor for the ectodomain of Cst-1 are unknown so far.

Interesting in this context are preliminary data from a proteomic screen to identify extracellular ligands of Cst-1 performed by Kerstin Leuthäuser in Peter Sonderegger's laboratory. Vitreous fluid from E14 chicken embryos was loaded on CNBr activated sepharose columns, which were coupled to his-tagged Cst-1 fusion proteins. Data from this assay suggested Cst-1 to bind secreted frizzled related protein 1 (sFRP-1). This interaction occurs at the cysteine-rich domain (CRD) of sFRP-1, a domain that is highly conserved in the frizzled receptor, which is part of the wnt signaling pathway and contributes to a multitude of cellular processes. sFRP-1 is known to bind to wnt and/or frizzled and thereby antagonizes wnt signaling (Wang et al., 1997, Bafico et al., 1999). Importantly, it has been shown that the wnt pathway in *C. elegans* affects the abundance of GLR-

1 receptors (Dreier et al., 2005). Taken together, this interaction may offer an explanation for the CASY-1 mutant phenotype in *C. elegans*. Based on these data the interaction of Cst-1 and sFRP-1 and the influence of Cst-1 on wnt signaling were investigated.

1.5 Wnt signaling

The wnt signaling pathways are highly conserved among species. They are essential and well characterized in developmental processes, including synaptic differentiation. In addition wnt signaling also plays part in synaptic maintenance and function, like modulation of synaptic vesicle cycle and trafficking of neurotransmitter receptors (Inestrosa and Arenas, 2010).

The protein wnt was first discovered in *Drosophila* (Sharma and Chopra, 1976). Mutation caused loss of wings and halteres which leads to the gene name *wingless*. Mutation of the gene in mice caused malignant transformation of mammary tissues which provided the name *int*. As *wingless* and *int* are homologs the name *wnt* was established as a combination of both names.

Wnt signaling is divided into two major parts: canonical and non-canonical wnt signaling. The canonical wnt signaling has been extensively studied. The main regulator in this pathway is the transcriptional co-activator β -catenin (section 1.5.1). Non-canonical wnt signaling pathways are highly diverse but they have in common to be β -catenin independent. An overview is provided in the work of Semenov (Semenov et al., 2007). There are at least two major non-canonical pathways: the planar cell polarity (PCP) pathway and the Ca^{2+} pathway. In the Wnt/PCP pathway activation of frizzled (Frzl) receptor leads to activation of the GTPases Rho and Rac which in turn stimulate ROCK and c-Jun N-terminal kinase (JNK), respectively. Therefore the Wnt/PCP pathway is also called Wnt/JNK pathway. The Wnt/ Ca^{2+} signaling pathway is initiated by activation of phospholipase C (PLC) which produces inositol 1,4,5-triphosphate (IP3) and 1,2 diacylglycerol (DAG). These products lead to an increase in cytosolic Ca^{2+} level, which subsequently activates several pathways, for example CaMKII that affects via phosphorylation of the cAMP response element-binding protein (CREB) transcription of wnt target genes (De, 2011). Non-canonical pathways will not be detailed here, as they are not investigated in this work.

There are 19 *Wnt* genes and 12 Frzl receptors in vertebrates. It is hard to classify wnt ligands as 'canonical' or 'non-canonical'. From a classical point of view wnt-

1, wnt-3a, wnt-8 and wnt-8b act in the canonical and wnt-4 and wnt-5a play the major part in non-canonical wnt signaling (De, 2011). But this classification is highly controversial and further depends on the specific combination of a certain wnt ligand binding to a certain Frzl receptor.

1.5.1 Canonical wnt signaling

The wnt ligand is a secreted, lipid-modified glycoprotein (Kurayoshi et al., 2007) that binds to its cell surface receptor Frzl, which is a seven-transmembrane spanning G-protein coupled receptor (Schulte and Bryja, 2007). The extracellular N-terminus of Frzl contains a Cysteine-rich domain (CRD), which forms the wnt ligand binding motif. Stimulation of Frzl and its co-receptor, the low-density lipoprotein receptor related protein (LRP), activates the intracellular signaling machinery including the activation of disheveled protein (DVL). This results in the deactivation of a so-called destruction complex, which contains proteins like glycogen synthase kinase-3 β (GSK-3 β) and adenomatous polyposis coli (APC). Normally the destruction complex keeps cytosolic β -catenin phosphorylated, which tags β -catenin for proteasomal degradation. Non-phosphorylated β -catenin accumulates in the cytosol and translocates into the nucleus. There it associates with the T-cell factor/lymphoid enhancer factor-1 (Tcf/Lef) family of transcription factors and initiates transcription of target genes (Oliva et al., 2013).

1.5.2 Function of sFRPs

There are several secreted antagonists of wnt signaling. Dickkopf-related protein 1 (Dkk-1) blocks the interaction of wnt with Frzl and LRPs (Mao et al., 2001), the wnt inhibitory factor (WIF), sclerostin, cerebus, Wise/SOST and others (Cruciat and Niehrs, 2013). The most prominent antagonist of wnt signaling is the family of sFRPs (Finch et al., 1997, Rattner et al., 1997). The sFRP family consists of five members, sFRP-1-5. They all contain two major domains: the netrin-related domain (NTR) and CRD. The C-terminal NTR domain is defined by segments of positively charged residues and by six cysteine residues (Uren et al., 2000, Chong et al., 2002). The CRD contains 10 conserved cysteine residues which build disulfide bridges (Rehn et al., 1998, Chong et al., 2002). The CRDs of sFRPs display 30 – 50% sequence similarity with the CRDs of Frzl (Rehn et al., 1998). It is proposed that sFRPs inhibit wnt signaling by binding wnt ligands that prevents their binding to Frzl. It was demonstrated that the CRD domain of sFRP-1 is necessary and sufficient to bind wnt and to inhibit wnt signaling (Lin et

al., 1997). More recent studies open a new discussion as for instance a CRD-lacking mutant of sFRP-1 still binds to wntless (Uren et al., 2000). In addition, optimal wnt inhibition is only achieved by both protein domains, CRD and NTR (Bhat et al., 2007). These contradictions imply that sFRPs have multiple wnt binding sites which could explain observed different affinities of certain sFRPs for different wnt ligands. Additionally the CRD shows the ability to dimerize (Dann et al., 2001) and to build homo- and heteromeric complexes of sFRPs and Frzl (Bafico et al., 1999, Rodriguez et al., 2005).

As the CRD domain of sFRPs and Frzl is highly homolog, it is nearby to investigate if Cst-1, as it binds to the CRD of sFRP-1, binds to the CRD of Frzl.

1.5.3 Wnt signaling at the mature neuronal synapse

It was shown that wnt-4, -5a, -7a and -11 are present in hippocampal neurons of rat embryo and adult rat (Cerpa et al., 2008). Several studies demonstrate an influence of wnt signaling on the functionality of mature synapses (Ahmad-Annur et al., 2006, Cerpa et al., 2008, Farias et al., 2009, Cerpa et al., 2010).

At presynaptic sites it was shown that wnt-7a fast and robustly stimulates the recycling of presynaptic vesicles, whereas wnt-3a shows only moderate effect. Wnt-1 and wnt-5a do not affect vesicle recycling (Cerpa et al., 2008). Application of wnt-7a further increases synaptic vesicle exocytosis at least temporally. Finally the number and size of synaptic vesicle recycling sites is increased by wnt-7a treatment, without affecting the protein level (Cerpa et al., 2008). In line with this a double-mutant mice lacking wnt-7a and Dvl exhibit decreased frequency in the release of neurotransmitter and altered synaptic protein localization (Ahmad-Annur et al., 2006). These data suggest that the presynaptic function of wnt-7a is driven by β -catenin-dependent signaling but without demanding gene transcription. Supporting evidence comes from studies showing that wnt-7a regulates trafficking of α_7 -nicotinic acetylcholine receptors (α_7 -nAChR) to the plasma membrane (Farias et al., 2007). Activation of α_7 -nAChR increases neurotransmitter release in hippocampal cells (Gray et al., 1996). The regulation of α_7 -nAChR by wnt-7a involves APC, which is highly expressed in hippocampal neurons (Brakeman et al., 1999) and builds a cytoplasmic complex with β -catenin (Rubinfeld et al., 1993). Wnt-7a induces the dissociation of β -catenin from APC, promoting the interaction of APC with α_7 -nAChR to induce its trafficking to the

plasma membrane (Farias et al., 2007). This represents an example of a β -catenin-dependent signaling without affecting gene transcription.

At postsynaptic sites it was shown that application of wnt-5a to rat hippocampal slices increases the amplitude of field EPSPs by modulation of NMDA- and AMPA receptor mediated currents (Cerpa et al., 2010). In line with this wnt-5a leads to rapid insertion of NMDA receptors into the postsynaptic membrane and increases the number of PSD-95 clusters (Farias et al., 2009, Cerpa et al., 2010). These effects are mediated via CaMKII and JNK phosphorylation indicating that wnt-5a acts via non-canonical signaling in the postsynapse.

Since Cst-1 was shown to bind to sFRP-1, it is tempting to speculate that Cst-1 may also influence synaptic properties via wnt signaling, which is addressed in the course of my PhD thesis.

1.6 Aims

There are two major parts in this thesis:

- I. The effect of the ECM on the expression and dynamics of GluN2B-NMDA receptors
- II. Cellular effects of Calsyntenin-1's ectodomain

Part I

The ECM plays an important role in the development of the brain and in the regulation of synaptic function. It has been shown that removal of the ECM in the visual cortex after the critical period rejuvenates ocular dominance plasticity, but the underlying molecular mechanisms are not clear. It is known that the GluN2A/GluN2B ratio of NMDA receptors at the synapse is crucial for the threshold to induce synaptic plasticity. This ratio is decreasing during the critical period. If removal of the ECM brings plasticity back into a juvenile stage, does it also rejuvenate the GluN2A/GluN2B ratio? Does the ECM removal increase the abundance of GluN2B-NMDA receptors that probably lead to increased plasticity? If so, what is the signaling mechanism that transfers the information of the ECM removal into the cell and changes the expression profile of NMDA receptors? The aims of this part are summarized here:

- Does the digestion of ECM alter NMDA receptor-driven synaptic currents?
- Does the digestion of ECM influence expression levels of GluN2B-NMDA receptors?
- Does the digestion of ECM alter surface abundance of GluN2B-NMDA receptors? Is the signaling mechanism integrin dependent?
- Does the digestion of ECM change GluN2B phosphorylation?
- Does the digestion of ECM change mobility of GluN2B-NMDA receptors?

Part II

The activity of extracellular proteases is known to yield new signaling molecules to affect synaptic transmission. The effect of ectodomain shedding of the cadherin superfamily member Cst is poorly described. Published data demonstrate a rescuing effect of this ectodomain in *C. elegans* Cst-1 mutants that show an impaired associative learning. But the involved signaling mechanisms are still not known. Unpublished data suggested that Cst-1 binds sFRP1, a protein related to wnt signaling. This binding needs the CRD of sFRP-1, which is homologous to the CRD of Frzl. These observations lead to the hypothesis that Cst-1 could also bind to Frzl, which would provide a possible receptor for the ectodomain of Cst-1. Further it was questioned if Cst-1 influences wnt signaling-dependent gene transcription as it could affect the activity of the pathway by interacting with sFRP-1. Further, wnt signaling was shown to influence presynaptic activity which led to the investigation of the effect of Cst-1 on presynaptic activity. The aims of this part are summarized here:

- Does Cst-1 act on canonical wnt signaling activity?
- Does Cst-1 bind Frzl?
- Does Cst-1 influence presynaptic activity?

2 Material and Methods

Chemicals were purchased from Roth or the companies indicated. The quality of the reagents was of analytical grade.

2.1 Neuronal cell cultures

Rat hippocampal and cortical cultures were prepared by Heidi Wickborn, Anika Lenuweit, Bettina Kracht, Anita Heine and Kathrin Hartung. All media and solutions were warmed (37°C) before use. Dissociated hippocampal cultures were prepared as Banker type cultures as described from Kaech & Banker (Kaech and Banker, 2006).

Table 1: Media and reagents for neuronal cell cultures

| Media and reagents | Ingredients/Company |
|---|---|
| DMEM full | 10 % FCS (Gibco); 1 % Penicillin/Streptomycin 100x (Gibco); 2 mM L-Glutamine 100x (Gibco) in DMEM (Gibco) |
| NB+ (Neurobasal) | 2 % B27 (Gibco); 2 mM L-glutamine (Gibco); 1 % Penicillin/Streptomycin 100x (Gibco) in Neurobasal (Gibco) |
| Distilled Water | Gibco /Millipore |
| HBSS+ (with Mg ²⁺ and Ca ²⁺) | Gibco |
| HBSS- | Gibco |
| AraC 1.5 mM | Calbiochem |
| 10x Trypsin | Gibco |
| 10x Trypsin + EDTA 0.5 % | Gibco |
| Paraffin | Paraplast embedding medium (Fischer) |
| Freezing medium | DMEM full, 10 % DMSO |
| Poly-L-Lysin | 100 mg/l poly-L-lysin in 100 mM boric acid, pH 8,5, sterile filtered |
| Poly-D-Lysin | 100 mg/l poly-D-lysin in 100 mM boric acid, pH 8,5, sterile filtered |

2.1.1 Glia cells

Preparation: P0-P2 pups from Wistar rats were decapitated and both hemispheres were isolated and freed by the meninges in ice cold HBSS+. After three washing steps with ice cold HBSS- 10x trypsin was added and incubated for 20 min at 37 °C. The hemispheres were washed three times with HBSS- and dissociated in 1ml DMEM full by using 1 ml pipette. Cells were plated in 10 ml DMEM full in 75 cm² flasks and kept in the incubator at 37 °C, 5 % CO₂ and a humidity of 95 %. The media was changed the following day and then every 4-5 days. After 10-14 days cells were confluent and split in a 1:4 ratio. After being confluent again cells were frozen.

Freezing: The flasks were washed with HBSS-, 10x Trypsin + EDTA was added and incubated at 37 °C until all cells were detached. Cells were re-suspended in DMEM full and centrifuged for 5 min at 1000 x g followed by re-suspension in

1 ml freezing media. The aliquots were slowly frozen in “isopropanol containing boxes” at -80 °C and on the following day the frozen aliquots were transferred to -150 °C and stored until usage.

Plating: Frozen aliquots were quickly thawed at 37 °C. Two aliquots were diluted in 48 ml DMEM full and plated into 10 Ø 6 cm plates with a final volume of 5 ml each.

2.1.2 Preparation of glass coverslips

18 mm glass coverslips for dissociated hippocampal cultures were incubated in 69 % HNO₃ in an end-over-end rotator overnight. The next day coverslips were neutralized by rinsing with ultra-pure water. Afterwards, coverslips were boiled three times in the microwave oven with exchanging water in between. Thereupon, coverslips were dried separately on a paper tissue and subsequently sterilized at 225 °C for 16 h. Paraffin puncta were applied and coverslips were coated with Poly-L-Lysin overnight at 37 °C and then washed three times with ultra-pure water. Finally, coverslips were stored for 3-4 days until the day of preparation.

Coverslips used for dissociated cortical cultures were only sterilized without any previous washing procedure, coated with Poly-D-Lysin, washed with ultra-pure water und stored in HBSS- until day of preparation.

2.1.3 Preparation of neuronal cultures

E18-19 embryos of Wistar rats were decapitated and both hemispheres were isolated and freed by the meninges in ice cold HBSS+. The hippocampi were isolated from the cortex and both cortices and hippocampi were treated in the same way from now on. After three washing steps with HBSS- 10x trypsin was added and incubated for 20 min at 37 °C. Tissues were washed again with HBSS- and dissociated with two syringes of different diameter (first 0.9 mm, then 0.45 mm). Using a cell mesh cells were further dissociated and diluted with DMEM full to different plating concentrations. Dissociated cortical cultures were plated in 24 or 6 well plates with a density of 50.000 or 500.000 cells per well, respectively. On the following day DMEM full was replaced by NB+. Dissociated hippocampal cultures were plated with a density of 30.000 cells per coverslip. After 1 h coverslips were placed into prepared Ø 6 cm plates containing the glia

feeding layer, cells facing down. At DIV 4 AraC was added to the hippocampal cultures. Cells were fed once a week.

2.2 Stable HEK293-T cell line cultures

Table 2: Media and reagents for stable HEK293-T cell line cultures

| Media and reagents | Ingredients/Company |
|--------------------|---|
| DMEM full | 10 % FCS (Gibco); 1 % Penicillin/Streptomycin 100x (Gibco); 2 mM L-Glutamine 100x (Gibco) in DMEM (Gibco) |
| HBSS- | Hank's balanced salt solution, Ca ²⁺ and Mg ²⁺ free (Invitrogen) |
| 10x Trypsin + EDTA | Gibco |
| 1x Trypsin | 10 % 10x Trypsin + EDTA (Gibco) in HBSS- |
| Poly-D-Lysin | 100 mg/l poly-D-lysine in 100 mM boric acid, pH 8,5, sterile filtered |

Human Embryonic Kidney Cells (HEK293-T) (ATCC) were mainly cultured by Kathrin Gruss and cultured in DMEM full. Cells were split twice a week until they reached passage P30 – P40. If cells were plated on glass coverslips those were treated with Poly-D-Lysin for 1 h and washed three times with ultra-pure water.

2.3 Molecular Biology

2.3.1 DNA constructs (commercially available)

- pCI-SEP_Glu2B (Plasmid #23998) purchased from addgene. Depositing Laboratory: Robert Malinow (Kopec et al., 2006)
- rat Frizzled-1-HA-pCD (Plasmid #16818) purchased from addgene. Depositing Laboratory: Randall Moon (Xenopus Expression Plasmids, unpublished)
- Super 8x TOPFlash (Plasmid #12456) purchased from addgene. Depositing Laboratory: Randall Moon (Veeman et al., 2003)
- Super 8x FOPFlash (Plasmid #12457) purchased from addgene. Depositing Laboratory: Randall Moon (Veeman et al., 2003)
- 7-TGC (Plasmid #24304) purchased from addgene. Depositing Laboratory: Roel Nusse (Fuerer and Nusse, 2010)

2.3.2 DNA constructs (custom-made)

Table 3: DNA constructs (custom made)

| Construct | Vector backbone | Insert | Source |
|-----------------|-----------------|------------------------------------|---------------------------------------|
| Cst1Clea-myc | pcDNA3.1. (A+) | Cst1 aa 1 - 822 (mouse) | self-made |
| Cst1Cad-myc | pcDNA3.1. (A+) | Cst1 aa 1 – 263 (mouse) | self-made |
| Cst1LamG-myc | pcDNA3.1. (A+) | Cst1 aa 1 – 28 + 362 - 508 (mouse) | self-made |
| Cst3Clea-myc | pcDNA3.1. (A+) | Cst1 aa 1 - 811 (mouse) | self-made |
| Wnt8a-myc | pcDNA3.1. (A+) | Wnt8a aa 1 – 68 (mouse) | self-made |
| GluN1-wt | pRcCMV | GluN1 (rat) | gift from Dr. Paoletti (Bordeaux) |
| Neurofascin 186 | | Neurofascin 186 | gift from Dr. Dirk Montag (Magdeburg) |
| Cst1 | pcDNA3.1. (A+) | Cst1 (mouse) | Prof. Sonderegger (Zurich) |
| Cst3 | pcDNA3.1. (A+) | Cst3 (mouse) | Prof. Sonderegger (Zurich) |

2.3.3 Transfection of dissociated hippocampal neurons

For Quantum Dot experiments dissociated hippocampal neurons grown on Ø 18 mm coverslips were transfected by using Effectene Transfection Reagent (QIAGEN) following the protocol offered by the company. Cells were transfected at DIV 5 with two DNA constructs: pCI-SEP_GluN2B and GluN1-wt (0.75 µg each). DNA was diluted with Buffer EC and Enhancer solution was added and mixed. After incubation of 5 min at RT Effectene reagent was added and mixed. 10 min of incubation at RT were followed by diluting the mix 1:1 with cell media. Coverslips were placed in a separate petri dish filled with NB+ with cells facing up. Transfection mix was distributed over each coverslips and incubated for 1 h at 37 °C. Afterwards cells were placed back into the former petri dish containing the glia feeding layer.

2.3.4 Transfection of HEK293-T cells

Table 4: Buffer for transfection of HEK293-T cells

| Buffer | Composition |
|------------|--|
| Solution A | 500 mM CaCl ₂ |
| Solution B | 140 mM NaCl, 50 mM HEPES, 1.5 mM Na ₂ PO ₄ , pH 7.05 |

Table 5: Quantities of buffers and DNA for transfection of HEK293-T cells

| plate / flask | V of media (ml) | DNA (µg) | Sol A / Sol B (µl) |
|--------------------------|-----------------|----------|--------------------|
| 24 well plate | 0.5 | 1 | 25 |
| 12 well plate | 1 | 2 | 50 |
| 25 cm ² flask | 5 | 8 | 175 |
| 75 cm ² flask | 10 | 25 | 500 |

| | | | |
|---------------------------|----|----|------|
| 150 cm ² flask | 30 | 75 | 1500 |
|---------------------------|----|----|------|

HEK293-T cells were transfected with a CaPO₄ method. Confluent cells were split the day before transfection in a 1:5 ratio. DNA was diluted in a certain amount (Table 5) in Solution A. Solution B was added and incubated for 1 min at RT. The mix was added to the cells and 4 – 10 h later the cell media was exchanged. In general cells were used for experiments after 48 h.

2.3.5 PCR to amplify defined DNA fragments

Table 6: Primer sequences for Cst constructs

| Construct | Primer forward | Primer reverse |
|--------------|---|---|
| Cst1Clea-myc | Cst1full-fw 5' TTAAGCTTATGCTGCGCCGCC 3' | Cst1clea-rev 5'AAGAATTCGGCATGTTCCACGGGGTTGG 3' |
| Cst1Cad-myc | Cst1Cad-fw 5'AAGGATCCATGCTGCGCCGCCCT 3' | Cst1Cad-rev 5'TTGAATTCGGGGCTGCAGGTGGGCTTGA 3' |
| Cst1LamG-myc | Cst1LamG-fw 5'AAGTTAACCATGACAGTGACCAGGTCTTT 3' | Cst1LamG-rev 5'TTGAATTCATACTCTTGCCAGCAAGCTC 3' |
| Cst3Clea-myc | Cst3Cleafw_ms 5'AAAAGCTTATGACCCTCTGCTGGT 3' | Cst3Clearev_ms 5'AACTCGAGACTGGGATGGGCCACC 3' |

Table 7: PCR protocol / Cycles

| Process | Temperature and Time | Cycles |
|----------------------|----------------------|---------|
| Initial denaturation | 95 °C, 3 min | 1 |
| Denaturation | 95 °C, 20 sec | 30 - 40 |
| Annealing | 57 °C, 20 sec | |
| Extension | 72 °C, 60 - 90 sec | |
| Final extension | 72 °C, 5 min | 1 |

Table 8: Buffers for PCR

| Buffer / Item | Composition / Company |
|--|-----------------------|
| Taq Polymerase | QIAGEN |
| 5x Phusion GC Buffer | QIAGEN |
| MgCl ₂ 25 mM | QIAGEN |
| Q-Solution | QIAGEN |
| Deoxynucleotide Triphosphate Set (dNTPs) | Fermentas |
| DMSO | QIAGEN |
| Smart Ladder DNA Marker 200 – 10 kb | Eurogentec |
| GeneRuler™ 1 kb Plus DANN Ladder | Life Technologies |

To investigate cellular functions of the ectodomain of Cst three DNA constructs were produced: Cst1Clea-myc/his (Cst1Clea) or Cst3Clea-myc/his (Cst3Clea), containing both cadherin and LamG domains; Cst1Cad-myc/his (Cst1Cad), containing only two cadherin domains and Cst1LamG-myc/his (Cst1LamG), containing only the LamG domain. All constructs were tagged with an N-terminal myc/his tag. Table 6 depicts the primers that were used for each

construct. The template DNA was either Cst1 or Cst3 provided by Prof. Sonderegger (Table 3).

When cDNA constructs were generated by PCR, specific primers were re-suspended at a concentration of 100 pmol/ μ l and used in the amplification reaction at a final concentration of 10 pmol/ μ l. The final concentration of the PCR reagents were: template DNA 20 ng / 50 μ l, 0.2 mM dNTPs, 0.02 units/ μ l of Phusion DNA Polymerase, 3 % DMSO in Phusion GC Buffer (5 x). The temperature profile used for PCR is highlighted in Table 7.

2.3.6 DNA agarose gel electrophoresis

Table 9: Buffers for DNA gel electrophoresis

| Buffer / Item | Composition / Company |
|------------------|--|
| Agarose | Bio&SELL / BIOZYM |
| 50x TAE buffer | 4.84 g Tris, 114.2 ml Acetic acid, 37,3 g EDTA |
| Ethidium bromide | Roth (0.5 μ g/ml working concentration) |

DNA fragments, e.g. PCR products were separated by one dimensional agarose gel electrophoresis according to their size. Agarose gels were prepared as 1 – 2 % w / v dependent on the fragment size. Agarose was melted in 1x TAE buffer by heating in a microwave. 5 – 10 μ l ethidium bromide solution were added before polymerization to visualize the DNA at a later time. Gels were run in an electrophoresis chamber (Sub-Cell®, BioRad) with 60 – 100 V (depending on the size of the gel) in 1x TAE buffer until DNA fragments were separated properly. The DNA fragments were visualized under UV-light and photographed with an Eagle-Eye (Stratagene) using the gel documentation system Gel Doc (Biorad).

To isolate the DNA out of the agarose Gel the PCR cleanup gel extraction kit (Macherey-Nagel) was used.

2.3.7 DNA digestion by restriction enzymes and ligation of DNA fragments

Table 10: Buffers for DNA digestion by restriction enzymes

| Buffer / Item | Composition / Company |
|---------------------|-----------------------|
| Buffer 10x | Fermentas / NEB |
| Restriction enzymes | Fermentas / NEB |
| Ligation Buffer 10x | Fermentas / NEB |
| T4 DNA Ligase | Fermentas / NEB |

To ligate different DNA fragments with each other the DNA needs to have appropriate ends. Therefore the DNA gets digested by restriction enzymes that cut the DNA at specific sequences. That results in defined overhangs (sticky end)

or blunt ends, which can be ligated with the suitable partner. In most of the cases a target vector and a smaller construct (insert) should be ligated and therefore need to be digested with the same enzymes. Depending on whether an analytic or a preparative digestion should be performed, the amounts of ingredients varied: 0.5 - 1 μg DNA, 0.5 – 2 μl restriction enzyme and Buffer (10x) were diluted in nuclease free water. The buffer and the concentration of enzymes varied upon different combinations of enzymes.

To ligate the predigested vector and insert these two are mixed in a 1 : 7 ratio with T4 ligase in Ligation Buffer (10x). Reaction was performed at 16 – 20 °C for 2 – 8 h. To select successful ligations, DNA constructs were transformed into E. coli XL10 Gold competent cells for subsequent DNA mini-prep isolation.

2.3.8 Transformation of E. coli XL10 Gold competent cells

Table 11: Items for bacteria transformation

| Item | Composition / Company |
|---------------------------|--|
| E.coli XL10 Gold Bacteria | Stratagene |
| LB medium | 20 g LB Broth Base (Invitrogen) / 1000 ml H ₂ O |
| LB Agar | 15 g Select Agar (Invitrogen) / 1000 ml LB-medium |
| Antibiotics | Roth |
| X-Gal | Roth |
| IPTG | Roth |

To transform DNA constructs into E. coli competent cells a heat shock protocol was used. DNA was incubated with 100 μl competent E. coli cells on ice. After heat shock at 42 °C for 30 sec cells were cooled down on ice for 2 min and diluted in 1 ml warm LB medium without antibiotics. Cells were gently shaken for 1 h at 37 °C, subsequently centrifuged at 1000 x g for 1 min and re-suspended in 100 μl LB medium. The whole suspension was plated on an LB Agar plate containing the corresponding antibiotic and in case of a blue-white-screening X-Gal and IPTG. Plates were placed at 37 °C over night.

2.3.9 Plasmid Isolation (Mini Preparation)

Table 12: Buffers for plasmid isolation

| Buffer | Composition |
|-----------|---|
| P1 Buffer | 50 mM Tris/HCl pH 8.0, 10 mM EDTA, 100 $\mu\text{g}/\text{ml}$ RNase A (4 °C) |
| P2 Buffer | 200 mM NaOH, 1 % (w/v) SDS |
| P3 Buffer | 3 M potassium acetate, pH 5.5 (4 °C) |

One colony from an agar plate was picked and transferred into a 2 ml LB medium overnight culture. Plasmids were isolated by an alkaline lysis. After

centrifugation with 5500 rpm for 5 min cells were re-suspended in 300 μ l P1 buffer and 300 μ l P2 buffer were added. Probes were gently pivoted and incubated at RT for 5 min. Ice cold P3 buffer was added, pivoted and incubated on ice for 5 min. After centrifugation with 14000 rpm for 10 min supernatants were transferred into a new reaction tube, 510 μ l isopropanol were added and pivoted. After 5 min incubation at RT the plasmids were spun down with maximum speed for 10 min. Supernatants were removed and the pellets washed with 1 ml 70% Ethanol (v / v). Afterwards the pellets were centrifuged again and supernatants removed. After drying, the pellets were diluted in 50 μ l dH₂O each and stored at -20 °C. For mammalian cell transfection, DNA with high concentration and purity was prepared using the NucleoBond® Xtra Midi EF Kit (Macherey-Nagel). DNA concentration was measured with NanoDrop1000 (peQLab).

For sequencing the DNA constructs were sent to SeqLab (Sequence Laboratories Göttingen)

2.4 Antibodies

Table 13: List of primary antibodies, origin and working concentrations

| Primary antibody | Species | Company | Cat-No. | ICC dilution | WB dilution |
|-------------------------------------|---------|------------------------------------|-------------|------------------------|-------------|
| α GluN2B | rb | Alomone labs | AGC-003 | 1:400/ 1:25/ 1:1000 | |
| α GluN2B N59/36 | ms | NeuroMab | 75-101 | | 1:500 |
| α pGluN2BY472 | rb | AAT Bioquest | 8A0526 | | 1:500 |
| α pGluN2BS133 | rb | Millipore | 06-519 | | 1:500 |
| α PSD-95 | ms | NeuroMab | | 1:1000 | |
| α Map2 | ms | Sigma-Aldrich | | 1:2000 | |
| α β 3-tubulin | ms | Synaptic System | | | 1:1000 |
| α GFP | ms | | | 1:1000 | |
| α Synaptotagmin 1-550 Oyster | ms | Synaptic System | | 1 : 750 | |
| α β 1-integrin (CD29) | rat | BD Pharmingen | 555002 | 1:25 | |
| α Brevican | gp | PD Seidenbecher / Dr. Frischknecht | | 1:1000 | |
| α Neurofascin | rb | abcam | ab31719 | 1:1000 | |
| α myc | ms | abcam | ab18185 | 1:1000 | |
| α HA | rat | Roche | 11867423001 | 1:500 | |

Species: rabbit (rb), mouse (ms), guinea pig (gp), rat. Fluorescently labelled secondary antibodies that were used for ICC were purchased from Invitrogen (Alexa Fluor 488, 568, 647 1:1000) or from Dianova (Cy3, Cy5 1:1000). Fluorescently labelled secondary antibodies that were used for quantitative

immunoblotting were purchased from Invitrogen (ms Alexa Fluor 680, 1:20.000) and from Rockland (rb IRDye 800 W, 1:20.000).

Table 14: List of enzymes and drugs

| Drug | Company | Cat-No. | ICC dilution |
|------------------------|-----------|---------|---------------------|
| Hyaluronidase (Hya) | Millipore | 38594 | 250 u / 500 μ l |
| Chondroitinase (ChABC) | Sigma | C3667 | 0.1 u / 500 μ l |
| PP2 | Tocris | 1407 | 1 – 10 μ M |

2.5 Immunocytochemistry

Table 15: Buffers for immunocytochemistry

| Buffer | Composition |
|-------------------|--|
| 4 % PFA (w / v) | 4 % PFA in PBS pH 7.4 |
| Blocking Solution | 10 % FCS in PBS, 0,1 % Glycin, 0,1 % Triton X-100 |
| 1x PBS | 2,7 mM KCl, 1,5 mM KH ₂ PO ₄ , 137 mM NaCl, 8 mM Na ₂ HPO ₄ , pH 7,4 |
| Mowiol (96 ml) | 9.6 g Mowiol, 24 ml H ₂ O, 24 g Glycerol → 2 h stirring, 48 ml 0.2 M Tris pH 8.5 → 10 min 50 °C, 2.5 g DABCO |
| Tyrode buffer | 145 mM NaCl, 5 mM KCl, 10 mM glucose, 10 mM HEPES, 2 mM MgCl ₂ , 2 mM CaCl ₂ , pH 7.4, osmolarity 300 mosmol |

2.5.1 Immunostainings of dissociated neuronal cultures

Rat cortical neurons were grown on Ø 12 mm coverslips in NB+ medium. If surface or extracellular proteins should be stained, antibodies were diluted in NB+ medium. A wet chamber was covered with Parafilm and drops of the antibody solution were pipetted on it. Coverslips were turned, cells facing down, on top of the drop and incubated at 37 °C for 20 min. After 5 min fixation with 4 % PFA cells were incubated in Blocking Solution to block PFA reactivity and unspecific binding sites and to permeabilize the cells. Primary antibodies against intracellular proteins were diluted in Blocking Solution and dropped on Parafilm. Coverslips with cells facing down were incubated with primary antibodies for 90 min at room temperature or overnight at 4 °C. Afterwards cells were washed three times with 1x PBS. Secondary antibodies were again diluted in Blocking Solution and incubated with the cells for 45 min at room temperature in darkness. Following three washing steps coverslips were mounted with Mowiol on object slides and stored at 4 °C until usage.

If no surface or extracellular proteins were stained, the protocol started with the PFA fixation of the cells.

Synaptotagmin antibody uptake

To investigate presynaptic activity an antibody against the luminal domain of synaptotagmin-1 coupled with a fluorophore was used in the same way as antibodies for surface expressed receptors. If synapses are active and fuse their neurotransmitter vesicles with the cell membrane the luminal part of synaptotagmin-1 gets exposed to the neuronal surface and the antibody can bind and is taken up when vesicular membranes are endocytosed. In this way the fluorescence intensity of this antibody reflects the activity state of the single synapses.

2.5.2 Binding Assay

To investigate if extracellular proteins bind to surface expressed receptors a binding protocol was established. Cst1Clea, Cst3Clea and Cst1Cad were overexpressed in HEK293-T cells. The proteins were secreted into the supernatant which was collected. Alpex cells, constantly expressing brevicin, secrete the protein and these supernatants were collected as well. HEK293-T cells were transfected with either Frzl-1-HA or neurofascin. After 48 h cells were plated on coated Ø 12 mm coverslips. When cells were settled down they were briefly washed with warmed HBSS+. The collected supernatants were diluted in FKS free DMEM full (1 : 2.5) and cells were incubated in these dilutions at 18 °C for 1 h. Afterwards cells were washed with HBSS+ and fixed with 4 % PFA. In this experiment the Blocking Solution did not contain Triton, since all the antibodies that were used should only label surface expressed or surface bounded proteins. Apart from that the immunostaining protocol followed the same procedure as described in section 2.5.1.

2.5.3 Microscopy and image analysis

Images were taken using a Zeiss Axioplan 2 epifluorescence microscope equipped with a camera (Cool Snap EZ camera; Visitron Systems, or Spot RT-KE; Diagnostic Instruments, Inc.) and MetaView software (MDS Analytical Technologies). Image processing and analysis were performed using ImageJ (MacBiophotonics ImageJ Version 1.41a) and OpenView (Version 1.5 from Noam Ziv) software.

2.5.4 Quantum Dot experiments

Dissociated hippocampal neurons grown on Ø 18 mm coverslips and transfected at DIV 5 (see 2.3.3) were used for Quantum Dot (QD) experiments from DIV 21 – 26. Some coverslips were treated with Hya overnight, some with Hya for 10 min. QDs (Life Technologies) were centrifuged before use for 10 min at 10.000 × g. 0.5 µl GFP antibody were incubated with 1 µl QD-655 in 1x PBS for 10 min under gentle shaking. 1 µl Casein was added to reduce the formation of aggregates and the master mix was incubated for another 15 min. 1 µl of the master mix was diluted in 100 µl cell media and dropped on a petri dish covered with Parafilm (final concentration of antibody / QD-655: 1:2000 / 1:1000). The coverslip was incubated with cells facing down for 2 min at 37 °C. Subsequently cells were washed in Tyrode buffer containing 0.1 % BSA and fixed in an imaging-chamber (Low Profile Open Bath Chamber, Warner Instruments) and filled with warmed Tyrode buffer.

Live imaging was performed at 37 °C using an inverted microscope (Observer. D1; Carl Zeiss, Inc.) in a heated imaging chamber TC-344B (Warner Instruments) and an EMCCD camera (Evolve 512; Photometrics) controlled by MetaMorph Imaging (MDS Analytical Technologies) and VisiView (Visitron Systems GmbH) software. Live streams were acquired every 30 ms (33 Hz) for 30 sec.

Data analysis was performed with custom-made software (Groc et al., 2007). Two parameters were analyzed the Mean Square Displacement (MSD) and the Instantaneous Diffusion Coefficient (D_{inst}). The MSD is calculated by the distance that a QD moves in between two images, for example between the 1th and 2th picture and the 2th and 3th image. The second MSD is based on the covered distance between the 1th and 3th and the 2th and 4th image. The MSD provides information about the area a QD explores within a defined time window. The D_{inst} describes the velocity of a QD calculated out of the first 4 images of the stream.

2.6 Biochemistry

Table 16: Buffers for biochemistry

| Buffer | Composition |
|--|---|
| 4x SDS sample buffer | 250 mM Tris, pH 6.8, 1 % (w/v) SDS, 40% (v/v), glycerol, 4 % β -mercaptoethanol, 0.02 % bromophenol blue |
| Cell lysis buffer | 10 mM Tris, pH 7.4, 150 mM NaCl, 2 % SDS, 1 % deoxycholate, 1 % Triton X-100, Complete Protease Inhibitor Cocktail (Roche) 1 Tbl. per 10 ml, PhosSTOP Phosphatase Inhibitor Cocktail (Roche) 1 Tbl. per ml, 1 % NaVO_3 |
| Electrophoresis buffer | 192 mM glycine, 0.1 % (w/v) SDS, 25 mM Tris, pH 8.3 |
| Separation buffer | 1.5 mM Tris pH 8.8 |
| Stacking buffer | 0.5 M Tris pH 6.8 |
| Separation gel (20 %) | 8.25 ml separation buffer, 7.5 ml 87 % Glycerol, 16.5 ml 40 % Acrylamide, 330 μl EDTA (0.2 M), 22 μl TEMED, 120 μl 0.5 % Bromophenol blue and 75 μl 10 % APS |
| Separation gel (5 %) | 8.25 ml separation buffer, 17.94 ml dH_2O , 1.89 ml 87 % Glycerol, 4.12 ml 40 % Acrylamide, 330 μl EDTA (0.2 M), 22 μl TEMED and 118 μl APS |
| Stacking gel (5%) | 6 ml stacking buffer, 7.95 ml dH_2O , 5.52 ml 87% Glycerol, 3.90 ml 30 % Acrylamide, 240 μl EDTA (0.2 M), 240 μl 10% SDS, 17.2 μl TEMED, 30 μl Phenol red and 137 μl 10% APS |
| Coomassie brilliant blue staining solution | 1 mg/1000 ml Coomassie brilliant blue R-250, 60 % (v/v) methanol, 10 % (v/v) acetic acid |
| Destaining solution | 7 % (v/v) acetic acid, 5 % (v/v) methanol |
| Blotting buffer | 192 mM Glycine, 0.2 % (w/v) SDS, 18 % (v/v) methanol, 25 mM Tris pH 8.3 |
| 1x TBS | 50 mM Tris, 150 mM NaCl, pH 7.5 |
| 1x TBS-T | 50 mM Tris, 150 mM NaCl, 1 % Tween-20 pH 7.5 |
| ACSF | 125 mM NaCl, 2.5 mM KCl, 1.25 mM NaH_2PO_4 , 25 mM NaHCO_3 , 2 mM CaCl_2 , 1 mM MgCl_2 , 25 mM glucose |

2.6.1 Acute hippocampal slices

Acute hippocampal slices were prepared with the help of Jeet Singh.

10 weeks old Wistar rats were anesthetized with isoflurane. After decapitation the brain was rapidly removed and immersed in oxygenated ice-cold ACSF. Hippocampi were isolated and transverse slices (350 μm) were produced using a Vibratome (The Vibratome Company). After recovery in ACSF (32 $^\circ\text{C}$) the slices were treated with Hya (500 u / ml) for 3 h. Three slices were triturated with a pipette in 90 μl of cell lysis buffer supplemented with Complete Protease Inhibitor Cocktail (Roche), PhosSTOP Phosphatase Inhibitor Cocktail (Roche) and 1 % NaVO_3 before adding 4x SDS sample buffer. Samples were stored at -80 $^\circ\text{C}$ until they were used for SDS page.

2.6.2 SDS-Page using Laemmli system

Proteins were separated using a one-dimensional sodium dodecyl sulfate polyacrylamide gel electrophoresis (SDS-PAGE) under fully denaturing conditions. Gradient gels were used in which the separating gel had an

acrylamide concentration of 5 % on top and 20 % at the bottom. The stacking gel was covering the separating gel to focus the proteins. Gels were placed in an electrophoresis chamber (Mighty Small II MINI Vertical Electrophoresis Unit, Hoefer) and filled with electrophoresis buffer. Protein samples were diluted with 4x SDS buffer and boiled at 95 °C for 5 min, centrifuged with full speed for 10 min to load the supernatants on the gel. The gel run was performed with constant 8 mA within the stacking gel and 10 mA during the separation phase. After SDS-page gels were either used for Western Blotting or they were stained with Coomassie solution for 30 min. By incubation with destaining solution for 2 h or overnight the proteins get visible. For quantification the gels were scanned by Odyssey Infrared Imaging System (LI-COR Bioscience).

2.6.3 Western Blotting

Proteins were electrotransferred from polyacrylamide gels to Millipore Immobilon-FL transfer membranes (polyvinylidene fluoride membrane; PVDF). The membrane was activated in methanol for 30 sec. The transfer was performed in a Western Blot chamber (Mighty Small Transfer Tank, Hoefer) filled with Blotting buffer at 4 °C for 1.45 h with 200 mA. After the transfer the membrane was rinsed again with methanol and air dried.

2.6.4 Immunoblot detection

The PVDF membrane was blocked in 5 % BSA containing TBS-T for 30 min at RT. Primary antibodies were diluted in 2 % BSA containing TBS-T and probed for 90 min at RT or overnight at 4 °C. After three times washing with TBS-T secondary antibodies diluted in TBS-T were incubated for 45 min at RT. After further washing steps with TBS-T the final washing needs to be done with TBS, since Tween-20 interferes with the upcoming scanning procedure. Immunodetection was performed with an Odyssey Infrared Imaging Scanner (LI-COR Bioscience).

2.6.5 Purification of eukaryotic expressed fusion proteins

Table 17: Buffer for protein purification

| Buffer | Composition / Company |
|--------------------|---|
| Binding buffer 10x | 200 mM sodium phosphate, 5 M NaCl, 200 mM imidazole, 0.45 µm filtered |
| Binding buffer 1x | 20 mM sodium phosphate, 0.5 M NaCl, 20 mM imidazole, pH 7.4, 0.45 µm filtered |
| Elution buffer 1x | 20 mM sodium phosphate, 0.5 M NaCl, 0.5 M imidazole, pH 7.4, 0.45 µm filtered |

To investigate the functions of extracellular shed proteins I produced fusion proteins, which can be purified by affinity chromatography. The aim was to get purified proteins of the following constructs: Cst1Clea, Cst1Cad, Cst1LamG, Cst3Clea (see Table 3). All proteins produced by these constructs are secreted into the cell medium. The procedure was the same for all constructs, since they all contain a myc / his tag which was used for purification.

As an expression system eukaryotic cells (HEK293-T cells) were chosen because all proteins needed posttranslational modifications such as N- or O-glycosylation that can only be produced in eukaryotic cells. Therefore HEK293-T cells were transfected with one of the constructs. After 48 h of protein expression cell medium was collected and fresh medium was added. After further 12 h the cell medium was collected again. Combined media were centrifuged to remove remaining cells or cell debris.

The ÄKTAprime™Plus system (GE Healthcare) with the preinstalled “Histidine-tagged protein purification, gradient elution” program was used to purify overexpressed proteins. HisTrap FF columns (GE Healthcare) were used, which are packed with precharged Ni²⁺ Sepharose 6 for preparative purification of histidine-tagged recombinant proteins by immobilized metal ion affinity chromatography (IMAC). The procedure was fully automatic, controlled and

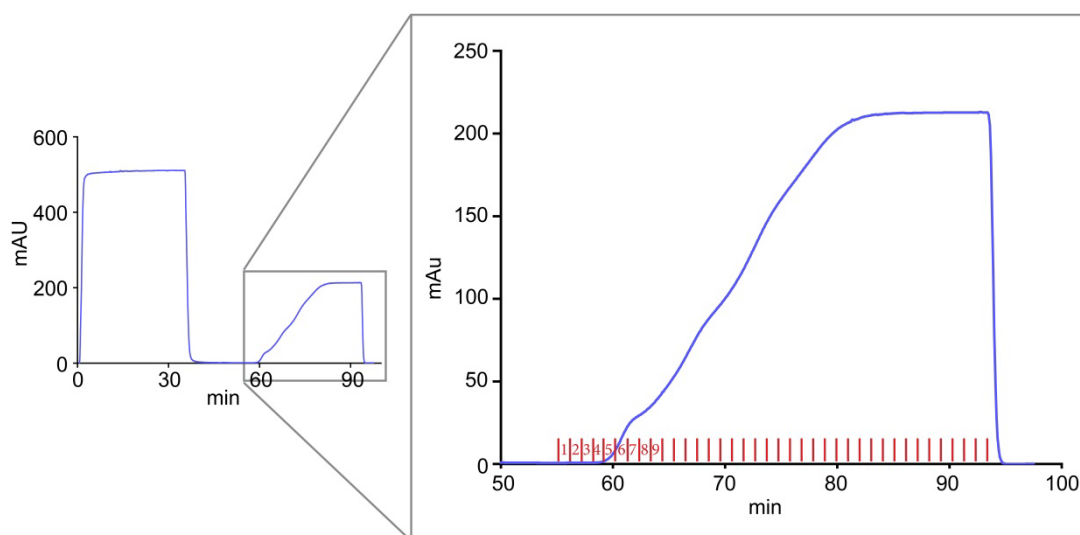


Figure 3: Plot of the UV absorption (A280 nm) during protein purification

Throughout the whole purification procedure, the fluid that exits the column is controlled for its UV absorption.

On the right side, the elution phase is enlarged with 37 fractions á 1 ml (first 9 are indicated). Surrounding fraction 7 a shoulder in the UV absorption is detectable, which represents the eluted fusion protein.

visualized by the Software PrimeView 5.31 (GE Healthcare). Right after the column exit, fluids are tested for their potential to absorb UV 280nm (Figure 3), which provides information about the protein content in the fluid.

Collected cell media were diluted with 10x binding buffer to adjust the sample to composition of 1x binding buffer. The pH was set to 7.4 and the solution was filled in a super-loop of appropriate size (150 ml). After equilibration of the column with 1x binding buffer the Sample was loaded on the column and subsequently washed with 1x binding buffer. Figure 3 shows the plot of the 280 nm absorption (mAU) acquired during the purification of Cst1Clea as an example. The curve increases during the loading phase of the column, due to the large amount of proteins in the flow-through, originating from the cell culture medium. During the washing step the absorption decreases again. The gradient elution increases the concentration of imidazole containing elution buffer continuously over 20 min to 100 %. Imidazole replaces and thus elutes the protein of the column. Imidazole itself shows absorption at 280 nm therefore the absorption rises with increasing imidazole concentration. During elution fractions of 1 ml are collected. Elution is followed by a washing step with 100 % elution buffer. The fractions which include the desired fusion protein can be detected by a peak within the absorption plot, which starts in the plotted example in fraction 7 (Figure 3). Samples of those fractions were separated by SDS-Page and the gels were stained with Coomassie solution. The positive fractions needed to be dialyzed since they contain imidazol. Dialysis tubes with a filtering rate of 3.5 and a Molecular Weight Cut Off (MWCO) of 4.000 – 6.000 D were used to transfer the purified proteins into 1x PBS. Fractions were filled into the dialysis tubes and then incubated in 1x PBS for 3 - 4 hours in which PBS was always exchanged. Protein concentration was measured with NanoDrop1000 (peQLab). Afterwards proteins were stored at -80 °C.

2.7 Electrophysiology

Table 18: Buffers and drugs for electrophysiology

| Buffer | Composition / Company |
|----------------------------------|--|
| Extracellular solution | 145 mM NaCl, 5 mM KCl, 0 mM MgCl ₂ , 1 mM / 2 mM CaCl ₂ , 10 mM HEPES, 10 mM D-glucose, 15 μM Glycine pH 7.4 |
| Intracellular / Pipette solution | 140 mM potassium gluconate, 2 mM MgCl ₂ , 4 mM NaATP, 0.1 mM EGTA, 10 mM HEPES, 10 mM phosphocreatine, 0.4 mM GTP, 10 mM QX-314 pH 7.25 |
| CNQX | 5 μM (Tocris) |
| Bicuculline (BCC) | 10 μM (Tocris) |
| APV | 10 μM (Tocris) |
| Ifenprodil (Ifen) | 3 μM (Tocris) |
| Tetrodotoxin (TTX) | 0.5 μM (Tocris) |

For electrophysiological recordings dissociated hippocampal cultures (DIV 21-26), grown on Ø 18 mm coverslips were used. Coverslips were fixed in an imaging-chamber (Low Profile Open Bath Chamber, Warner Instruments) and continuously perfused with warmed extracellular solution containing the desired drugs if needed (Ismatec™ Reglo tubing pump). Patch pipettes were prepared of borosilicate glass capillaries (major diameter: 1.5 mm, inner diameter: 0.86 mm, length: 100 mm) using a Flaming/Brown Micropipette Puller (Model P-97, Sutter Instruments). The resistance of the pipettes fluctuated between 2.5 – 5 MΩ. Under visual control using an inverse microscope (Zeiss Axio Observer A1) with a 63x objective the pipette was placed onto the cells working with a micromanipulator (SM-5 Manipulator, Luigs & Neumann). To measure synaptic currents a computer controlled patch clamp amplifier was used (HEKA EPC10, Software: PatchMaster 2.11 HEKA). The serial resistances of the patch pipettes were allowed to fluctuate between 5 and 11 MΩ.

2.7.1 Miniature Excitatory Synaptic Currents (mEPSCs)

mEPSCs were measured during my diploma thesis. The extracellular Solution contained TTX to block action potentials, BCC to inhibit GABA_A receptors and 2 mM CaCl₂ to increase the release probability. The holding potential was clamped at -40 mV. To analyze the NMDA receptor component of the mEPSCs APV was applied and currents were compared to control currents.

2.7.2 Spontaneous Excitatory Synaptic Currents (sEPSCs)

In order to isolate NMDA receptor mediated synaptic currents I added the AMPA receptor blocking agent CNQX to the extracellular solution. Ca²⁺

concentration was reduced to 1 mM to decrease the release probability. The holding potential was clamped at -70 mV. In order to verify that measured currents are completely driven by NMDA receptor APV was added. Application of ifenprodil shows the amount of GluN2B-NMDA receptor-mediated currents.

2.8 Wnt signaling reporter systems

To investigate the influence of Cst-1 on canonical wnt signaling two reporter systems were used. The first one is based on a GFP expression (7-TGC) and the other one on luciferase expression (Super 8x TOP/FOPFlash) if canonical wnt signaling is active. In both cases the reporter gene is under control of the Tcf/Lef binding site that respond to β -catenin-mediated activation. For further information on the constructs see section 2.3.1 and the listed publications.

2.8.1 Reportersystem based on GFP expression

HEK293-T cells were plated on \varnothing 12 mm coated coverslips and transfected with the 7-TGC construct which is a reporter system for canonical wnt signaling based on GFP expression. In a first set of experiments additionally to the transfection with 7-TGC, cells were co-transfected with either cDNA for wnt-8a or Cst-1. Then cells were incubated for 48 h. Since it was not possible to estimate the concentration of the desired protein in the extracellular space I continued to work with purified proteins like Cst1Clea and wnt-3a to add specific amounts (which are stated in the results) for better comparability. Cells were incubated for 6 h. In both experimental approaches cells were fixed, stained with DAPI to visualize the nuclei and without any further immunostaining mounted with Mowiol. The 7-TGC construct leads to a constitutively expressed mCherry protein to localize the transfected cells. Both mCherry and GFP signals were acquired. The intensity of the GFP signal was later normalized to the intensity of mCherry because it reflects the expression level of the construct in each cell.

2.8.2 Reporter system based on luciferase expression

HEK293-T cells were transfected in flasks with either the Super 8x TOPFlash or Super8x FOPFlash construct. The Super 8x TOPFlash construct reports the activity of the canonical wnt signaling by expressing luciferase under control of the Tcf/Lef promotor. The Super8x FOPFlash construct contains a mutated version of the Tcf/Lef promotor and serves as a control. After approximately 12 h

the cells were plated in a 96 well plate, containing 100 μ l per well. Another 12 h later purified proteins such as Cst1Clea, Cst1Cad and wnt-3a were added to the HEK293-T cells expressing the reporter system and incubated for 6 h. The detection of luciferase expression was performed with the ONE-Glo™ Luciferase Assay System (Promega). It is important to work at RT since luciferase has a temperature optimum of 22.5 °C (Ueda et al., 1994). Therefore the cells were cooled down to RT for 30 min after incubation at 37 °C and the ONE-Glo reaction buffer was thawed at RT. 100 μ l ONE-Glo reaction buffer were added in each well and kept for 3 min at RT. Subsequently luminescence was measured with GENios (TECAN). The luminescence values of the Super 8x TOPFlash transfected cells were normalized to the values of corresponding cells transfected with Super 8x FOPFlash, which contains a mutated version of the Tcf/Lef binding site.

3 Results

The results of my thesis consist of two parts. The first part describes the effect of an ECM removal on surface expression of GluN2B-NMDA receptors, which was the main part of my thesis. The second part contains the results of a side project that was started within the last year of my PhD. This part is about a protein called calyntenin and its role in cellular functions. This project is in a preliminary state, but provides hints for future research directions.

Part I: The effect of the ECM on the expression and dynamics of GluN2B-NMDA receptors

The ECM of the brain is formed during the first postnatal weeks and coincides with a switch in brain plasticity and in NMDA-receptor subunit composition. NMDA receptors are essential modulators for synaptic plasticity, thus I was interested in whether these two developmental changes are in a causal relationship. In order to investigate the role of ECM on the composition of NMDA receptors, I digested the ECM by making use of the glycosidase hyaluronidase (Hya) as published in (Frischknecht et al., 2009). This enzyme dissolves the hyaluronic acid backbone of the ECM and destroys its dense net-like structure surrounding the cells (see Figure 8). This work is based on preliminary data that I obtained during my diploma thesis. For a comprehensive description I will refer to some data from my diploma thesis, which will be clearly marked as such.

3.1 Electrophysiological recordings after ECM removal

To analyze basal synaptic activity measurements of miniature excitatory postsynaptic currents (mEPSCs) are an established method. During my diploma thesis I measured mEPSCs in dissociated hippocampal cultures (DIV 21-26) before and after overnight Hya treatment. mEPSCs were analyzed for their amplitude, frequency, rise- and decay-time. None of these characteristics were affected by the ECM digestion, which is in line with previously published data from our laboratory (Frischknecht et al., 2009). Further blockage of NMDA receptors by (2R)-amino-5-phosphonovaleric acid (APV) did not show any significant differences in all analyzed parameters. I concluded that under tetrodotoxin (TTX) treatment the majority of activated channels are AMPA

receptors in our neuronal cultures. Due to that it was essential to develop a protocol to measure isolated NMDA receptor-mediated synaptic currents.

3.1.1 Isolation of NMDA receptor-mediated synaptic currents in dissociated cultures

Using TTX, I was not able to isolate NMDA receptor-dependent currents, which might be due to insufficient activation under these conditions. Therefore I performed measurements without TTX and made use of the spontaneous, intrinsic activity present in these cultures. Spontaneous excitatory synaptic currents (sEPSCs) driven by AMPA and NMDA receptors showed clearly detectable single peaks in the current traces, which are above noise (filled stars, Figure 4A). Figure 4C shows the same current trace as Figure 4A but with a lower magnification. There are periods of high frequent events with high amplitudes

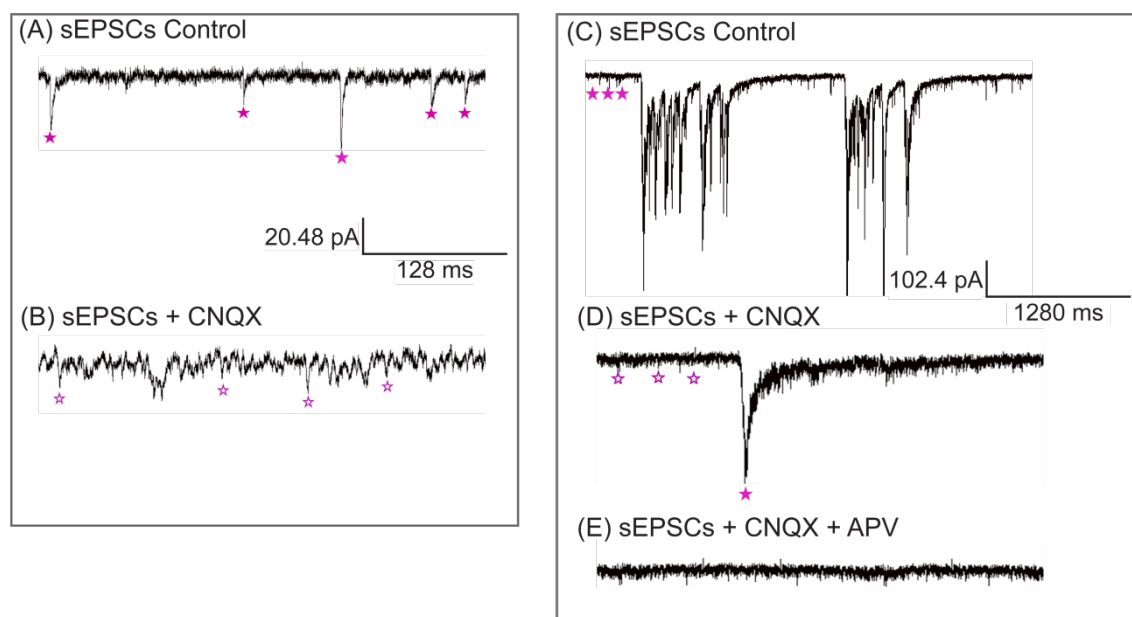


Figure 4: Isolation of NMDA receptor mediated currents

(A) sEPSCs under control conditions, driven by AMPARs and NMDA receptors. Single peaks (filled stars) are clearly above noise.

(B) sEPSCs under CNQX treatment, driven only by NMDA receptors. The amplitudes of potential peaks are not clearly separable from the noise of the setup. Potential peaks are marked with blank stars.

(C) sEPSCs under control conditions, driven by AMPARs and NMDA receptors. Note that the trace is displayed with lower magnification as in (A) and (B) (see scale bar). Besides smooth baseline, periods of high, burst-like activity are visible.

(D) sEPSCs under CNQX treatment, driven only by NMDA receptors. Note that the trace is displayed with lower magnification as in (A) and (B) (see scale bar). Single peaks (filled stars) with large amplitudes are detectable.

(E) sEPSCs under CNQX + APV treatment. Single peaks that were detected in (D) disappeared, which proves that those currents were driven by NMDA receptors

that varied between ~ 400 - 1600 pA and lasted for ~ 1500 ms. In between these burst-like events a “smooth” baseline is present, which includes the single events described in Figure 4A (filled stars). To separate NMDA receptor mediated synaptic currents the competitive inhibitor of AMPA receptors 6-cyano-7-nitroquinoxaline-2,3-dione (CNQX) was added. Under high magnification the clearly detectable events from Figure 4A disappeared. Amplitudes of potential peaks were indistinguishable from the noise of the setup (blank stars, Figure 4B). These events could not be analyzed. Figure 4D shows this current trace with lower magnification to visualize again periods of high current amplitudes. Application of CNQX shrunk the high frequency periods observed under control conditions (Figure 4C) to individual, clearly detectable peaks (Figure 4D). These peaks disappeared after application of APV which demonstrates that these currents were exclusively driven by NMDA receptors (Figure 4E). With this protocol it was possible to measure isolated NMDA mediated synaptic currents before and after Hya treatment.

3.1.2 Increased NMDA receptor-mediated sEPSCs after ECM removal

I measured NMDA mediated sEPSCs in dissociated hippocampal cultures (DIV 21-26), as described in 3.1.1. Neurons were treated with Hya overnight. I found no obvious changes in the current traces before or after Hya treatment (Figure 5A). The amplitudes of single peaks were quantified and no significant difference between the two groups was observed (Figure 5B). To further separate the currents into GluN2A- and GluN2B-NMDA receptor-mediated portions ifenprodil (Ifen) was used to selectively block GluN2B-NMDA receptors. Again no difference was detectable in the amplitudes (Figure 5B), which are obviously driven by GluN2A-NMDA receptors. Further information about involved receptors is contained in the total charge transfer, which is transferred during one single event. Especially the decay-time is determined by the composition of activated receptors. Before analyzing the total charge transfer, the amplitudes were normalized to accentuate differences within the decay-times of the peaks, which represent the subunit composition of NMDA receptors. GluN2A-NMDA receptors have shorter decay-times compared to GluN2B-NMDA receptors and therefore, unlike the amplitude, the decay-time is dominated by the GluN2B-NMDA receptor. The total charge transfer was calculated by the integral of the mean peak per cell. I found a 38 % increase in total charge transfer after ECM digestion (Figure 5C), which was erased after application of Ifen that blocks

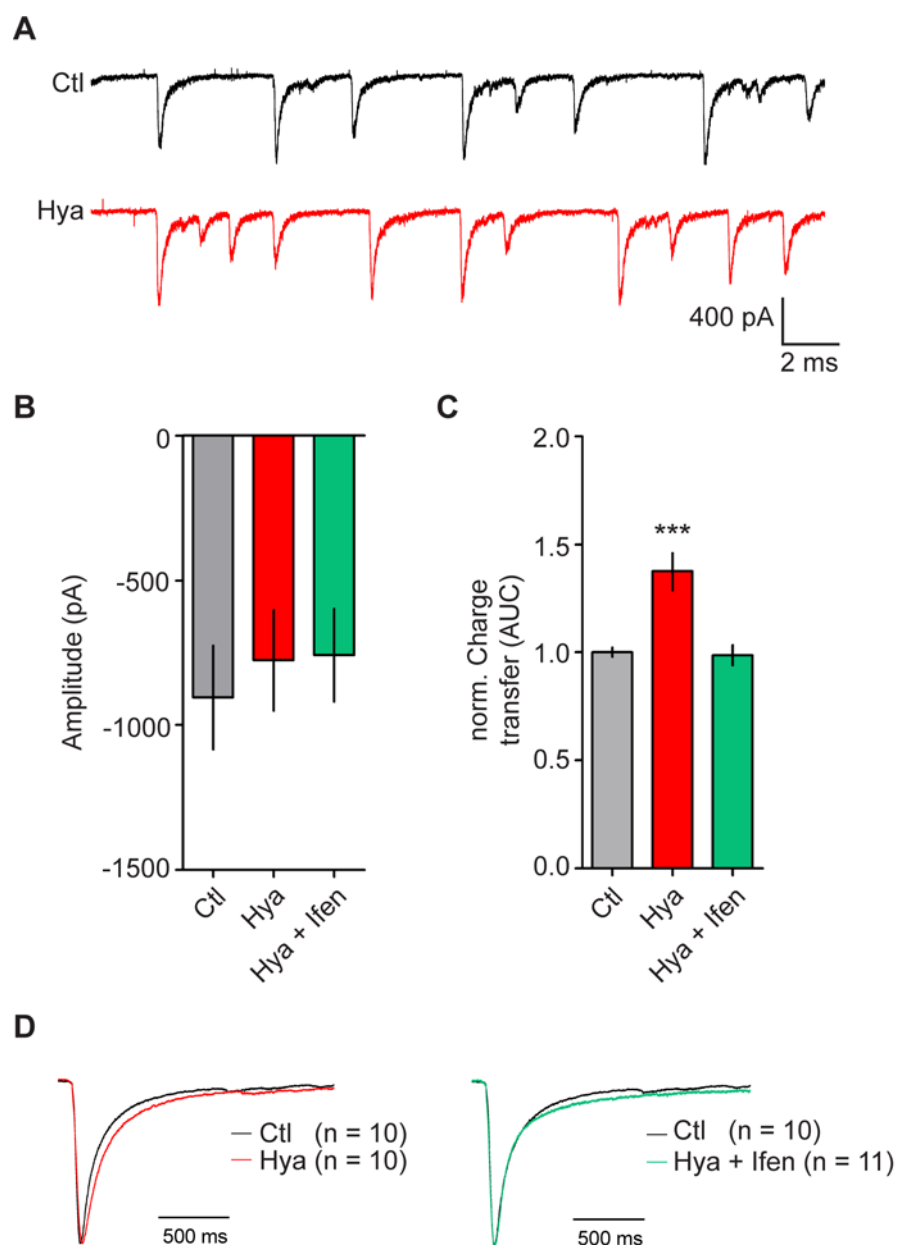


Figure 5: ECM removal enhances GluN2B-NMDA receptor-mediated synaptic currents

(A) Example traces of NMDA receptor-mediated sEPSCs before and after Hya treatment in dissociated hippocampal cultures (DIV21-26).

(B) Amplitudes of single peaks showed no significant differences to Ctl neither after Hya treatment nor after Hya plus Ifen treatment. (Ctl, -905.5 ± 179.4 , $n = 10$; Hya -776.2 ± 174.8 , $n = 10$; Hya + Ifen, -758.2 ± 161.7 , $n = 11$; average \pm SEM; One-way ANOVA, $P = 0.7991$).

(C) Quantification of the area under the curve (AUC) which represents the total charge transfer. Peaks of the recorded sEPSCs were normalized by their amplitudes before AUC calculation. It revealed a bigger charge transfer after ECM removal that decreased to Ctl levels after blocking GluN2B-NMDA receptors with Ifen. (Ctl, 1 ± 0.02 , $n = 10$; Hya, 1.38 ± 0.09 , $n = 10$; Hya + Ifen, 0.98 ± 0.05 , $n = 11$; average \pm SEM; One-way ANOVA, $P < 0.0001$, Dunnett's Multiple Comparison Test, $*** P < 0.05$).

(D) Average of single peaks before and after Hya treatment and after Ifen application. Normalization of the amplitude illustrates the increased decay-time after Hya treatment (red line) in comparison to Ctl (black line). This can be restored after Ifen application (green line). Ctl traces are identical.

GluN2B-NMDA receptor-mediated currents. After the block of GluN2B-NMDA receptors the charge transfer was indistinguishable from control (Ctl) conditions. Further comparison of mean traces before (black) and after Hya treatment (red) showed a clear increase in the decay-time of the currents after ECM removal, which could be blocked by application of Ifen (green) (Figure 5D).

This clearly indicates that Hya treatment increases GluN2B-NMDA receptor-mediated synaptic currents. Whether this increase is due to altered gene expression, trafficking or receptor modification was subject to following experiments.

3.2 Unaffected GluN2B protein level after ECM removal

Increased GluN2B-NMDA receptor-mediated synaptic currents may be due to an increased GluN2B protein level. During my diploma thesis I showed, using immunocytochemistry experiments on permeabilized dissociated cortical neurons (DIV 21-24), that the total level of GluN2B proteins is not affected by the Hya treatment, neither in dendrites nor at synapses.

Here I investigated the GluN2B protein level by biochemical methods. Therefore western blot (WB) experiments of dissociated cortical neurons were performed to compare Hya and untreated cells. 6 well plates of cortical cultures were treated

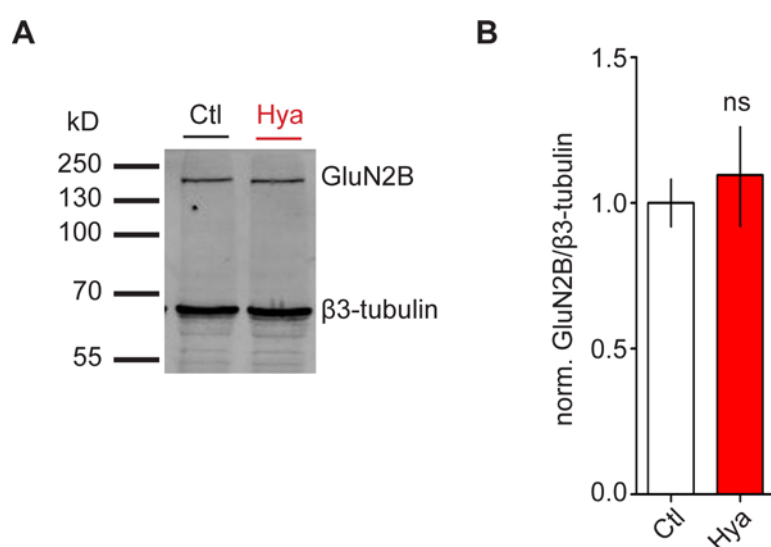


Figure 6: Total GluN2B protein level stays unaffected after ECM removal

(A) Quantitative WB of cortical cultures lysates (DIV 21) pre-treated with Hya over night. Western blot was incubated with antibodies against GluN2B and β 3-tubulin.

(B) Quantification of WB showed no significant change in GluN2B immunoreactivity after normalizing to the loading control β 3-tubulin (Ctl 1 ± 0.08 , $n=9$; Hya 1.1 ± 0.18 , average \pm SEM; $n=9$, $P = 0.6282$, unpaired t-test).

with Hya overnight and subsequently lysed in 1x SDS buffer. Probes were subjected to SDS Page and WB and the membranes were probed with antibodies against GluN2B and β 3-tubulin as a loading control (Figure 6A). There was no difference in the total expression level of GluN2B between treated and untreated cells (Figure 6B). Taken together, these results suggest that ECM removal results in increased GluN2B-NMDA receptor mediated charge transfer without affecting the total amount of GluN2B.

3.3 GluN2B surface expression is increased after ECM removal in a β 1-integrin-dependent manner

Since the protein level of GluN2B is not affected by the ECM removal I followed the line of an altered balance of intracellular and surface expressed GluN2B-NMDA receptors. During my diploma thesis I obtained preliminary data regarding the surface expression of GluN2B-NMDA receptors after ECM removal using immunocytochemistry. In order to verify that enhanced GluN2B-NMDA receptor-mediated currents are due to an increased abundance of these receptors at the cell surface, immunocytochemistry experiments were performed on living, non-permeabilized hippocampal neurons (DIV 21-24). Surface GluN2B were labeled with an antibody raised against their extracellular N-terminus. Subsequently cells were fixed, permeabilized and synapses were labeled with an antibody against the postsynaptic protein PSD-95 (Figure 7A). Fluorescence intensity analyzes revealed an increase of about 25 % in surface expressed synaptic GluN2B after Hya treatment (Figure 7B). Measuring surface expression of GluN2B on whole dendrites, using a Map-2 mask, exhibited an increase of about 78 % in surface GluN2B after ECM removal (Figure 7C). This indicates that increased surface expression of GluN2B is not synapse specific but affects also the extrasynaptic population of GluN2B-NMDA receptors. These data demonstrate that the increased GluN2B-NMDA receptor mediated synaptic currents after ECM removal are due to an increased surface abundance of these receptors.

Next I wondered about signaling mechanisms that sense changes in the ECM and trigger molecular changes at the synapse like altered receptor expression. Most promising candidates are integrins, which are known to interact with several ECM molecules and have been reported to modulate NMDA receptor abundance at the neuronal cell surface (Lin et al., 2003, Bernard-Trifilo et al., 2005). Further, chondroitin sulfates within the ECM have been suggested to inhibit integrin

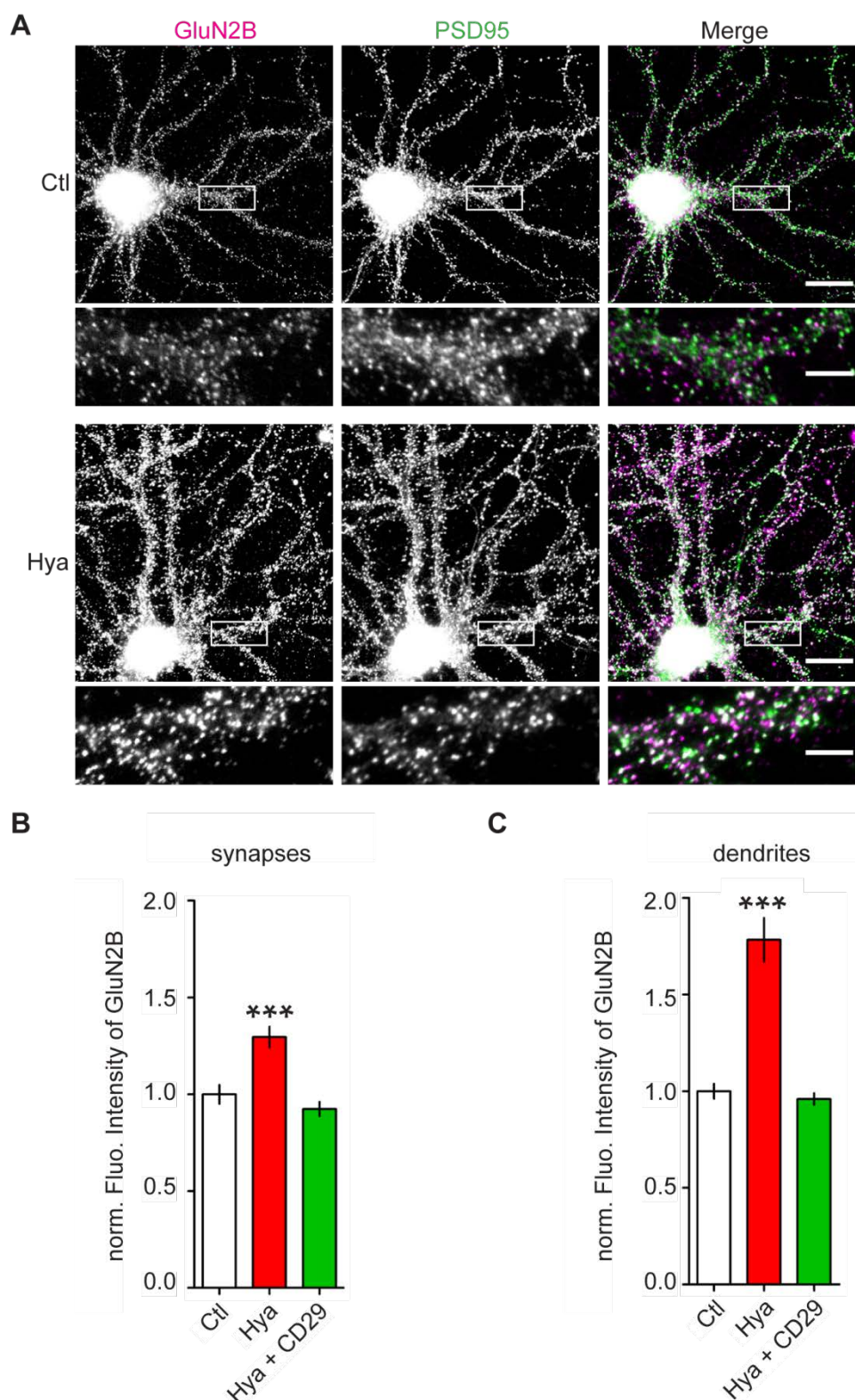


Figure 7: ECM removal increases surface expression of GluN2B in a β 1-integrin dependent manner

(A) Dissociated hippocampal cultures (DIV 21-24) were treated with Hya over night and stained against surface GluN2B (nonpermeabilised) (magenta) and the synaptic marker PSD-95 (permeabilised) (green). GluN2B intensities at the synapses were quantified using ImageJ and OpenView (scalebars, 20 μ m, inset: 5 μ m).

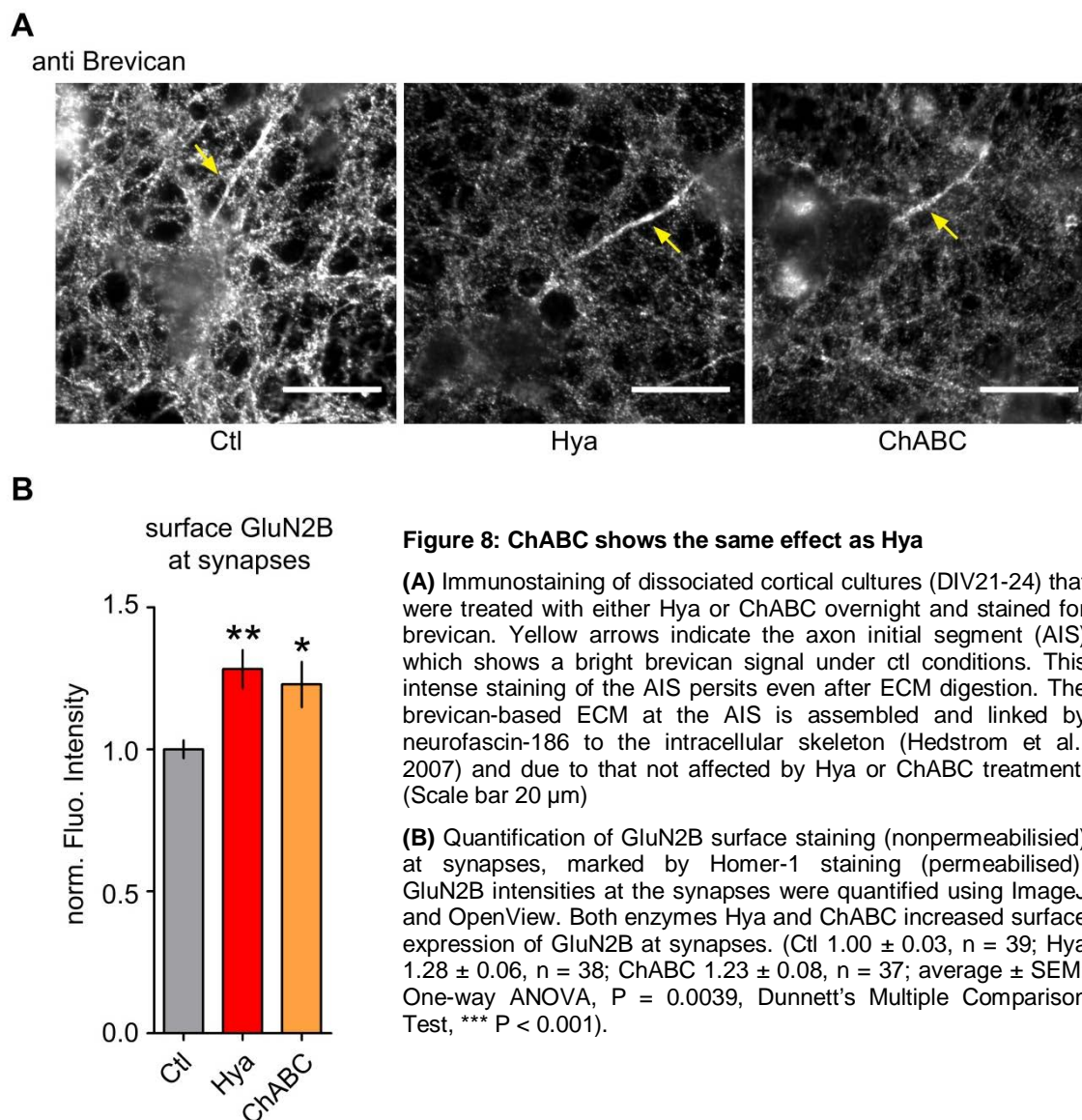
(B, C) The GluN2B surface expression at synapses and dendrites increased after ECM degradation and could be restored by simultaneous application of the β 1-integrin function-blocking antibody CD29 (**B**) Synapses: Ctl 1.0 ± 0.05 , $n = 68$; Hya 1.3 ± 0.05 , $n = 70$; Hya +CD29 0.7 ± 0.03 , $n = 51$; (**C**) Dendrites: Ctl 1.00 ± 0.04 , $n = 36$; Hya 1.78 ± 0.11 , $n = 35$; Hya+CD29 0.96 ± 0.03 , $n = 34$; average \pm SEM; One-way ANOVA, $P < 0.0001$, Dunnett's Multiple Comparison Test, *** $P < 0.001$).

signaling (Tan et al., 2011). I tested whether the increased surface expression of GluN2B after Hya treatment could be prevented by blockage of integrin signaling. For this purpose I added in parallel to Hya a function-blocking β 1-integrin antibody (CD29) to neuronal cultures. On the next day GluN2B surface staining was performed as described above. In both, synapses and dendrites the observed increased GluN2B surface expression was abolished after application of CD29 (Figure 7B, C). This suggests that removal of the ECM via Hya treatment increases β 1-integrin signaling, which in turn regulates surface abundance of GluN2B-NMDA receptors.

3.4 ChABC treatment increases surface expression of GluN2B-NMDA receptors

Both ChABC and Hya are ECM-degrading enzymes cleaving glycosaminoglycan chains. Hya degrades preferentially hyaluronic acid whereas ChABC favors chondroitin sulfate chains. However, Hya has an intrinsic chondroitinase activity while ChABC endows hyaluronidase activity. Many studies concerning the influence of the ECM on plasticity or integrin function used ChABC in their experiments (Orlando et al., 2012, de Vivo et al., 2013). In order to better compare my data with other work in the field and to exclude unspecific effects caused by Hya I repeated the experiments using ChABC.

In a parallel approach using dissociated cortical cultures (DIV 21-24) I treated cells either with Hya or ChABC overnight and stained for surface expressed GluN2B receptors. For quantification I focused on synaptically expressed receptors by co-staining with Homer-1. Figure 8A shows the immunostaining for brevicin under control, Hya and ChABC conditions. Brevican immunofluorescence was brighter and more compact under control compared to the ECM degrading conditions. What is more important, the brevicin immunostaining was comparable under Hya and ChABC treatment. Quantification of surface expressed GluN2B-NMDA receptors revealed that Hya as well as ChABC treatment increased GluN2B surface abundance by 28 % and 23 %, respectively (Figure 8B), which demonstrates that the increased surface expression of GluN2B is no artificial effect of Hya treatment.



3.5 Hya treatment does not alter GluN2B expression in DIV 11 neurons

To verify that the observed effect of Hya treatment on the surface expression of GluN2B-NMDA receptors was due to the degradation of the hyaluronan-based matrix the analysis of surface expressed GluN2B after Hya was performed in DIV 11 cultures. Previous experiments were all performed in DIV 21-24 dissociated neuronal cultures because the hyaluronan-based ECM is fully developed at this age, whereas it is not yet established in younger neurons (John et al., 2006). Figure 9A shows comparative immunostaining against brevicin before and after Hya treatment in DIV 11 and DIV 21 neurons. Neurons at DIV 11 do not show the intense brevicin staining as found in DIV 21 neurons. Hence Hya treatment

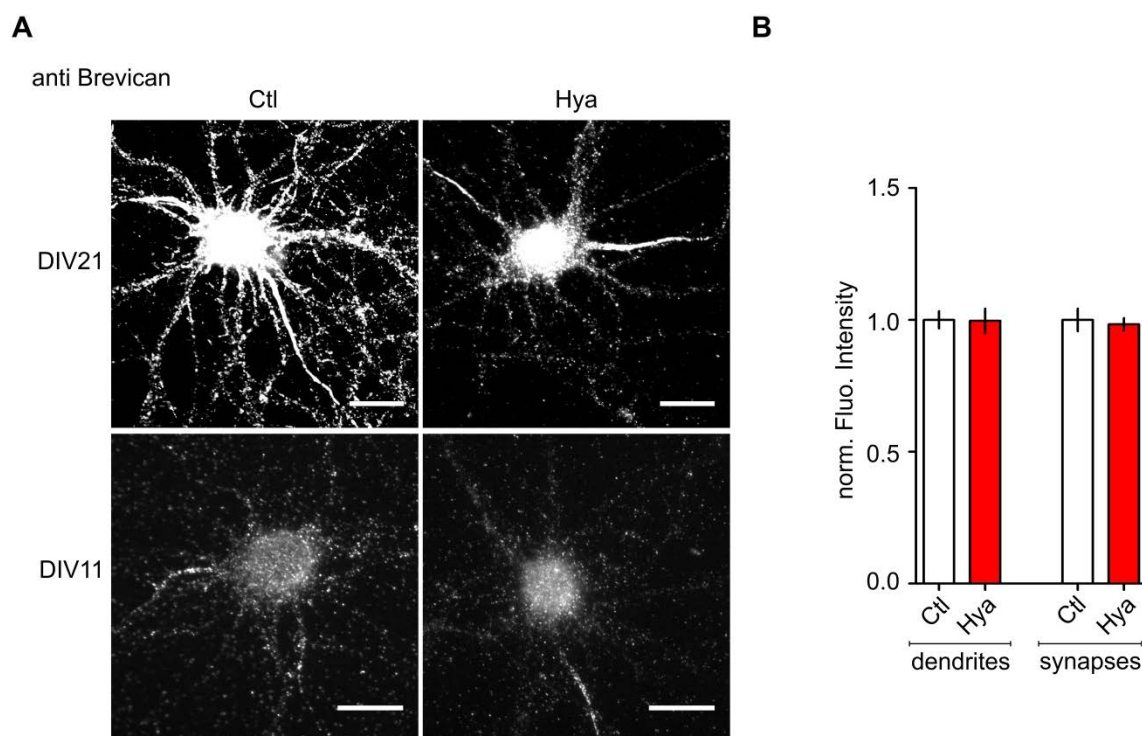


Figure 9: Surface expression of GluN2B-NMDA receptors was unaffected by Hya treatment in DIV 11 neurons

(A) Primary cortical cultures (DIV 21 or DIV 11) were treated with Hya over night and stained against brevicane. At DIV 21 a well-developed ECM surrounds neurons under Ctl conditions. After Hya treatment the net-like structure is abolished, remaining just at the axon initial segment. In DIV 11 neurons no developed ECM can be visualized. (Scalebars, 20 μ m)

(B) Hya treatment in DIV 11 neurons did not affect the surface expression of GluN2B neither at dendrites (Map-2 mask) nor at synapses (PSD-95 mask). (Synapses: Ctl 1.0 ± 0.04 , $n = 25$; Hya 0.98 ± 0.02 , $n = 24$; average \pm SE, unpaired t-test, $P = 0.7341$; Dendrites: Ctl 1.00 ± 0.03 , $n = 39$; Hya 0.99 ± 0.05 , $n = 40$; average \pm SEM; unpaired t-test, $P = 0.9488$)

showed much stronger effect in DIV 21 neurons compared to DIV 11 neurons. Figure 9B shows that Hya treatment did not affect the surface expression of GluN2B-NMDA receptors neither at dendrites nor at synapses. These data diminish the possibility of unspecific side effects of the enzyme that could cause the observed effect on GluN2B-NMDA receptors. It gives evidence that the rearrangement of the matrix after Hya manipulation indeed is responsible for the increased surface abundance of GluN2B.

3.6 ECM digestion increases phosphorylation of GluN2B and decreases its endocytosis

I have shown that ECM removal increased surface expression of GluN2B in a β 1-integrin-dependent manner. During my diploma thesis I developed a protocol to measure the amount of endocytosed receptors within a defined time window.

Indeed treatment with Hya diminished the endocytosis rate of GluN2B-NMDA receptors to 90% of control conditions. It was suggested that the endocytosis of GluN2B-NMDA receptors is regulated via phosphorylation of a tyrosin (Y1472) within the YEKL motif, which builds the binding site for the adaptor protein AP-2. If Y1472 is phosphorylated AP-2 cannot bind the subunit and the receptor is stabilized at the surface. Therefore I investigated whether the phosphorylation state of Y1472-GluN2B after ECM removal was altered.

In a first set of experiments high density cortical cultures (DIV 21) were treated with Hya overnight. On the next day cell lysates were prepared, separated by SDS page and blotted on PVDF membranes. By using an antibody against pY1472-GluN2B and an antibody against pan-GluN2B (Figure 10A) it was possible to analyze the ratio of pY1472-GluN2B to the entire population of GluN2B proteins. Figure 10A shows a WB of acute hippocampal slices to illustrate the signal of both antibodies against pan-GluN2B and pY1472-GluN2B. The signals at the predicted molecular weight are co-localizing (arrows) in both channels. As the other visible bands do not co-localize, they can be assumed to be unspecific. Figure 10A shows that the ratio of pY1472/GluN2B was increased after Hya treatment of dissociated cortical cultures. In a parallel approach, the

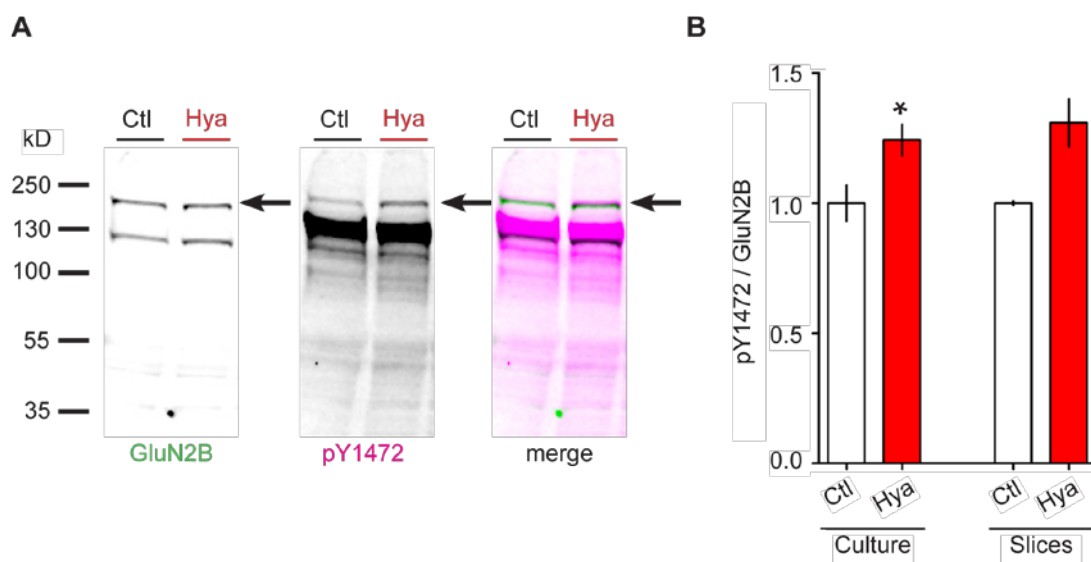


Figure 10: Hya increases phosphorylation of GluN2B and decreases its endocytosis

(A) Quantitative Western Blots of acute hippocampal cultures under Ctl and Hya conditions. Antibodies: α pGluN2B pY1472 (AP2 binding site) and α GluN2B

(B) Quantification of Western Blots of cortical cultures (DIV 21-24) and acute hippocampal cultures. In both cases the amount of phosphorylated GluN2B, normalized to the total amount of GluN2B, was increasing after Hya treatment (overnight for cultures; 3h for slices). (Culture: Ctl 1.00 ± 0.07 , $n = 5$; Hya 1.24 ± 0.06 , $n = 5$, average \pm SEM Unpaired t-test, * $P = 0.0296$; Slices Ctl 1.00 ± 0.01 , $n = 2$; Hya 1.31 ± 0.1 , $n = 2$, average \pm SEM Unpaired t-test, $P = 0.0794$)

phosphorylation state of GluN2B was analyzed in acute hippocampal slices from 10 weeks old rats. Acute hippocampal slices were treated with Hya for 3 h and subsequently triturated and lysed. Immunodetection of pY1472-GluN2B and GluN2B revealed higher ratio of phosphorylated vs. total GluN2B after ECM removal and thus confirmed the data obtained from dissociated cultures (Figure 10A).

3.7 Mobility of GluN2B-NMDA receptors

In previous studies from my laboratory it was shown that digestion of the ECM with Hya increases lateral mobility of GluA1-AMPA receptors (Frischknecht et al., 2009). In contrast GluN2A-NMDA receptors were found unaffected in their mobility, and GluN2B-NMDA receptors had not been tested. Since GluN2B-NMDA receptors have to move out of the synapse to be endocytosed and I found decreased endocytosis upon ECM removal, it is tempting to speculate that their lateral mobility is also affected by ECM removal.

Dissociated hippocampal cultures were co-transfected with GluN1 and GluN2B-subunit fused to an extracellular superecliptic pHluorin (SEP). SEP is a mutant of the *Aequorea* green fluorescent protein, which is pH-sensitive with a pK of 7.1 (Sankaranarayanan et al., 2000). Only surface-expressed GluN2B subunits are visible by the fluorescent signal of the SEP tag as the extracellular milieu has a pH of 7.4 that overlaps with the pH optimum of SEP. Intracellular vesicles are more acidic (pH 5.6), which quenches the fluorescence signal of SEP. Overexpression of SEP-GluN2B + GluN1 revealed both a diffuse expression within dendrites and accumulated expression at spots, most probably representing synapses (Figure 11B). The maximum projections of QD traces are presented in red in Figure 11B. Some QDs were sticking to the glass, as they did not co-localize with neurons, which were visualized in a differential interference contrast (DIC) image. The other QDs co-localized with the SEP-GluN2B signals.

Cells were treated with Hya either overnight or for 10 minutes. Frischknecht et al. showed that the lateral mobility of AMPA receptors is increased after an acute ECM digestion with Hya (Frischknecht et al., 2009). Based on this observation, I included an acute ECM digestion in the mobility experiments. The receptors were labeled with an antibody against GFP pre-coupled with a QD (Figure 11A). Mobility was acquired every 30 ms (33 Hz) for 30 sec. The trajectories were analyzed for the Instantaneous Diffusion Coefficient (D_{inst}) and the Mean Square

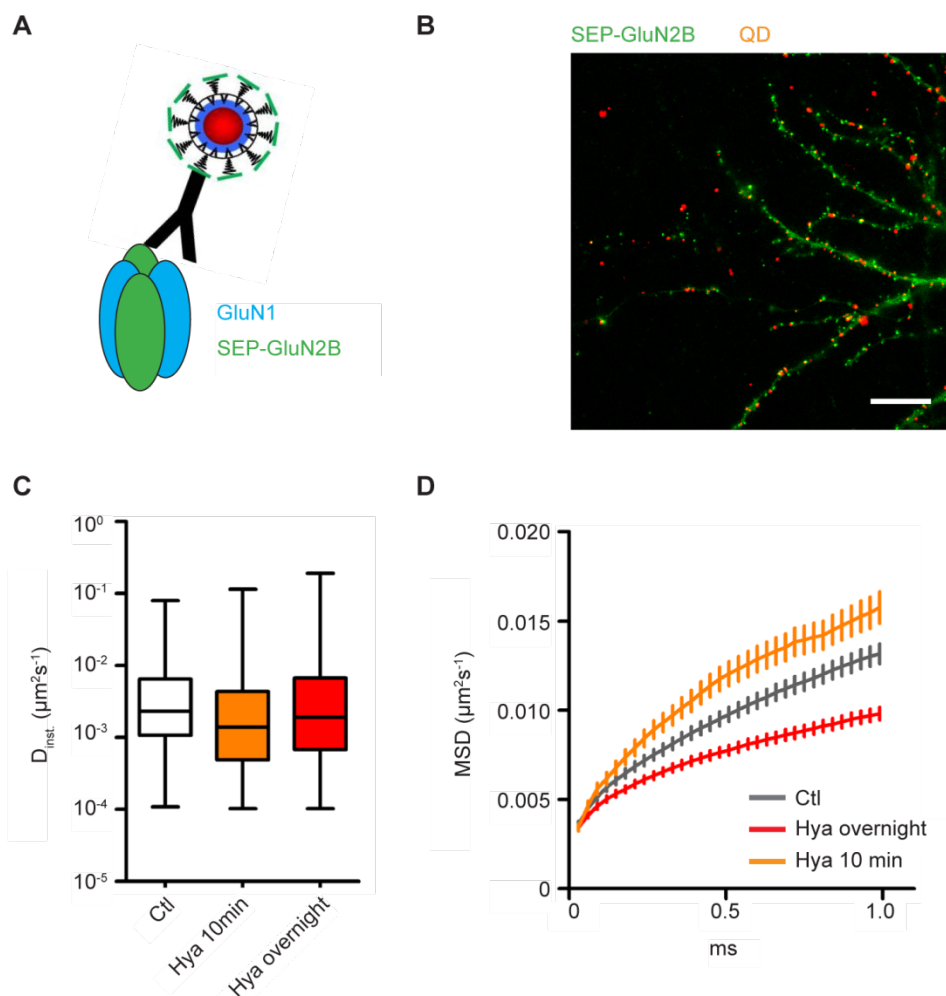


Figure 11: Prolonged ECM digestion increased confinement of GluN2B-NMDA receptors

(A) Schematic presentation of the overexpressed constructs: GluN1 wt and SEP-GluN2B. QDs were coupled to an antibody against GFP. Image is not drawn to scale.

(B) Dissociated hippocampal cultures (DIV 21-24) were treated with Hya either for 10 min or overnight. QDs were coupled with the GFP antibody and living cells were labeled. The maximum projection of QD trajectories is presented in red and GluN2B overexpressed channels are presented in green. (scalebar 20 μ m)

(C) The D_{inst} did not reveal any differences between controls or Hya treated cells. The velocity of GluN2B-NMDA receptors was not affected by ECM digestion. (Ctl 0.0023, Hya 10 min 0.2214, Hya overnight 0.0019)

(D) The mean square displacement (MSD) showed that GluN2B-NMDA receptors were less confined in their explored surface area after 10 min of ECM digestion. In contrast, a prolonged overnight Hya treatment increased their confinement.

Displacement (MSD) that represent the velocity and the confinement of the receptors, respectively. Quantification revealed that the D_{inst} was not affected by ECM digestion, meaning that the velocity of the receptors stayed the same (Figure 11C). The MSD illustrated that the receptors were less confined after 10 min of ECM removal, but in contrast more restricted after overnight incubation with Hya (Figure 11D). To sum up, after 10 min of Hya action the GluN2B-NMDA receptors explore a bigger area but are not increased in their surface

expression. After an overnight incubation with Hya GluN2B-NMDA receptors are more abundant at the surface and additionally more confined in their mobility.

Part II: Cellular effects of Calsyntenin-1's ectodomain

Cellular functions of the ectodomain of Cst-1 are poorly described. The only published data are coming from a *C. elegans* study in which Cst-1 mutants were shown to have an impaired associative learning performance, which could be rescued by expressing the ectodomain of Cst-1 (Hoerndli et al., 2009). Neither surface receptors nor signaling pathways are known, which lead to cellular changes upon Cst-1 shedding.

3.8 Purification of proteins

First, in order to perform cell biological assays and to test for biochemical interactions of Cst with potential ligands, I designed DNA constructs for different protein fragments of Cst-1 and Cst-3 and produced them in eukaryotic expression systems (all tagged with a his / myc tag). Figure 12A shows the scheme of the domain structure for two fusion protein constructs. The first one is Cst1Clea-myc/his (Cst1Clea), which starts at the N-terminus with two cadherin domains (CAD), followed by the laminin-G domain (LamG) and is terminated exactly upstream of the α -secretase cleavage site, which is substituted by the myc/his tag. A similar construct was produced for Cst-3. The second construct Cst1Cad-myc/his (Cst1Cad) contains only the two CAD domains fused to the myc/his tag. Proteins were expressed in HEK293-T cells and purified as described in section 2.6.5. Elution fractions that contain the purified proteins were visualized by coomassie brilliant blue stained SDS pages and WBs that were incubated with an anti his antibody (Figure 12 B-E). Additionally to the elution fractions, the unpurified HEK293-T cell supernatant (input) and the flow-through were loaded. In Figure 12 B, C the coomassie gel (B) and the WB (C) of Cst1Clea purification are shown. Cst1Clea has a calculated size of 94 kD without the signal peptide. Both the coomassie gel and the WB show a signal within the purification fractions at ~120 kD. This discrepancy in molecular weight is potentially due to posttranslational modifications and the intrinsic charge of the protein that influences its behavior in SDS page (Rath et al., 2009, Shi et al., 2012). Further the observed apparent molecular weight is in line with previous publications (Vogt

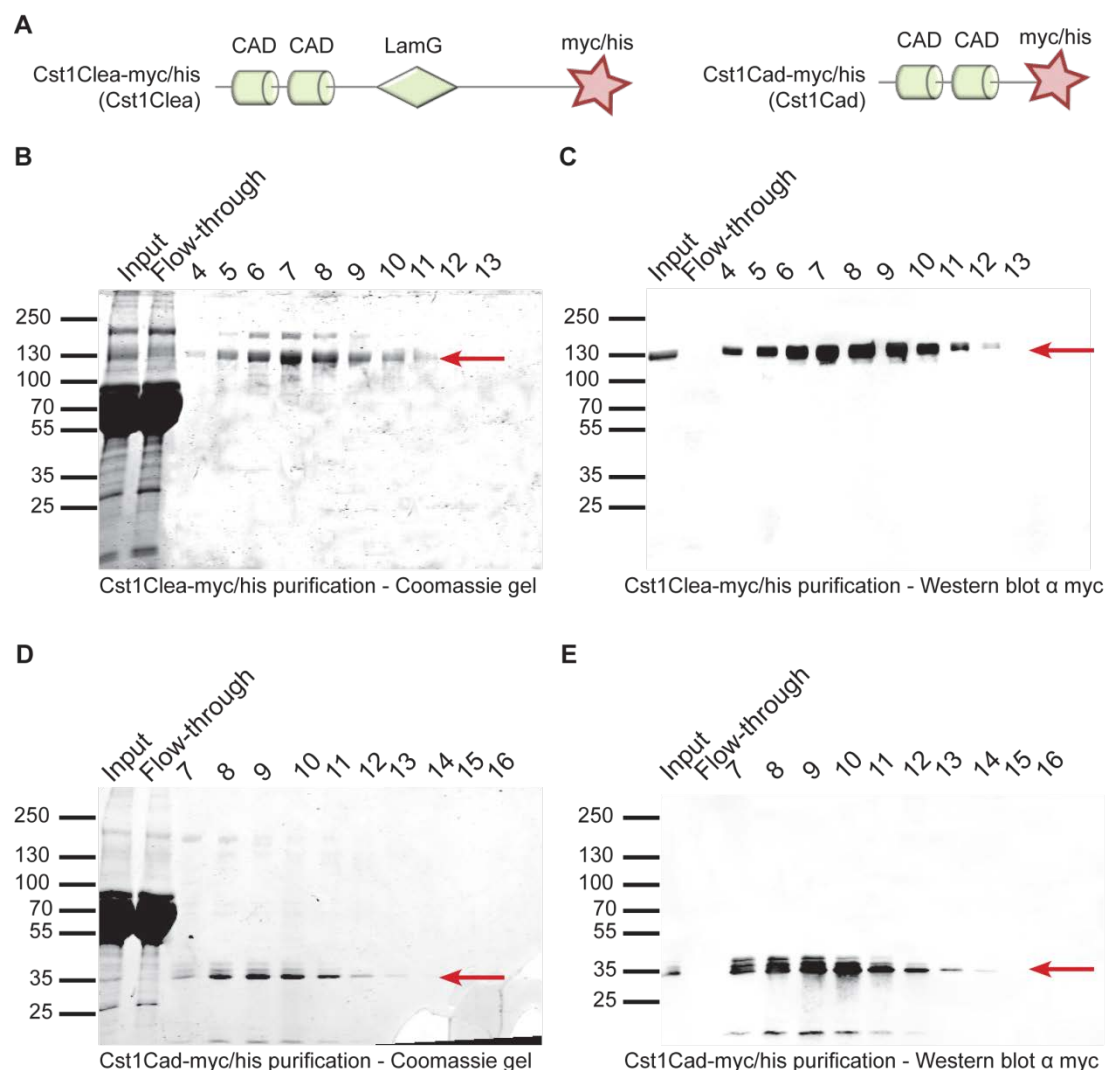


Figure 12: Purification of fusion proteins

(A) Scheme of fusion protein constructs. Both constructs are tagged with a myc/his tag. Cst1Clea contains two CAD domains and one LamG domain, whereas Cst1Cad lacks the LamG domain.

(C, D) Coomassie gel (C) and WB (D) treated with an antibody against his-tag of the Cst1Clea fusion protein.

(E, F) Coomassie gel (E) and WB (F) treated with an antibody against his-tag of the Cst1Cad fusion protein.

et al., 2001). The signal of the WB proves that the protein of ~120 kD in fraction 4 – 11 is his tagged and therefore the desired Cst1Clea fusion protein. As expected this signal is present in the input, but not in the flow-through. Figure 12 D, E shows the coomassie gel (D) and the WB (E) of the Cst1Cad purification. As expected from the calculated size of Cst1Cad (30 kD) both detection methods yield a signal at ~35 kD, which is present in the input, but not in the flow-through. The WB shows a second his tag positive band significantly smaller than 25 kD. The size of this protein argues for the isolated his/myc tag.

The two coomassie gels show a second signal (~200 kD) above the his tag-positive band, but this band is not his tag-positive and it is further visible in the supernatant. The signal is present in both Cst1Clea and Cst1Cad purifications, which points this band out to represent a protein which is part of HEK cell supernatants and unspecifically bound to the Ni²⁺ sepharose. This possibility could be investigated by loading HEK293-T cell supernatants from untransfected cells on the Ni²⁺ sepharose columns. If the band is not visible in this control experiment the protein could be a co-purified binding partner of Cst-1.

3.9 Cst-1 in canonical wnt signaling: GFP reporter system

Unpublished data from Kerstin Leuthäuser suggested that Cst-1 binds sFRP-1, which is an antagonist for wnt signaling. This proposed interaction with sFRP-1 suggests that Cst-1 might affect wnt signaling. To elucidate this question a genetic reporter system was used in which GFP is expressed upon activation of the Tcf/Lef promotor which is the target promotor of canonical wnt signaling. HEK293-T cells were transfected with the reporter system. Figure 13A shows the GFP expression, which indicates the activity of the canonical wnt signaling. The constitutive expression of mCherry allows the localization of transfected cells and the DAPI staining is used to visualize nuclei of the cells. In the course of quantification I noticed a positive linear relationship between the intensities of the GFP signal and the mCherry signal (Figure 13B). That means that the GFP signal is partially dependent on the expression level of the DNA construct in each cell. Therefore GFP values were normalized to mCherry values. In a first set of experiments (Figure 13C) the reporter system was co-expressed with cDNA for wnt-8a and Cst-1 and incubated for 48 h. Wnt-8a was chosen because it is highly expressed in the brain (www.brain-map.org). Unfortunately, expression of wnt-8a did not increase the activity of the canonical wnt signaling. Expression of Cst-1 only slightly increased GFP expression (Figure 13C). This experimental setup did not include a control of the expression efficacy of wnt-8a and Cst-1. Too low expression levels of wnt-8a could be the reason why Cst-1 co-expression increased canonical wnt signaling while wnt-8a did not. For that reason a new experimental setup was chosen based on HEK293-T cells, which were only transfected with the reporter system and wnt and Cst1Clea were added as purified proteins in defined amounts. Here, wnt-3a was used instead of wnt-8a, as wnt-3a is the most commonly used activator of canonical wnt signaling in the field (von Marschall and Fisher, 2010, Ring et al., 2011, Ring et al., 2014). Wnt-3a

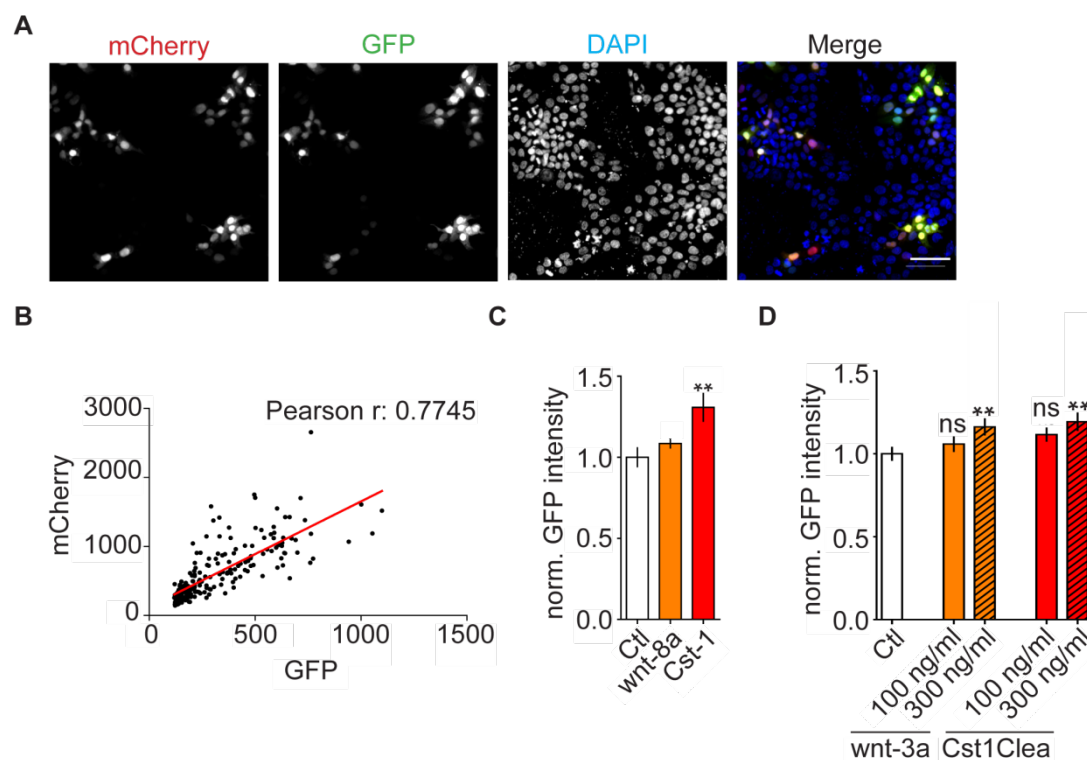


Figure 13: GFP based reporter system to analyze the influence of Cst1 on canonical wnt signaling

(A) HEK293-T cells were transfected with the GFP based reporter system of Tcf/Lef activity. Constitutive expression of mCherry visualizes transfected cells and the GFP signal represents the activation of Tcf/Lef promoter. DAPI staining visualizes the nuclei of plated cells.

(B) Plot of GFP intensities per cell with the corresponding mCherry signal. Calculation of the Pearson correlation value $r = 0.7745$ revealed an increasing linear relationship of both signals. For further quantifications GFP signal was normalized to mCherry intensity.

(C) HEK293-T cells were co-transfected with the GFP reportersystem and either wnt-8a or Cst-1 (48 h). Cst-1 but not wnt-8a increased GFP intensity (Ctl 1.00 ± 0.06 , $n = 23$; wnt-8a 1.09 ± 0.03 , $n = 8$; Cst-1 1.31 ± 0.09 , $n = 12$, average \pm SEM; One-way ANOVA, $P = 0.0065$, Dunnett's Multiple Comparison Test, * $P < 0.05$).

(D) HEK293-T cells were transfected with the GFP reporter system and defined amounts of purified proteins wnt-3a and Cst1Clea were added (6h). Both proteins increased GFP expression when added with 300ng/ml but not with 100ng/ml. (Ctl 1.00 ± 0.04 , $n = 21$; wnt-3a 100ng/ml 1.06 ± 0.05 , $n = 20$; wnt-3a 300ng/ml 1.16 ± 0.05 , $n = 21$; Cst1 100ng/ml 1.12 ± 0.04 , $n = 22$; Cst1 300ng/ml 1.19 ± 0.05 , $n = 21$, average \pm SEM; One-way ANOVA, $P = 0.0192$, Dunnett's Multiple Comparison Test, * $P < 0.05$).

was commercially available whereas Cst1Clea was purified as described in section 2.6.5 and represents the extracellular cleavage product of Cst-1 after α -secretase cleavage (Figure 12A). Figure 13D shows that both wnt-3a and Cst1Clea could increase canonical wnt signaling in higher doses (300ng/ml) but not in lower concentration (100ng/ml). To survey these results I used a more sensitive reporter system for canonical wnt signaling. The most accepted one is the so called Super 8x TOP/FOPFlash system which is based on the expression of luciferase upon Tcf/Lef promoter activation.

3.10 Cst-1 in canonical wnt signaling: luciferase reporter system

Similar to previous experiments HEK293-T cells were transfected either with the Super 8x TOPFlash or Super 8x FOPFlash constructs. Cells were plated in 96 well plates and treated with purified wnt-3a at different concentrations overnight. Figure 14A shows the results of this assay after normalization of the Super 8x TOPFlash to Super8x FOPFlash signal. With increasing amounts of wnt-3a (4 – 16 pmol/ml) canonical wnt signaling was activated. 16 pmol/ml wnt-3a protein led to an almost 10 fold increase in luciferase activity. In the next experiment 16 pmol/ml wnt-3a were used as a positive control and different amounts of Cst1Clea or Cst1Cad were applied overnight (Figure 14B). None of the used concentration of Cst1Clea or Cst1Cad changed luciferase activity. In order to

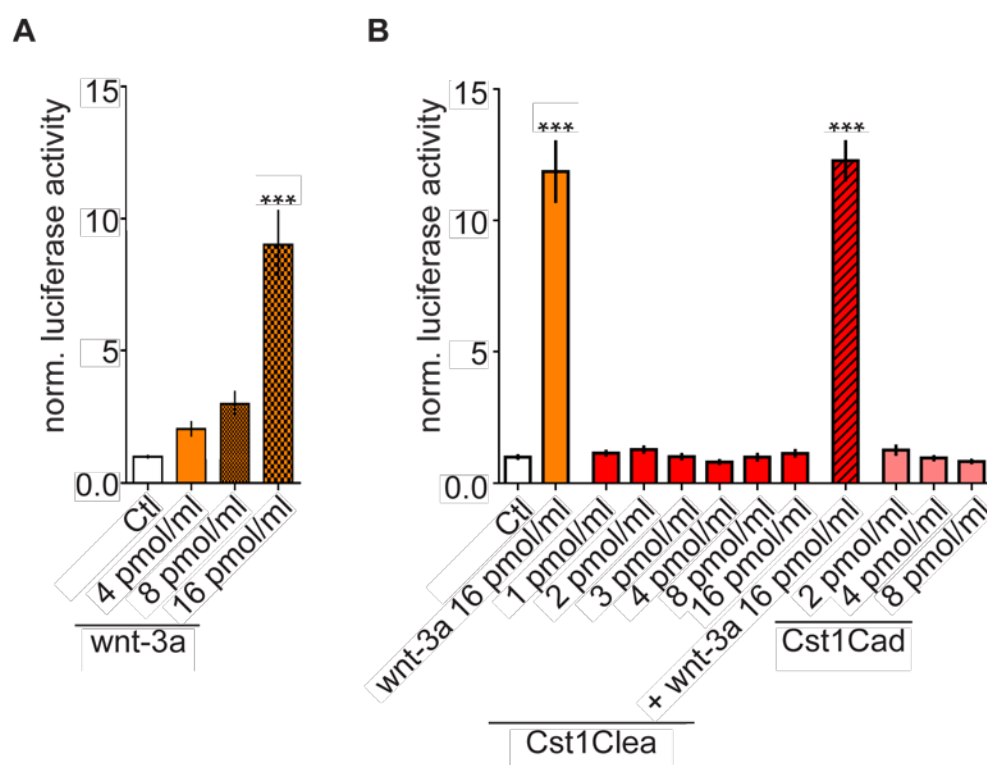


Figure 14: Cst-1 does not affect canonical wnt signaling / Tcf/Lef promotor activation

(A) HEK293-T cells were transfected with the luciferase reporter system and treated with defined amounts of purified wnt-3a (overnight). 4 pmol/ml and 8 pmol/ml wnt-3a slightly increased luciferase activity, whereas 16 pmol/ml wnt-3a significantly enhanced luciferase activity. (Ctl 1.00 ± 0.03 , $n = 18$; wnt-3a: 4 pmol/ml 2.06 ± 0.26 , $n = 12$; 8 pmol/ml 3.00 ± 0.43 , $n = 12$; 16 pmol/ml 9.01 ± 0.43 , $n = 18$; average \pm SEM; One-way ANOVA, $P < 0.0001$, Dunnett's Multiple Comparison Test, *** $P < 0.0001$).

(B) HEK293-T cells were transfected with the luciferase reporter system and treated with defined amounts of purified wnt-3a, Cst1Clea or Cst1Cad (overnight). Only 16 pmol/ml wnt-3a increased luciferase activity significantly. Simultaneous application of equal amounts of wnt-3a and Cst1Clea had the same effect as wnt-3a alone. (Ctl 1.00 ± 0.05 , $n = 8$; wnt-3a 16 pmol/ml 11.86 ± 1.34 , $n = 8$; Cst1Clea: 1 pmol/ml 1.15 ± 0.08 , $n = 8$, 2 pmol/ml 1.23 ± 0.1 , $n = 8$, 4 pmol/ml 1.02 ± 0.09 , $n = 8$, 8 pmol/ml 1.00 ± 0.11 , $n = 8$, 16 pmol/ml 1.14 ± 0.11 , $n = 8$; wnt-3a + Cst1Clea 16pmol/ml 12.27 ± 0.73 , $n = 8$; Cst1Cad: 2 pmol/ml 1.26 ± 0.15 , $n = 8$, 4 pmol/ml 0.96 ± 0.07 , $n = 8$, 8 pmol/ml 0.83 ± 0.05 , $n = 8$; average \pm SEM; One-way ANOVA, $P < 0.0001$, Dunnett's Multiple Comparison Test, *** $P < 0.0001$).

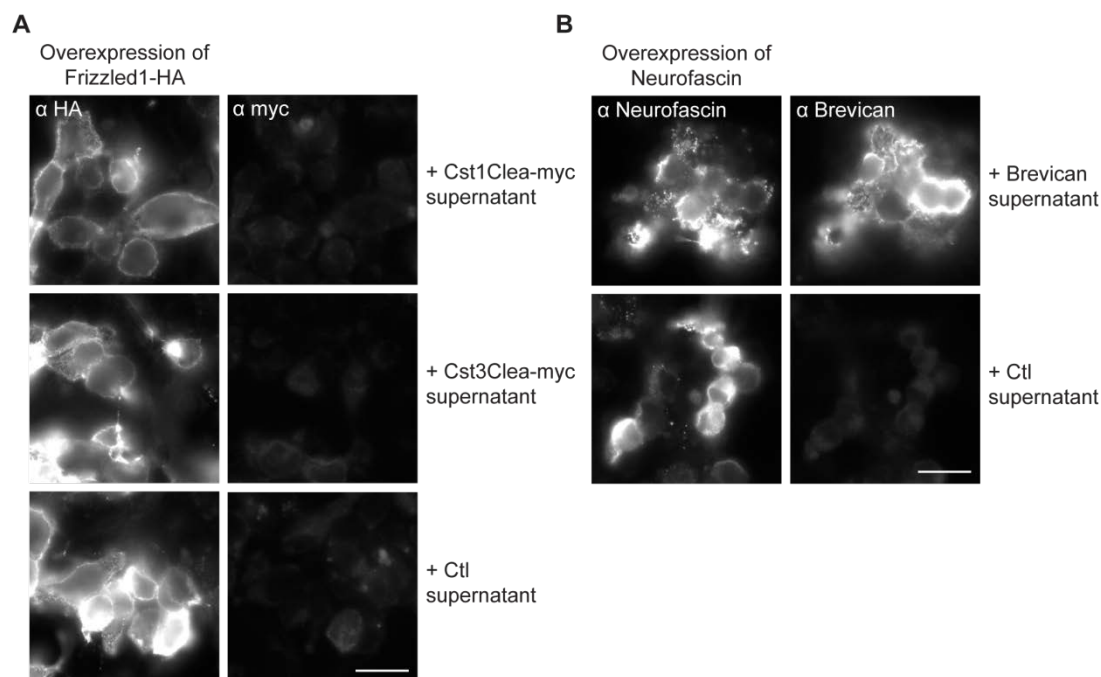


Figure 15: Neither Cst1Clea nor Cst3Clea bind to Frzl-1

(A) HEK293-T cells were transfected with HA tagged Frzl-1 and treated with supernatants from either Cst1Clea-myc or Cst3Clea-myc expressing HEK293-T cells. Living cells were stained for HA and myc tags. Neither Cst1Clea nor Cst3Clea bound to the Frzl-1-transfected cells. (scalebar 20 μ m)

(B) To verify the experimental setup the binding assay was performed with a known interacting protein. HEK293-T cells were transfected with neurofascin and supernatants from HEK293-T cells expressing brevicane were added. Living cells were stained against neurofascin and brevicane. The brevicane staining co-localized with the neurofascin staining, underlying the binding of these proteins. (scalebar 20 μ m)

clarify whether wnt-3a and Cst1Clea show any competitive behavior, wnt-3a and Cst1Clea were added together in equal amounts. Nevertheless the results did not change compared to the case where only wnt-3a was added. These data suggest that Cst-1 has no influence on canonical wnt signaling.

3.11 Binding assay: Cst1Clea and Frizzled-1

Even though I could not show an influence of Cst-1 on canonical wnt signaling-dependent gene expression, an influence of Cst-1 on other wnt signaling pathways cannot be excluded. After identifying Cst-1 as a binding partner of sFRP-1 different deletion mutants were created to localize the binding region within sFRP-1. It was shown that the CRD of sFRP-1 is essential for Cst-1 binding (Leuthäuser et al., unpubl.). CRDs are conserved between sFRPs and Frzl. Therefore it was feasible to test whether Cst-1 could also bind to Frzl. For that reason HEK293-T cells were transfected with an extracellular HA-tagged Frzl-1. Frzl-1 was chosen because it is highly expressed in hippocampal synapses

(Varela-Nallar et al., 2009). Supernatants of Cst1Clea- or Cst3Clea-expressing HEK293-T cells were added to the cells. Figure 15A presents microscopic images that show surface staining for HA tag (Frzl-1-HA) and myc tag (Cst1Clea-myc / Cst3Clea-myc). None of these proteins bound Frzl-1. The supernatant of non-transfected HEK293-T cells (Ctl supernatant) was used as a negative control and it shows the same result. As a positive control for the experimental design I chose brevican that interacts with neurofascin and is recruited to neurofascin overexpressing COS-7 cells (Hedstrom et al., 2007). Figure 15B shows clear recruitment of brevican to transfected cells. The application of control supernatants shows no signal of the brevican antibody that confirms its specificity. In the end these experiments show that under these conditions neither Cst1Clea nor Cst3Clea bind to Frzl-1.

3.12 Cst-1 in presynaptic activity

To date, a potential role of Cst-1 in wnt signaling remains to be clarified. Of note, wnt signaling is more diverse than the classical canonical and non-canonical pathways. It increases for example recycling of presynaptic vesicles (Ahmad-Annur et al., 2006, Cerpa et al., 2008) and is involved in targeting $\alpha 7$ -nAChR to the plasma membrane, whose activation affects neurotransmitter release (Farias et al., 2007). Due to these phenomena a role for Cst-1 in presynaptic activity was considered. To investigate this, a well-established protocol was chosen to measure presynaptic activity: synaptotagmin-1 antibody uptake. Figure 16A shows a schematic illustration of this method. Dissociated rat cortical neurons (DIV 14-17) were incubated with different purified proteins for 1 h. In case of additional application of channel blockers like Bungarotoxin (BgTx) those were applied 30 min before addition of purified proteins to ensure that the channel cannot be activated upon protein application. Cells were then incubated with an antibody against the luminal domain of synaptotagmin-1. With every fusion event of a synaptic vesicle, the antibody is taken up. The higher the fluorescent signal the higher is the presynaptic activity. Application of Cst1Clea increased the fluorescence intensity (Figure 16B). This demonstrates that the average activity of presynapses is increased. Neither Cst1Cad nor Cst3Clea changed presynaptic activity significantly, indicating specificity of the effect for the full-length ectodomain of Cst-1. The question arose which signaling pathway enables Cst1Clea to act on the presynapse. So far, I did not find a proof for the interaction of Cst-1 and Frzl-1, but the suggested interaction of Cst-1 and sFRP-1 made me to

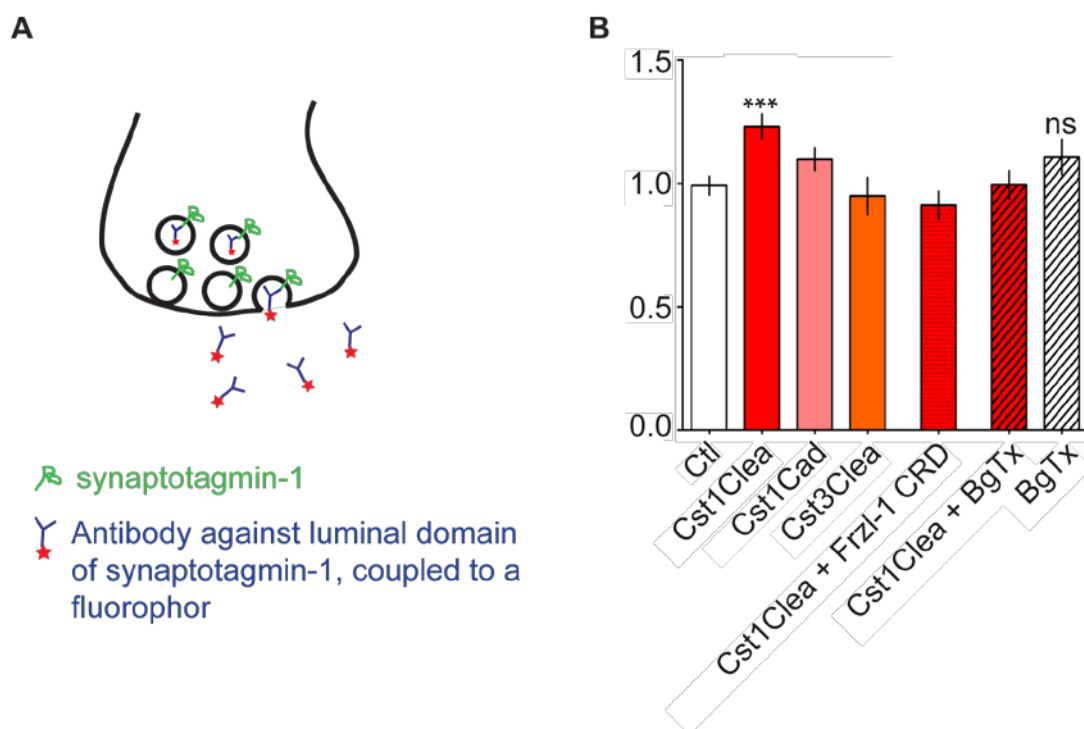


Figure 16: Cst1Clea increased presynaptic activity

(A) Scheme to illustrate synaptotagmin-1 antibody uptake. Fluorescently labeled antibodies against synaptotagmin-1 were added to the cell media of dissociated cortical cultures (DIV 14-17). The antibody was taken up when a neurotransmitter vesicle was fused to the membrane and recycled. In this way presynaptic activity is visualized by the intensity of the uptaken antibodies.

(B) Cst1Clea, but not Cst1Cad or Cst3Clea increased presynaptic activity. The effect of Cst1Clea could be inhibited by simultaneous application of soluble Frzl-1 CRD or by preincubation with BgTx to block $\alpha 7$ -nAChRs. BgTx alone did not affect presynaptic activity. (Ctl 1.00 ± 0.04 , $n = 113$; Cst1Clea 1.23 ± 0.05 , $n = 124$; Cst1Cad 1.10 ± 0.05 , $n = 78$; Cst3Clea 0.95 ± 0.07 , $n = 53$; Cst1Clea + Frzl-1 CRD 0.91 ± 0.06 , $n = 26$; Cst1Clea + BgTx 0.99 ± 0.06 , $n = 38$; BgTx 1.11 ± 0.07 , $n = 38$; average \pm SEM; One-way ANOVA, $P = 0.0002$. Dunnett's Multiple Comparison Test. *** $P < 0.0001$).

test if the effect of Cst-1 on presynaptic activity can be prevented by inhibition of wnt signaling. A tool to inhibit wnt signaling at the presynapse is a soluble Frzl-1 CRD (Varela-Nallar et al., 2009). I added simultaneously Frzl-1 CRD and Cst1Clea to the cells and prevented the activating influence of Cst1Clea alone (Figure 16B). Further, $\alpha 7$ -nAChRs are one target of wnt signaling within the presynapse (Farias et al., 2007). By treatment with Cst1Clea and BgTx, an inhibitor of $\alpha 7$ -nAChRs, the positive effect of Cst1Clea on presynaptic activity was inhibited (Figure 16B). BgTx alone did not change presynaptic activity.

4 Discussion

The aim of my thesis was to investigate the influence of the hyaluronan-based ECM and the extracellular cleaved molecule Cst-1 on synaptic transmission. I could show in the main project that enzymatic remodeling of the ECM leads to an enhanced surface expression of GluN2B-NMDA receptors in a β 1-integrin-dependent manner. In the side project I demonstrated that the ectodomain of Cst-1, which originates upon ectodomain shedding, enhances presynaptic activity. Cellular consequences, potential signaling mechanisms and the impact of these observations will be discussed in the following.

4.1 Regulation of surface expression of GluN2B-NMDA receptors

The regulation of NMDA receptors is an important feature in terms of plasticity processes. Due to their Ca^{2+} permeability, coincident detection of pre- and postsynaptic activity and their intracellular coupling to signaling cascades NMDA receptors are attractive modulators for plasticity. In particular GluN2B-NMDA receptors undergo activity-dependent changes in their surface abundance (Carmignoto and Vicini, 1992). It has previously been suggested that surface expression and endocytosis of GluN2B are regulated by phosphorylation of Y1472 within the YEKL-motif of GluN2B. This phosphorylation prevents the binding of the adapter protein AP-2 and subsequently inhibits the endocytosis of GluN2B-NMDA receptors (Nakazawa et al., 2001, Roche et al., 2001, Lavezzari et al., 2003, Prybylowski et al., 2005). Indeed, the presented data provide evidence that ECM digestion by Hya increased pY1472 of GluN2B and consequently decreased endocytosis of the receptor. However, it remains elusive which kinase phosphorylates GluN2B upon ECM degradation and this will be discussed.

4.1.1 Src and Fyn kinase phosphorylate GluN2B-NMDA receptors

Two kinases have been suggested to phosphorylate GluN2B at Y1472, namely the src kinase family (SFK) members Fyn and Src (Nakazawa et al., 2001, Zhang et al., 2008a). Nakazawa et al. showed that in HEK293-T cells Fyn phosphorylates GluN2B subunits at seven residues, including Y1472. Further, the phosphorylation was greatly reduced but not abolished in Fyn-mutant mice (Nakazawa et al., 2001). Zhang et al. suggested Src to phosphorylate GluN2B at Y1472 in a Cdk5-dependent manner, whereas phosphorylation by Fyn seems to

be Cdk5 independent. They propose Src to be responsible for the residual phosphorylation of Y1472 in Fyn mutant mice (Zhang et al., 2008a). There are further evidences in the study that the responsible kinase is member of the SFK. Interestingly, it was shown that application of integrin-ligand peptides evokes rapid increase in tyrosine phosphorylation by SFKs. This was followed by elevated NMDA receptor-mediated synaptic responses (Lin et al., 2003, Bernard-Trifilo et al., 2005). However, it remains open whether increased NMDA currents were due to direct effects on the channel properties or were caused indirectly, by affecting the membrane trafficking of the receptor. Indeed phosphorylation of Y1472 of GluN2B regulates surface trafficking of the receptor (Lavezzari et al., 2003). The YEKL motif, which includes Y1472, is the binding site for AP-2 that mediates clathrin-dependent endocytosis of the NMDA receptor. When Y1472 is phosphorylated AP-2 cannot bind anymore which results in stabilization of GluN2B-NMDA receptors at the surface. Based on that it was interesting to investigate whether the increased NMDA receptor mediated currents after application of integrin ligand peptides are due to an increased surface expression of GluN2B-NMDA receptors. The data in this study support this idea since it was shown that β 1-integrin-dependent signaling increased surface expression of GluN2B which was paralleled by higher phosphorylation of Y1472 (Figure 17). My attempts to confirm SFKs as responsible enzymes using PP2 as an selective inhibitor (see Table 14) did not reveal explicit results. Thus, based on the described literature the kinase mechanism needs to be unraveled in this experimental setup using other kinase inhibitors.

4.1.2 Lateral mobility of GluN2B-NMDA receptors

Endocytosis of GluN2B takes place at perisynaptic sites where the endocytotic pits are localized (Blanpied et al., 2002) and starts with a CKII dependent phosphorylation of S1480 within the MAGUK/PDZ binding motif (Sanz-Clemente et al., 2010). This motif binds to MAGUKs like PSD-95 or SAP-102 to tether the receptors within the post synaptic density. Phosphorylation of S1480 leads to a disruption of the interaction of MAGUKs with GluN2B as well as to lateral movement of GluN2B to extrasynaptic sites where the endocytotic zones are localized (Clapp et al., 2010, Chen et al., 2012). In fact, after ECM digestion there was increased pY1472 and decreased endocytosis found. However, my attempts to quantify pS1480 failed due to poor detection with corresponding antibody (see Table 13). Thus, it remains to be investigated if the phosphorylation

state of S1480 is also affected, which would argue for a coordinated extra- and intracellular mobilization of the receptors.

An indicator for altered association to the postsynaptic density is provided by the results of the mobility experiments presented here. Overnight treatment with Hya did not affect the velocity of surface expressed GluN2B-NMDA receptors but it decreased the explored surface area of the receptor. This could imply that GluN2B-NMDA receptors are more stabilized at synaptic sites, which is achieved by a higher binding to MAGUKs. Therefore it is tempting to speculate that long-term ECM digestion decreases phosphorylation of S1480 to promote association of GluN2B with MAGUKs (Figure 17).

Unfortunately the mobility experiments did not distinguish between synaptic and extrasynaptic receptors and thereby give no information about the exchange rate of those receptors. As my immunocytochemistry experiments revealed an increase in both synaptic and dendritic (extrasynaptic) receptors, one may speculate that both populations become more confined. Stabilization of GluN2B-NMDA receptors at extrasynaptic sites could be a cellular mechanism to react faster on upcoming network changes that provoke molecular adjustments of the synapse. Having more receptors available at the surface, the regulation of synaptic receptor abundance can be carried out much faster as well. In addition, enhanced abundance of GluN2B-NMDA receptors at extrasynaptic sites itself can influence the fate of neurons as extrasynaptic NMDA receptor-mediated signaling differs from synaptic NMDA receptor-mediated signaling (Gladding and Raymond, 2011). Extrasynaptic NMDA receptors are likely to be activated upon glutamate spill-over during high-frequency repetitive activity or by glutamate release from other sources like surrounding glia (Rusakov and Kullmann, 1998, Le Meur et al., 2007, Chalifoux and Carter, 2011). Ca^{2+} transients mediated by synaptic NMDA receptors were shown to activate CREB and subsequently enhance transcription of pro-survival genes, whereas extrasynaptic NMDA receptors inactivate CREB, thus dominating the activating effect of synaptic ones (Hardingham et al., 2002). The question whether GluN2B-NMDA receptors lead to cell death and GluN2A-NMDA receptor to cell survival remains contradictory (Liu et al., 2007, von Engelhardt et al., 2007, Martel et al., 2009). However, as both compartments, synaptic and extrasynaptic sites, show higher abundance of GluN2B-NMDA receptors the ratio of activated synaptic versus extrasynaptic receptors remains probably the same and may not drive the neurons into a CREB-inactive status.

Acute Hya treatment increases lateral mobility of GluA1-AMPA receptors and by that enhances short-term plasticity (Frischknecht et al., 2009). In line with that, acute ECM digestion increased the explored area of GluN2B-NMDA receptors. It is proposed that the ECM forms surface compartments with varying size that operate as lateral diffusion barriers for surface molecules. Short-term Hya treatment supports this idea also for GluN2B-NMDA receptors. By regulating the lateral diffusion of receptors from one compartment to the other may allow synapse specific adjustments of receptors without producing global effects. Another advantage of a decreased confinement of GluN2B-NMDA receptors after acute ECM digestion could be that extrasynaptic receptors can move easily into the synapse. In contrast, overnight treatment with Hya led to a decreased mobility of GluN2B-NMDA receptors. This may be due to stimulation of intracellular signaling mechanism including activation of kinases and phosphatases that lead to the association of the NMDA receptors with MAGUKs that anchor the receptors at synapses. The increased anchoring at synaptic sites is visualized by the decreased lateral mobility (Clapp et al., 2010, Chen et al., 2012).

4.1.3 Integrins regulate NMDA receptors

As already mentioned integrin-ligand peptides are known to influence NMDA receptor currents and properties (Lin et al., 2003, Bernard-Trifilo et al., 2005, Watson et al., 2007). In this thesis it was demonstrated that a function-blocking β 1-integrin antibody could inhibit ECM digestion-elicited increase of surface abundance of GluN2B (Figure 17). Increased NMDA receptor-mediated currents upon enhanced activation of β 1-integrins are in line with previously published data. Activation of integrins with RGD peptides affect the phosphorylation state of GluN2A and GluN2B NMDA receptor subunits via increased SFK activity (Bernard-Trifilo et al., 2005). This could be blocked by a function-blocking antibody against β 1-integrins. In line, application of the SFK inhibitor PP2 eliminated an RGD-induced increase of NMDA receptor-mediated currents in acute hippocampal slices (Lin et al., 2003). Supporting evidence came from calcium imaging experiments that showed higher intracellular calcium levels after RGD-induced integrin activation. Interestingly, this increase was blocked by the GluN2B specific inhibitor ifenprodil and the SFK inhibitor PP2 (Watson et al., 2007), suggesting that indeed GluN2B and SFKs were responsible for the increased Ca^{2+} transients after integrin activation.

4.2 ECM influences cellular properties via integrin signaling

Several studies showed that ECM molecules interact with integrins and change their intracellular signaling. β 1-integrins were shown to bind to the C-terminal domain of the CSPG versican and thereby activate the focal adhesion kinase (FAK) (Wu et al., 2002). Interestingly the peptide that is sufficient for this interaction does not contain the RGD consensus-binding motif, thus implementing a new binding mechanism. Another CSPG, which was shown to bind β 1-integrins, is aggrecan. It inhibits axon growth on laminin-coated substrata by impairing integrin signaling, which results in decreasing pY397 FAK and pY418Src level (Tan et al., 2011). These phosphorylation steps lead to enhanced kinase activity. Treatment with ChABC prevented the axon growth inhibition by aggrecan (Tan et al., 2011). Additionally manganese, a potent integrin activator that keeps integrins in a high ligand binding affinity conformation, was able to abolish the inhibitory effect of aggrecan, raising the hypothesis that aggrecan keeps integrins in an inactive conformation and thereby decreases integrin signaling. Supporting data came from Orlando et al. who showed that ChABC treatment of organotypic hippocampal slices induced activation of β 1-integrins and increased pY397 FAK levels (Orlando et al., 2012). Accordingly, structural changes were observed like enhanced spine motility and the formation of spine head protrusions. They propose CSPGs to “play a fundamental role in unmasking a cryptic binding motif that activates integrins and initiates both functional and structural plasticity”.

The application of ChABC does not represent an endogenous remodeling of the ECM, as ChABC is a bacterial enzyme (Yamagata et al., 1968). Thus the search for neural ECM remodeling mechanisms leads to experiments that focused on the effect of proteolytic activity on integrins. Indeed, application of recombinant MMP-9 was shown to potentiate synaptic responses in an integrin-dependent manner (Wang et al., 2008). The authors speculate that latent RGD recognition sequences in target proteins of MMP-9 could get exposed after cleavage and thereby activate integrins. Alternatively, they suggest that MMP-9 may directly bind to integrins (Wang et al., 2003).

In this thesis it was shown that both Hya and ChABC increase surface expression of GluN2B. Since Hya has an intrinsic chondroitinase function as well it is very likely that both enzymes decrease the inactivation of integrins due to degradation

of chondroitin sulfates. Thereby integrins are more activated and subsequently kinase activity is affected which leads to altered GluN2B phosphorylation.

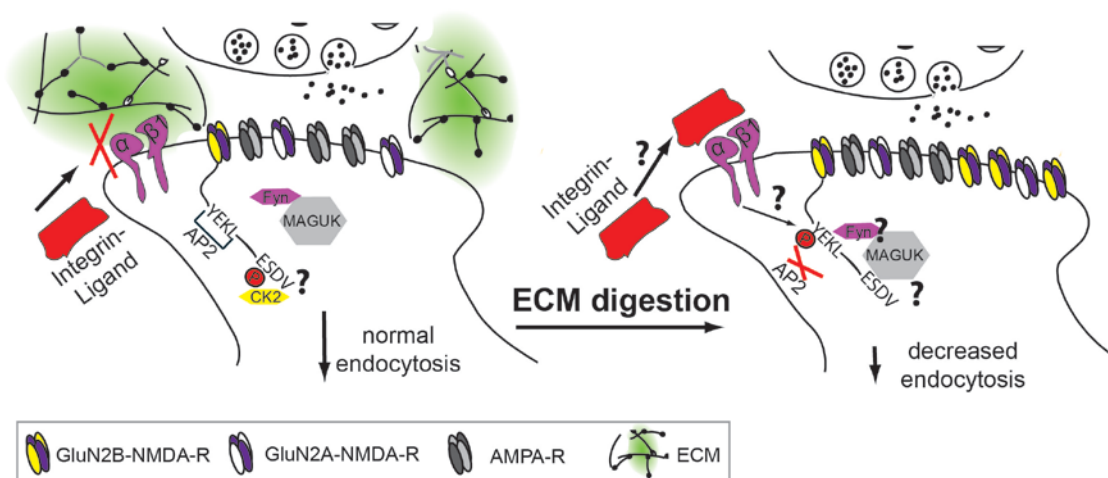


Figure 17: Schematic presentation of the putative signaling mechanism that increases GluN2B-NMDA receptor surface expression upon ECM removal

Adult synapses are surrounded by a dense ECM, which partially inhibits integrin signaling. The NMDA receptors are dominated by GluN2A-NMDA receptors, as the driving force for GluN2B-NMDA receptors is higher in comparison. The cytoplasmic tail of GluN2B contains two motifs, which are involved in the regulation of their trafficking. The ESDV motif is phosphorylated at this stage, which destabilizes the association to MAGUKs and allows the receptor to diffuse out of the synapse to the endocytotic pits. The YEKL motif is un-phosphorylated, which allows binding of AP-2 and results in endocytosis of the GluN2B-NMDA receptor.

In this thesis it is proposed that ECM digestion by Hya or ChABC leads to an increased surface expression of GluN2B-NMDA receptors. The proposed signaling mechanism starts with an enhanced activation of β 1-integrins, which leads to an increased phosphorylation of the YEKL motif. This prevents binding of AP-2 and results in a decreased endocytosis and a stabilization of the receptors at the surface. The question marks highlight ambiguity that needs to be clarified by further experiments. Elucidating the exact way of enhanced integrin activation, the responsible kinase to phosphorylate GluN2B (most likely Fyn or Src) and the phosphorylation state of the ESDV motif would help to understand the whole signaling mechanism.

4.2.1 Reelin regulates NMDA receptor properties

Several studies investigate the ECM protein reelin, which is involved in the developmental switch of NMDA receptor subunit composition, their mobility and physiological properties (Beffert et al., 2005, Qiu et al., 2006, Groc et al., 2007). Reelin, a secreted glycoprotein is well known for its crucial role in the development of laminar structure of the cortex (D'Arcangelo and Curran, 1998).

Blocking the function of reelin prevents the developmental subunit switch of NMDA receptors in a β 1-integrin-dependent manner. Further, it decreases lateral mobility of GluN2B-NMDA receptors but increases their synaptic dwell time. In contrast, application of recombinant reelin accelerates the switch of subunits and reduces the synaptic dwell time of the receptors. (Groc et al., 2007).

A well-established receptor for reelin is the Apolipoprotein E receptor 2 (Apoer2) which forms functional complexes with the NMDA receptor in the postsynaptic density (Beffert et al., 2005). Application of exogenous recombinant reelin leads to enhanced LTP, AMPA- and NMDA receptor-mediated postsynaptic currents and an enhanced tyrosine phosphorylation of NMDA receptors (Beffert et al., 2005, Qiu et al., 2006). Further, Qiu et al. showed that the enhanced synaptic NMDA currents were abolished by the SFK inhibitor PP1. But they also demonstrated that surface expression of NMDA receptor subunits is unchanged after reelin application.

There are parallels as well as differences between the studies mentioned above and the data of my thesis. The commonalities are that modulation of the ECM influences NMDA receptor subunit properties, by affecting the phosphorylation of the GluN2B subunit, partially stated to be β 1-integrin-dependent. Simulating an immature reelin function decreases receptor mobility, which is in line with the observation of a decreased mobility after prolonged Hya treatment. Strikingly, the modulation of reelin does not change NMDA receptor surface expression, whereas Hya treatment increased GluN2B-NMDA receptor surface expression. To date, no data are available that describe in which way reelin is influenced by Hya or ChABC treatment. Thus it remains elusive, if the regulative mechanisms by reelin or Hya/ChABC influencing NMDA receptors interfere with each other or if they are separated. It can be stated that different strategies to remodel the ECM influence NMDA receptor properties in different ways by using partially the same singling molecules. Therefore, the guided use of ECM remodeling strategies provides a tool to selectively affect synaptic properties.

4.3 Cellular consequences of an altered GluN2A/GluN2B ratio upon ECM remodeling

The subunit composition, in particular the abundance of GluN2A and/or GluN2B subunits, determines the kinetics of the receptors and the activated signaling cascades as they have diverse intracellular tails (section 1.2.2). This thesis demonstrates that removal of the ECM in adult neurons increases surface expression of GluN2B-NMDA receptors, which are predominantly expressed in juvenile synapses. Therefore, the question arises about the functional consequences of a decreased GluN2A/GluN2B ratio.

4.3.1 Tri-heteromeric NMDA receptors

In order to approach questions about cellular consequences of an altered GluN2A/GluN2B ratio, it is necessary to discuss the abundance of tri-heteromeric NMDA receptors. Most studies about NMDA receptor subunit composition focus on di-heteromeric receptors although 15 – 50% of the total receptor population are tri-heteromeric receptors (Sheng et al., 1994, Luo et al., 1997, Al-Hallaq et al., 2007, Rauner and Kohr, 2011, Tovar et al., 2013). In early studies it was shown by immunoprecipitation that the dominant NMDA receptor complex in adult rat cortex contains three different subunits (Sheng et al., 1994, Luo et al., 1997). Several studies evidenced that tri-heteromeric NMDA receptors exist at the synapse and have intermediate kinetics compared to di-heteromeric receptors. 3 μ M ifenprodil inhibit 80 % of di-heteromeric GluN2B-NMDA receptors, but has no effect on GluN2A-NMDA receptors (Tovar and Westbrook, 1999). This was shown in a heterologous expression system (HEK293-T cells). Gray et al. confirmed this finding in neurons by deleting either GluN2A or GluN2B and compared their sensitivity for ifenprodil with WT neurons. 3 μ M ifenprodil were demonstrated to exert an intermediate effect in WT neurons compared to GluN2A- or GluN2B-deficient neurons (Gray et al., 2011). Moreover, intermediate inactivation kinetics were shown by comparing neuronal cultures and acute slices of either GluN2A- or GluN2B knock-out mice with those from WT mice (Rauner and Kohr, 2011, Tovar et al., 2013).

In my experiments neuronal cultures of WT rats were used, implicating a dominant abundance of tri-heteromeric NMDA receptors at synapses. After Hya treatment the NMDA receptor mediated sEPSCs were increased by 38 %. This increase was completely blocked by application of 3 μ M ifenprodil. That suggests that those NMDA receptors that get stabilized at the surface are most probably di-heteromeric GluN2B-NMDA receptors. This result was confirmed by surface immunostainings of GluN2B subunits, which yielded 30 % more GluN2B-NMDA receptors at synapses after Hya treatment. Quantification of the surface GluN2B expression in the entire dendrite revealed an increase of 78 %. As only currents of synaptic NMDA receptors were measured in the sEPSCs experiments it stays ambiguous if the stabilized dendritic receptors are di- or tri-heteromeric receptors.

Most of the studies addressing consequences of an altered GluN2A/GluN2B ratio exclude to a certain degree the abundance of tri-heteromeric NMDA receptors. In

terms of plasticity processes synaptic NMDA receptors are the main actors. Since Hya treatment leads to an increase of di-heteromeric GluN2B-NMDA receptors at synapses in my experiments tri-heteromeres can be excluded for further discussions of my results.

4.3.2 Regulation of LTP by NMDA receptors and the ECM

The influence of NMDA receptors on LTP

Several partially controversial studies have shown that the GluN2A/GluN2B ratio critically affects various forms of synaptic plasticity such as LTP, LTD and metaplasticity (Paoletti et al., 2013, Shipton and Paulsen, 2014). The controversy whether GluN2A- or GluN2B-NMDA receptors were of higher importance to elicit LTP was studied during the last decades. The contradictions are often based on different experimental models (*in vivo* / *in vitro* / modeling), different protocols to induce LTP and different experimental setups (pharmacological / long-term or short-term genetic manipulation). Pharmacological studies suggested that inhibition of GluN2A-NMDA receptors prevented tetanus- and pairing-induced LTP but inhibition of GluN2B-NMDA receptors does not, but instead blocks LTD induction (Liu et al., 2004). That the frequency of stimulation can be crucial was shown as inhibition of GluN2B-NMDA receptors blocked the induction of spike-timing-dependent LTP (low-frequency paradigm) but it did not impair tetanus-induced LTP (Zhang et al., 2008b, Kohl et al., 2011). These different emphases of NMDA receptor subunits in responding to diverse stimulation frequencies can be important since network activity is changing upon behavior or molecular rearrangements. Overall, the pharmacological data do not provide a convincing evidence for a highly selective role of either subunit in LTP induction.

If the intracellular tail of the NMDA receptor subunit and thereby their coupling to signaling cascades influences the preference for any kind of plasticity cannot easily be deduced from receptor blocking studies. In 1998 it was demonstrated that the C-terminal tail of GluN2B but not GluN2A or GluN1 shows high affinity to bind CaMKII (Strack and Colbran, 1998). The expression of mutated GluN2B subunits that show a reduced association with CaMKII prevented LTP (Barria and Malinow, 2005). Strikingly, it was sufficient to express mutated GluN2A subunits with a higher CaMKII affinity to rescue LTP. That states that the intracellular tail of GluN2B is essential for LTP as it keeps CaMKII within the proximity of synaptic activity. This observation brings a new perspective into

pharmacological experiments. In 2010 it was shown that pairing-induced LTP was not impaired by the block of GluN2B-NMDA receptors, but it was impaired by RNAi knock-down of GluN2B (Foster et al., 2010). That provides the GluN2B-NMDA receptor a special role at the synapse, additional to its function as an ion channel.

Based on the available data, both GluN2A- and GluN2B-NMDA receptors support the essential Ca^{2+} influx, depending on the stimulation protocol and developmental stage. Additionally GluN2B-NMDA receptors carry a unique role to target CaMKII to the proximity of Ca^{2+} influx at the PSD. Thus, the decreased GluN2A/2B ratio, as was found after Hya treatment may enhance the probability of eliciting LTP by given stimuli. Concerning LTD the data are even more inconclusive since neither GluN2A nor GluN2B seem to have a dominant role in this process.

The influence of the ECM on LTP

Several studies have shown that the ECM influences different kinds of synaptic plasticity. However, depending on the form of plasticity and experimental system the outcomes of the experiments vary.

Prolonged ChABC treatment (3 days) in the visual cortex increased potentiation upon 3xTBS *in vivo* (de Vivo et al., 2013). Further the authors could show that chemical LTP combined with ChABC treatment potentiates visual responses. That provides a hint that prolonged ECM digestion can indeed increase functional plasticity, without providing precise molecular mechanisms yet. However, the authors speculate that this could be due to changes in receptor and channel surface localization, which would be in line with the altered GluN2A/GluN2B ratio after Hya or ChABC treatment in my experiments.

In contrast, 2h Hya treatment of hippocampal slices did not influence single TBS-induced LTP (Kochlamazashvili et al., 2010). However, the acute Hya treatment of hippocampal slices caused an impaired 5xTBS induced LTP, which was shown to be due to inhibited L-type Ca^{2+} -channel currents. The application of exogenous hyaluronic acid restored the calcium transients and LTP. These data argue against an effect of Hya treatment on the NMDA receptor-dependent machinery of LTP induction. This discrepancy to the observed effect of Hya in my thesis could be due to the shorter duration of ECM digestion that was used by Kochlamazashvili et al. The increased mobility upon short-term Hya treatment and the decreased mobility upon overnight treatment, which I observed in my

thesis, supports the idea that different durations of ECM digestion cause diverse effects.

Rearrangements of the ECM occur naturally by the action of proteases like MMP-9 for example. MMP-9 level and proteolytic activity are rapidly increased by stimuli that induce late-phase LTP (L-LTP) in an NMDA receptor dependent manner (Nagy et al., 2006). Nagy et al. could show that pharmacological inhibition of MMP-9 selectively prevents the induction of L-LTP. The same holds true for MMP-9 mutant mice (Nagy et al., 2006). Brief application of active MMP-9 leads to a potentiation in hippocampal area CA1, which could be erased by either echistatin, RGD peptides or integrin function-blocking antibodies suggesting that this potentiation is mediated by RGD-binding receptors (Nagy et al., 2006, Wang et al., 2008). These studies support findings of the present thesis unraveling a β 1-integrin-dependent mechanism how ECM remodeling can influence cellular properties. In which way MMP-9 activity or ECM remodeling in general activate integrin signaling stays elusive. The most favorable mechanism is the exposure of latent recognition sequences by proteolytic cleavage, which then activate cell-surface integrins. Enhanced exposure of recognition sites to cellular receptors like integrins is also a conceivable mechanism to occur upon Hya or ChABC treatment.

In studies that used either neurocan (Zhou et al., 2001) or brevican (Brakebusch et al., 2002) knock-out mice an impairment in the maintenance of LTP was detected, whereas no changes in the basal transmission or induction of LTP were observed. In addition Brakebusch et al. could show that application of an antibody against brevican mimicked the effect of the brevican KO animals. That presents again another effect of altered ECM composition on synaptic plasticity, as studies described before only observed effects in the induction of LTP. Tenascin-R deficient mice were shown to have a two-fold reduction in LTP (5xTBS), and short-term depression evoked by low-frequency stimulation was found reduced as well (Bukalo et al., 2001). In the same year a second study supported those data by showing an impaired NMDA receptor-dependent LTP (10xTBS) in tenascin-R deficient mice (Saghatelian et al., 2001). Both studies showed that the basal NMDA receptor component was unaffected. Saghatelian et al. state that amplitudes of NMDA receptor currents are normal, which is in line with my data. But they did not quantify decay times of the NMDA receptor-mediated currents, which could give more information about the subunit composition of NMDA receptors.

4.3.3 Regulation of metaplasticity by NMDA receptors and the ECM

Since it is not possible to determine fixed roles for either NMDA subunit to induce either LTP or LTD, the idea of metaplasticity (Abraham and Bear, 1996) was brought into focus of research. Metaplasticity describes the mechanisms that regulate the basal state of synapses which determines the threshold to induce plasticity. The subunit composition of NMDA receptors is known to be activity-dependent (Carmignoto and Vicini, 1992). Xu et al. demonstrated that the GluN2A/GluN2B ratio in acute hippocampal slices of 2-3 weeks old rats was decreased after high-frequency priming, which subsequently increased the magnitude of LTP but decreased LTD expression (Xu et al., 2009). For a higher GluN2A/GluN2B ratio they found an inverse relationship. Further, a plasticity protocol that induces no changes in 'naive' slices was able to induce LTP or LTD depending upon the previous priming protocol, as priming influences the GluN2A/GluN2B ratio to promote either LTP or LTD. In line, on a single synaptic level silencing led to enhanced GluN2B-NMDA receptor currents in comparison to naive synapses (Lee et al., 2010). Subsequently, the previously silenced synapses needed less intense protocols to elicit LTP and spine growth than previously active ones.

So far it clearly shows that the GluN2A/GluN2B ratio influences the fate of neurons in terms of their future plasticity processes. That supports my hypothesis that a decreased GluN2A/GluN2B ratio after ECM removal enhances the probability to induce plasticity as it is enhanced in juvenile networks. One may suggest that the ECM digestion in my experiments is analogous to the priming procedure used in other studies to alter the GluN2A/GluN2B ratio.

In line, tenascin-R-deficient mice were shown to exhibit elevated basal excitatory synaptic transmission and reduced perisomatic GABAergic inhibition, which could lead to metaplastic changes due to altered synaptic activity (Saghatelian et al., 2001). Indeed, Bukalo et al. found the threshold to induce LTP to be increased in tenascin-R-mutant mice, which is the key factor in metaplasticity (Bukalo et al., 2007). In turn a stimulation protocol that leads to LTP in WT mice induced LTD in tenascin-R-deficient mice. After several rescue experiments they proposed a chain of events including altered activity of GABA_B and GABA_A receptors, L-type Ca²⁺ channels and protein phosphatases, which all result in the metaplastic increase of LTP threshold in tenascin-R-deficient mice. This model does not consider NMDA receptor-mediated effects but the molecular mechanisms that

lead to metaplastic changes in mutant mice might be different than those after an enzymatic degradation of the ECM. Although individual components of the ECM may not be present in mutant mice, an alternative form of the mature ECM is formed and neurons may have established other compensatory mechanism than upon an acute ECM digestion.

Comparable to the controversy about LTP dependence on the GluN2A/GluN2B ratio, the data related to its involvement in metaplasticity are not completely consistent. In 2012, Yang et al. presented a study in which they altered the GluN2A/GluN2B ratio by activating G-protein-coupled receptors (GPCRs) such as pituitary adenylate cyclase activating peptide 1 receptors (PAC1Rs) or dopamine 1 receptors (D1 receptors) (Yang et al., 2012). Depending on the activated GPCR they found a lower LTP threshold upon enhanced GluN2A-NMDA receptor-mediated currents and a higher LTP threshold in case of enhanced GluN2B-NMDA receptor-mediated currents. These results are contradictory to the previously described effects of altered GluN2A/GluN2B ratio (Xu et al., 2009, Lee et al., 2010). It needs to be mentioned that Yang et al. used a unique method, in which they isolated single CA1 neurons out of acute hippocampal slices of two weeks old rats. This is a very artificial and isolated system and provides a lot of stress to the neurons. This could be one reason why results differ from other studies. Further they used another protocol to affect the GluN2A/GluN2B ratio. To change the ratio by altering network activity induces many more changes than only affecting the NMDA receptor; the same holds true for the activation of GPCRs. But both treatments have diverse side effects that could influence metaplasticity in different ways.

Based on the controversy regarding the effects of GluN2A/GluN2B ratio it has to be clarified in which direction the neurons are primed by ECM digestion-induced increased GluN2B-NMDA receptor surface expression. Regardless the direction of plasticity changes, the community agrees that the subunit composition of NMDA receptors is an important modulator of several plasticity phenomena. ECM remodeling that alters the GluN2A/GluN2B ratio describes an additional cellular mechanism to influence plasticity potential of neurons.

4.3.4 Regulation of structural plasticity by NMDA receptors and the ECM

It is well described that persistent changes during late-phase LTP and LTD involve structural changes (Carlisle and Kennedy, 2005). Structural plasticity in

the brain includes the ability to build new synapses, change their size, morphology and motility or degrade established ones. Similar to the involvement of NMDA receptors and ECM in functional plasticity, their role in structural plasticity was also shown in several studies.

Early expression of GluN2A in organotypic hippocampal slices reduces the number of synapses and dynamics of spines (Gambrill and Barria, 2011). In contrast the expression of GluN2B did not change synapse number but leads to increased spine motility and higher rates of spine additions and retractions. In line, knockdown of GluN2B decreased synapse number and spine motility. A study that supports this finding was performed in corticostriatal slices in which GluN2A-NMDA receptors were blocked, which resulted in an increase of spine head width (Vastagh et al., 2012). As in a metaplasticity study mentioned above (Yang et al., 2012) Vastagh et al. activated D1 receptors that decreased GluN2A-NMDA receptors at synaptic sites and increased spine head width. This effect could be blocked by application of ifenprodil. Whether increased spine volume is a direct effect of the decreased GluN2A/GluN2B ratio remains elusive as the prolonged treatment with D1 receptor agonists not only decreased the GluN2A/GluN2B ratio but also increased insertion of AMPA receptors into the synapse. Spine volume has been positively correlated with strength of AMPA receptor-mediated currents (Matsuzaki et al., 2001). These studies propose a mechanism in which decreased GluN2A/GluN2B ratio supports potentiation of present synapses and an increase in both AMPA receptor content and spine volume. This close relationship of induction of LTP and structural plasticity was also shown at single synaptic level (Lee et al., 2010), described already in section 4.3.3. Previously silenced synapses showed enhanced GluN2B-NMDA receptor mediated currents and needed lower stimulation to elicit LTP and spine growth (Lee et al., 2010).

MMP-9 was also shown to influence dendritic spine enlargement, beside its effect on LTP (Wang et al., 2008). On one hand, they could show that TBS induced maintenance of spine enlargement and potentiation is dependent on the activity of MMP-9. On the other hand, the authors proved that MMP-9 application itself is already sufficient to induce potentiation and spine enlargement. Finally they stated that these effects are β 1-integrin-dependent. In line ChABC treatment of organotypic hippocampal slices induced the appearance of spine head protrusions and enhanced the motility of dendritic spines in a β 1-integrin-dependent manner (Orlando et al., 2012). But the authors stated that this effect is

glutamate receptor independent, which would imply other underlying molecular mechanism than an altered GluN2A/GluN2B ratio. This could be due to shorter duration of ECM digestion in this study (4h) versus an overnight Hya/ChABC incubation in my work. A prolonged treatment *in vivo* with ChABC was shown to increase spine motility (de Vivo et al., 2013), without providing any molecular mechanism yet. The authors only speculate that the observed effects could be due to changes in receptor surface localization. As described previously, GluN2B-NMDA receptor activity seems to influence structural spine plasticity, thus the observations from de Vivo et al. could be explained by altered GluN2A/GluN2B ratio upon ECM remodeling. It would be interesting to analyze if the increased spine motility could be blocked via ifenprodil, or if the level of pY1472-GluN2B is altered in these animals used by de Vivo et al.

4.4 *In vivo* application of ECM digestion

A number of studies have demonstrated altered plasticity in adult animals after ECM digestion using ChABC or Hya *in vivo* (Bradbury et al., 2002, Pizzorusso et al., 2002, Gogolla et al., 2009, Kochlamazashvili et al., 2010, de Vivo et al., 2013, Happel et al., 2014).

4.4.1 ECM removal in the visual cortex and the role of NMDA receptors

In particular studies in the visual cortex improved the knowledge about the influence of the ECM on plasticity. Monocular deprivation leads to a rapid depression of the deprived-eye inputs and a delayed strengthening of the open-eye inputs (Frenkel and Bear, 2004). This adaption leads to an ocular dominance shift and is called ocular dominance plasticity. This shift can only be induced during the critical period of development and is not inducible in adults. However, enzymatic removal of the ECM in the visual cortex of adult rats can reactivate ocular dominance plasticity and therefore virtually rejuvenate the plasticity of the cortex (Pizzorusso et al., 2002). The molecular basis for this restoration is unknown to date. Several mechanisms are discussed, for example the GABA-mediated control of the critical period as preventing the maturation of GABA-transmission delayed the onset of the critical period (Hensch et al., 1998, Fagiolini and Hensch, 2000, Iwai et al., 2003). But Pizzorusso et al. state that treatment with ChABC does not lead to those alterations of visual cortical neurons that are observed after pharmacological treatments with GABA

antagonist (Pizzorusso et al., 2002). Therefore they exclude a general disinhibition to be the mechanism by that ChABC restores ocular dominance plasticity.

Interestingly, the NMDA receptor subunit composition switches from mainly GluN2B- to GluN2A-NMDA receptors during the critical period in an experience-dependent manner (Carmignoto and Vicini, 1992, Quinlan et al., 1999a, Quinlan et al., 1999b). Pizzorusso et al. described that dark rearing of animals prolongs the critical period and slows down the development of the ECM. One-week exposure to a normal light/dark cycle was enough to rapidly terminate ocular dominance plasticity and the formation of perineuronal nets (Pizzorusso et al., 2002). As I propose a connection between ECM digestion and the abundance of GluN2B-NMDA receptors it is interesting to mention that dark rearing of rats from birth onwards attenuated the developmental increase in GluN2A-NMDA receptors and increased the proportion of GluN2B-NMDA receptors. Visual experience exerted an opposite effect (Quinlan et al., 1999a, Philpot et al., 2001). In 2007 Chen et al. added the observation that visual deprivation changes NMDA receptor subunit composition by initially increasing GluN2B and later by decreasing GluN2A protein levels (Chen and Bear, 2007). But does this change in subunit composition affect functional properties of the visual cortex? The influential Bienenstock, Cooper and Munro (BCM) theory describes that reduction in overall cortical activity by closing the contralateral eye decreases the modification threshold and thereby facilitating potentiation of inputs (Bienenstock et al., 1982). This sliding threshold builds the basis of metaplastic changes. As described in section 4.3.3, NMDA receptor subunit composition plays a critical role in metaplastic changes and indeed those changes were found in the visual cortex. Already in 1996 it was shown that light-deprived rats show enhanced LTP and diminished LTD over a range of stimulation frequencies, which was reversible by two days of light exposure (Kirkwood et al., 1996). Further, dark reared animals showed a decreased LTD in response to 1 Hz stimulation, which is normally the optimal frequency for LTD, but an increased LTD in response to 0.5 Hz stimulation (Philpot et al., 2003). In line with the previous studies, brief dark exposure extended the integration temporal window for the induction of both spike-timing dependent LTP and LTD (Guo et al., 2012). This is based on the incorporation of GluN2B-NMDA receptors that prolongs the NMDA receptor mediated response and by that extends the window of coincidence detection of pre- and postsynaptic activity. This supports the idea that a sliding threshold to induce LTP/LTD is crucial for ocular dominance

plasticity. These results can be connected to the observed subunit changes of NMDA receptor upon light deprivation and light-exposure (Quinlan et al., 1999a, Philpot et al., 2001, Chen and Bear, 2007), supporting my proposed model of an altered GluN2A/GluN2B ratio upon ECM remodeling.

In summary, the importance of the plastic changes of the GluN2A/GluN2B ratio to induce ocular dominance plasticity is extensively demonstrated. Further, permissive effects of the ECM on ocular dominance plasticity are described as well. But there are no studies available yet that focus on a possible connection between ECM remodeling, the resulting increase in plasticity and changes in the GluN2A/GluN2B ratio. My thesis demonstrates that digestion of the ECM with Hya can, at least in neuronal cultures, decrease the GluN2A/GluN2B ratio. Based on the described literature it is justified to speculate about a putative signaling pathway in which the ECM removal increases ocular dominance plasticity by affecting the GluN2A/GluN2B ratio probably in a β 1-integrin-dependent manner as shown in my study. However this model needs further support. Clarifying experiments would include the blocking of β 1-integrins simultaneously to ECM digestion and to test for ocular dominance plasticity under these conditions. Further, pY1472-GluN2B levels could be analyzed in these animals. Electrophysiological recordings including selective inhibitors for either GluN2A- or GluN2B-NMDA receptors could elucidate the question about an altered subunit ratio in the visual cortex upon ECM remodeling.

4.4.2 Homeostatic plasticity as a model involved in ocular dominance plasticity

An alternative mechanism involved in ocular dominance plasticity is synaptic scaling. It was first described in rat cortical cultures in which activity was blocked with TTX resulting in an increase in mEPSCs reflecting a global upscaling of synaptic weights (Turrigiano et al., 1998). This phenomenon was also found in the visual cortex where visual deprivation increased amplitudes of mEPSCs measured in cortical slices (Desai et al., 2002, Goel et al., 2006). That supports the hypothesis that besides plasticity processes like LTP/LTD and metaplasticity homeostatic plasticity occurs in the visual cortex as well to balance visual deprivation. The interconnection of these different kinds of plasticity processes is strong and some processes are discussed to be the preceding step to allow or change upcoming plasticity processes. The GluN2A/GluN2B ratio was also shown to be decreased in synaptic scaling experiments upon chronic inactivation

with TTX (Ehlers, 2003). In adult animals the induction of ocular dominance plasticity is only possible via a preceding period (10 days) of visual deprivation (He et al., 2006). During these 10 days of deprivation it was shown that, besides other molecular changes, the GluN2A/GluN2B ratio is decreased. Given that a decreased GluN2A/GluN2B ratio is necessary for ocular dominance plasticity and that visual deprivation elicits a chronic inactivation, it is tempting to speculate that synaptic scaling mechanisms lead to the altered GluN2A/GluN2B ratio which results in a sliding threshold for plasticity. If Hya or ChABC treatment in the visual cortex would also lead to a decreased GluN2A/GluN2B ratio, as proposed in my theses, digestion of the ECM would be an alternative to network silencing for reactivating ocular dominance plasticity in adults, as both would target the same molecular changes.

Homeostatic plasticity occurring in the visual cortex provides another link to the ECM. Our group demonstrated that chronic deactivation of primary cortical cultures with TTX leads to an increased cleavage of brevican by ADAMTS4 at synaptic sites (Valenzuela et al., 2014). Subcellular fractionation suggested that the C-terminal fragment of brevican, which contains the chondroitin sulfate side chains, is enriched in the soluble fraction. The other fragment of brevican is more associated with cellular membranes. Consequently cleavage of brevican removes inhibiting chondroitin sulfate chains from synapses. Brevican is not the only substrate for ADAMTS4 since it also cleaves other lecticans like aggrecan, which is the main CSPG in the adult brain (Giamanco et al., 2010). Thus it is very intriguing that increased activity of ADAMTS4 leads to removal of permissive chondroitin sulfate side chains from the synapse. As described before removal of inhibiting chondroitin sulfate chains leads to increased structural plasticity and, as shown in my thesis, to a decreased GluN2A/GluN2B ratio. Based on these data it would be worth to investigate if a prolonged visual deprivation of adult animals (He et al., 2006) also affects the structural properties of the ECM (e.g. decreased abundance of chondroitin sulfates) and by that influences the GluN2A/GluN2B ratio. If this holds true, ECM digestion is not an alternative to network silencing to allow ocular dominance plasticity in adults (as suggested before), but ECM remodeling would be a direct effect of network silencing which then leads to further molecular changes.

As mentioned before for MMP-9, the activity of proteases is thought to expose hidden binding sites for integrins (Michaluk et al., 2009). Consequently the increased activity of ADAMTS4 upon network inactivation could also promote

the abundance of new signaling molecules or binding sites to induce further plasticity processes. It could be tested if TTX treatment leads also to enhanced integrin signaling, proposing another signaling mechanism by that prolonged inactivation could lead to altered GluN2A/GluN2B ratio.

Still, the complex molecular mechanisms underlying ocular dominance plasticity are partially controversial or not known. There are links between regaining plasticity in adults after ECM removal or prolonged visual deprivation. Further, the GluN2A/GluN2B ratio is a prominent candidate to regulate plasticity in the visual cortex. The work of my thesis provides a link between the ECM and the GluN2A/GluN2B ratio and by that proposes a mechanism by which ECM remodeling could influence plasticity.

4.4.3 ECM removal in memory processes

ECM digestion was not only investigated in terms of ocular dominance plasticity, a form of developmental plasticity necessary to establish and refine sensory input but it was also shown to influence learning processes (Happel et al., 2014) or the extinction of fear memories in the adult (Gogolla et al., 2009). For instance, Happel et al. could show that ECM digestion in the auditory cortex enhances cognitive flexibility, as treated animals developed better performance in a reversal learning task than untreated animals (Happel et al., 2014). Thus this study provides evidence that ECM modulation could be a potential target for guided neuroplasticity with therapeutic potential.

In terms of fear memory it was shown that ChABC injection into the amygdala of adult animals reopens the possibility to erase fear memories by extinction (Gogolla et al., 2009), a process that is only observed in juvenile animals and gets lost during adulthood (Bouton et al., 2006, Quirk, 2006, Myers and Davis, 2007). This demonstrated, comparable to the observations in the visual cortex, that plasticity mechanisms that drive juvenile plasticity are not completely lost in adults, but need some support to be reactivated. A recent study showed erasure of fear memories by extinction in adult reelin-haploinsufficient heterozygous reeler mice, like it is normally found in juvenile animals (Iafrati et al., 2014). In addition, it was suggested that the activity of GluN2B-NMDA receptors was crucial to erase fear memory. It is already well established that application of D-cycloserine, a partial NMDA agonist that binds to the glycine binding site, facilitates extinction and prevents the recovery of memories in rats, mice and

humans both before and after extinction training (Guastella et al., 2007, Otto et al., 2007, Weber et al., 2007, Matsuda et al., 2010).

Thus, in summary one may speculate that underlying mechanism of ChABC induced erasure of fear memory may also depend on GluN2B-NMDA receptor expression, like I showed in neuronal cultures. Therefore experiments as described in my thesis may help to understand molecular changes based on an ECM remodeling and to identify endogenous signaling pathways, which may promote similar changes in plasticity. These pathways may be good targets to replace the invasive treatment using glycosidases with more specific ones to avoid potential side effects, which becomes of particular interest for translational approaches. Especially, in terms of fear memory it could help to find potential therapies to prevent the development of extinction-resistant pathological fear and anxiety like it is the case in post-traumatic stress disorder (PTSD). The enhanced flexibility, the increased ability of relearning and of synaptic rearrangements after an ECM remodeling could be helpful for instance after the implantation of auditory prostheses to achieve long-lasting successful treatment (Lim et al., 2007, Deliano et al., 2009).

4.5 Cst-1 in wnt signaling

To date, the cellular function of Cst-1 and especially of Cst-1's ectodomain remains elusive. Cst-1 lacking *C. elegans* mutants show an impaired associative memory, which could be rescued by expression of the ectodomain of Cst-1 (Ikeda et al., 2008, Hoerndli et al., 2009). These data suggest that the ectodomain is sufficient to induce cellular changes, but the signaling pathway or surface receptors are not known. It was suggested that Cst-1 binds the wnt signaling antagonist sFRP-1 and that a specific protein domain, the CRD of sFRP-1 is sufficient for this interaction (Leuthäuser et al., unpubl.). The CRD is also involved in binding wnt ligands; therefore it is likely that binding of Cst-1 to the CRD interferes with the sFRP-1/wnt binding. Further, Frzl also contains a CRD where wnt ligands bind to activate intracellular signaling cascades. Cst-1 could influence the binding properties at this site of action as well. That led to the idea to investigate the role of Cst-1 in wnt signaling.

4.5.1 Does Cst-1 bind Frzl?

The aim was to investigate if Cst-1 shows binding potential to Frzl. Searching in the Allen Brain Atlas (www.brain-map.org), a database for mRNA localization by *in situ* hybridization on adult mouse brain, revealed that Frzl-1 is the most abundant member of the Frzl family. In addition it was shown that Frzl-1 is highly expressed at presynaptic sites in hippocampal cultures (Varela-Nallar et al., 2009). Therefore binding of Cst1Clea to Frzl-1 was tested. But no binding could be observed in our test system. The binding specificity of Frzl family members and their ligands is complex. In 2014 an overview about known interactions of wnt ligands and Frzl was published (Dijksterhuis et al., 2014), demonstrating that the majority of wnt ligands binds to Frzl-1, or at least activates Frzl-1-dependent signaling. Nevertheless, not all wnt ligands interact with Frzl-1. Thus it stays elusive if Cst1Clea interacts with another Frzl. Although under experimental conditions the CRD of sFRP-1 was sufficient to bind Cst-1 (Leuthäuser et al., unpubl.), it may well be that the NTR domain supports binding *in vivo*. Probably Cst1Clea cannot bind Frzl as it only contains the CRD and not the supporting NTR domain. Another possibility could be that an isolated, overexpressed CRD construct is able to bind Cst-1, as shown previously, but a CRD which is integrated into the N-terminal part of Frzl might exhibit another conformation that does not allow proper binding, at least not in my experimental design. Similar contradictions are observed in the binding properties of sFRPs to wnt ligands. First it was described that the CRD of sFRPs is sufficient to bind wnt ligands (Lin et al., 1997) but later studies describe that a CRD-lacking mutant of sFRP-1 still binds to wingless (Uren et al., 2000) and that optimal wnt inhibition is achieved only by combination of both protein domains, CRD and NTR (Bhat et al., 2007). Even though it is possible that Cst1Clea does not bind at all Frzl itself, it may influence wnt signaling activity by interacting with sFRP-1.

4.5.2 Does Cst-1 influence canonical wnt signaling?

The canonical wnt pathway leads to the activation of the Tcf/Lef promotor to induce transcription of wnt target genes. Therefore the experimental setups to investigate canonical wnt signaling are based on genetic reporter systems. A reporter gene, in this case either GFP or luciferase, gets expressed upon Tcf/Lef activation. In the wnt signaling field the reporter system of choice is based on luciferase expression. Indeed, application of wnt-3a decoupled the luciferase

signals, confirming the feasibility of the assay. In comparison Cst1Clea did not have any effect on the activity of the Tcf/Lef promotor, regardless of protein concentration or if Cst1Clea and wnt-3a were applied at the same time. These results suggest that Cst1Clea does not have any effect on the canonical wnt signaling, at least not in the regulation of Tcf/Lef activation. It is still plausible to assume that Cst1Clea acts on β -catenin-dependent wnt signaling that does not result in gene transcription changes. This was shown for instance for the signaling of wnt-7a in the presynapse, which regulates surface abundance of $\alpha 7$ -nAChR in a transcription-independent manner (Farias et al., 2007). Therefore it would be interesting to investigate whether Cst1Clea influences downstream molecules of the canonical wnt signaling like DVL and β -catenin which are upstream of gene transcription. To further stress possible effects of an interaction of Cst-1 with sFRP-1 it could help to apply exogenous sFRP-1 alone or in combination with Cst-1 to cell assays like the luciferase reporter system. Recently a study demonstrated that sFRP-1 acts dose-dependently on canonical wnt signaling. Nanomolar concentrations of sFRP-1 increased wnt-3a induced luciferase expression in HEK293-T cells whereas higher concentrations blocked it (Xavier et al., 2014). Therefore it could be interesting to investigate if there is any dose-dependent influence of Cst-1 on sFRP-1, or if Cst-1 changes the dose-dependency of the inhibitory effect of sFRP-1.

4.6 Cst1 increases presynaptic activity

Uptake of a fluorescently labeled antibody against the luminal domain of synaptotagmin-1 is an established cell biological measurement of presynaptic activity. The application of Cst1Clea increased the intensity of synaptotagmin-1 antibody uptake, which demonstrates that presynapses release more neurotransmitter vesicles within the observed time window. In contrast the treatment with Cst1Cad or Cst3Clea did not alter presynaptic activity. As Cst1Clea but not Cst1Cad increases presynaptic activity it implies that the LamG domain of the Cst-1 ectodomain is important to induce this effect. Application of the purified LamG domain may proof this assumption.

The principle of ectodomain shedding to generate signaling molecules is well known and Cst-1 is not the only transmembrane protein that is proposed to influence synaptic properties after ectodomain shedding (Ethell et al., 2002, Hinkle et al., 2006, Peixoto et al., 2012, Toth et al., 2013). For example A β , the

shedding product of APP, exerts activity-regulating functions at the presynapse (Abramov et al., 2009). A β binds selectively with picomolar affinity to α 7-nAChR (Wang et al., 2000) and subsequently increases presynaptic Ca²⁺ levels, which was blocked by the α 7-nAChR inhibitor BgTx (Dougherty et al., 2003). As A β is released from presynaptic sites but also from dendrites it functions as a trans-synaptic signal (Haass et al., 2012). The same holds true for Cst-1 as it is found in the postsynapse and its shedding product Cst1Clea acts on the presynapse. This trans-synaptic signaling is an important mechanism by which postsynaptic modifications lead to precisely coordinated changes in presynaptic structure and function. Along this line, enhanced neuronal activity leads to cleavage of the postsynaptic protein neuroligin-1 by MMP-9. This results in rapid destabilization of its presynaptic binding partner neurexin-1 β and subsequent in a decreased presynaptic release probability (Peixoto et al., 2012). An increased ectodomain shedding upon elevated activity was also shown for the α -secretase (Sakry et al., 2014), the same enzyme that sheds Cst1Clea from Cst-1 at postsynaptic sites. Activity-dependent α -secretase activity could lead to altered Cst-1 cleavage and which subsequently would influence presynaptic activity as a trans-synaptic regulator. This could be a new mechanism by which presynaptic activity can be adjusted upon altered network activity.

The signaling mechanism underlying Cst1Clea affecting presynaptic release probability remains elusive. It was shown that wnt signaling influences presynaptic function in several ways (Ahmad-Annuar et al., 2006, Farias et al., 2007, Cerpa et al., 2008, Farias et al., 2009, Cerpa et al., 2010). To investigate if the presynaptic effect of Cst1Clea application depends on wnt signaling a soluble Frzl-1 CRD was simultaneously added and abolished the effect of Cst1Clea on the presynapse. This soluble Frzl-1 CRD was shown to inhibit wnt-3a-induced changes at the presynapse (Varela-Nallar et al., 2009). Acute treatment of hippocampal cultures with wnt-3a leads to an increase in the number of bassoon and vGlut1 clusters and in the number of functional recycling sites. All these effects were inhibited by the application of Frzl-1 CRD. Furthermore wnt-3a treatment increases the intensity of FM dye puncta and speeds up unloading kinetics. Increased uptake and unloading represent higher efficacy of neurotransmitter release upon stimulation. The uptake of FM dye is analogous to the uptake of synaptotagmin-1 antibody. Therefore increasing effect of Cst1Clea on presynaptic activity can be compared with the effect of wnt-3a. Even though, the antibody uptake was performed under unstimulated conditions and not upon

a certain stimulus like KCl application, both, wnt-3a and Cst1Clea increased synaptic vesicle release and in both cases soluble Frzl-1 CRDs abolished this effect. It seems contradictory that the binding assay revealed no binding of Cst1Clea to Frzl-1 and here the Frzl-1 CRD abolishes an effect mediated by Cst1Clea. sFRP-1, which is proposed to bind Cst-1, was shown to inhibit wnt-3a induced β -catenin accumulation at least in L-cells (Galli et al., 2006). In hippocampal neurons sFRP-1 inhibits effects of wnt-7a at the presynapse, which are comparable with those changes wnt-3a induces (Cerpa et al., 2008). Therefore sFRP-1 might also inhibit wnt-3a activity at the presynapse, leading to a hypothetical mechanism that could explain the results from the synaptotagmin-1 antibody uptake experiment (Figure 18): applied Cst1Clea molecules may bind sFRP-1 and assuming that this binding detains sFRP-1 to inhibit wnt-3a, enhanced levels of free wnt-3a can stimulate presynaptic activity. In case of simultaneous application of Cst1Clea and Frzl-1 CRD enhanced levels of free wnt-3a bind to the soluble Frzl-1 CRD and by that do not activate presynaptic activity anymore. The most speculative assumption is that interaction of Cst1Clea and sFRP-1 prevents binding of wnt ligands to sFRP-1. Additionally, if this hypothesis holds true, one can conclude that the cadherin domain of Cst-1 alone is not able to bind sFRP-1, as Cst1Cad did not increase presynaptic activity. The interplay between these molecules needs to be further investigated. It would be possible to investigate binding properties of all three proteins, wnt, sFRP and Cst using the Biacore Plasmon Resonance system. This would clarify if the interaction of Cst-1 with sFRP-1 influences binding preferences of wnt ligands and sFRP-1.

Another way to inhibit the enhancing effect of Cst1Clea on presynaptic activity was to block α_7 -nAChR before adding Cst1Clea. α_7 -nAChR are highly Ca^{2+} permeable (Vernino et al., 1992) and enhance neurotransmitter release upon activation with nicotine (Gray et al., 1996). The question arises if α_7 -nAChRs are activated in my primary cortical cultures, as the mayor cholinergic projections to the cerebral cortex and hippocampus are coming from the basal forebrain cholinergic complex. But the media I used for the cell cultures (Table 1) contains choline chloride, which was shown to be an agonist for α_7 -nAChR (Mandelzys et al., 1995, Papke et al., 1996). Therefore I can assume that α_7 -nAChRs are activated, which is supported by the observation that BgTx blocks the effect of Cst1Clea, implementing that α_7 -nAChRs were active before.

It was shown that acute wnt-7a application increases the amount of $\alpha 7$ -nAChR on the surface of presynaptic sites (Farias et al., 2007). This effect was dependent on β -catenin as it dissociates from APC, which then induces enhanced trafficking of $\alpha 7$ -nAChR to the plasma membrane. But β -catenin dependent gene expression was not altered, at least not in short-term treatment. Farias et al. did not show that the enhanced surface abundance of $\alpha 7$ -nAChR leads to enhanced vesicle release. But wnt-7a was later shown to enhance the frequency of mEPSCs in hippocampal slices (Cerpa et al., 2008); the same effect is observed when activating $\alpha 7$ -nAChR with nicotine (Gray et al., 1996). Acute application of Cst1Clea enhanced presynaptic activity, which is inhibited by blocking $\alpha 7$ -nAChR with BgTx. Thus it is feasible to speculate that Cst1Clea leads to increased wnt signaling activity via binding to sFRP-1 resulting in enhanced

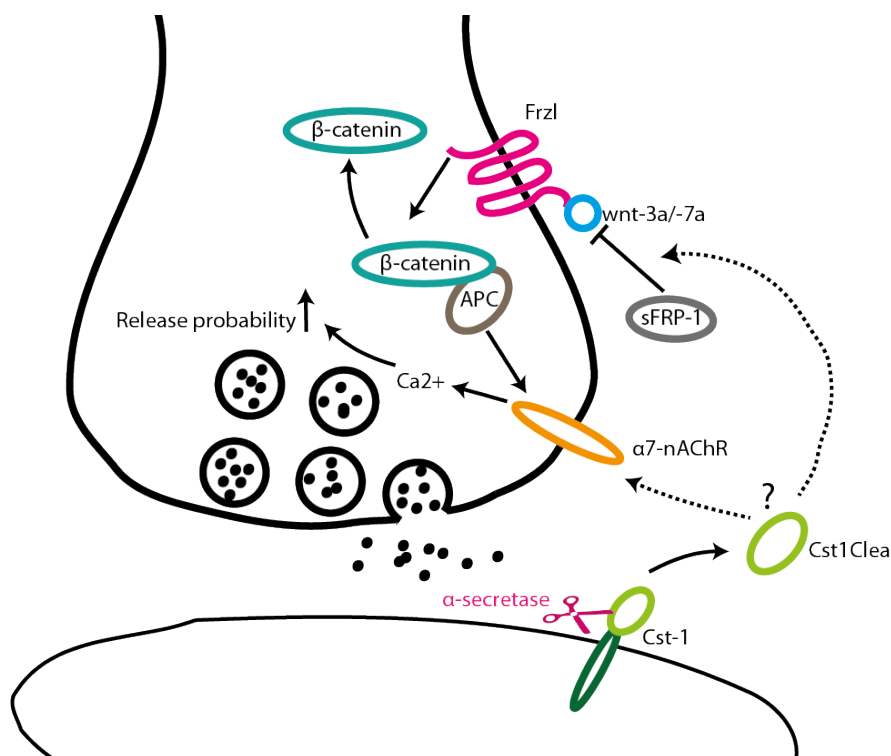


Figure 18: Scheme of potential signaling mechanisms involved in the stimulating effect of Cst1Clea on presynapses

In this thesis it was shown that Cst1Clea increases release probability at presynaptic sites. As α -secretase sheds it from the postsynapse, it is proposed to act as a trans-synaptic messenger protein. Two signaling mechanisms can be proposed: The first one includes an interaction of Cst1Clea with sFRP-1, which prevents binding of wnt ligands to sFRP-1. That would result in increased amount of free wnt ligands, which activate Frzl and result in a dissociation of β -catenin from APC. APC then stimulates trafficking of $\alpha 7$ -nAChR to the plasma membrane, which ends up in an increased release probability. This putative signaling mechanism is supported by two observations. The first one was that the effect of Cst1Clea can be prevented by application of soluble Frzl-1 CRD, which binds the enhanced level of free wnt ligands and therefore prevents increased activation of Frzl. The second was that the effect of Cst1Clea was inhibited by application of BgTx, which inhibits the increased signaling of $\alpha 7$ -nAChR. It cannot be excluded that Cst1Clea acts directly on $\alpha 7$ -nAChR, like A β does for example.

$\alpha 7$ -nAChR surface expression. Their activation triggers vesicle release, and application of BgTx prevents this effect. As shown before, Cst1Clea did not affect canonical wnt signaling in a luciferase-based reporter system. That seems to be contradictory to the proposed mechanism by which it alters presynaptic function via a β -catenin-dependent pathway. But the results from the reporter system experiment only show that Cst1Clea does not alter β -catenin-dependent gene expression. It is well possible that application of Cst1Clea affects β -catenin properties, for example its preference to build a complex with APC (Rubinfeld et al., 1993).

In summary, Cst1Clea was shown to influence presynaptic activity. Based on these data I raise the hypothesis that it acts via binding to sFRP-1, but not Frzl, thus influencing wnt signaling activity at the synapse. The prevention of its effect by application of either soluble Frzl-1 CRD or BgTx is both connected to wnt signaling effects but acts at two different steps in the proposed signaling mechanism (Figure 18). These signaling mechanisms for Cst-1 are yet highly speculative and need to be further investigated by targeting downstream molecules like β -catenin, DVL or APC as these were described to be involved in the wnt dependent regulation of presynaptic efficacy. Further it cannot be excluded that Cst-1 in addition acts via other mechanisms, i.e. in coordination with other extracellular proteins or directly on the $\alpha 7$ -nAChR, as the A β peptide binds the receptor (Wang et al., 2000). As the metabolisms of Cst-1 and APP are closely related (see 1.4.2) and Cst1Clea and A β seem to have similar effects on presynaptic activity, it is worth to investigate possible interactions of their signaling, by adding both proteins simultaneously to the cultures and measure presynaptic activity. With respect to Alzheimer's disease, it would be beneficial to get a better understanding of physiological and pathological effects of A β and of putative interactions with other molecules, like for example Cst-1.

5 Declaration

Barbara Schweitzer

Sternstraße 29

39104 Magdeburg

Email: barbara.schweitzer@gmx.net

Hiermit erkläre ich, dass ich die vorliegende Dissertation selbständig angefertigt habe. Es wurden nur die in der Arbeit ausdrücklich benannten Quellen und Hilfsmittel benutzt. Wörtlich oder sinngemäß übernommenes Gedankengut habe ich als solches kenntlich gemacht.

Magdeburg, 21.7.15 _____

6 Curriculum Vitae

Personal Data

| | |
|-----------------|-------------------------------|
| Name: | Barbara Christina |
| Family name: | Schweitzer |
| Family status: | unmarried |
| Date of birth: | 9 th of April 1986 |
| Place of birth: | Krefeld, Germany |
| Nationality: | German |

School Education

| | |
|-------------------|---|
| 1992 - 1996 | Basic primary school: Katholische Grundschule an der Burg, Krefeld, Germany |
| 1996 - 2005 | Secondary school: Ricarda-Huch-Gymnasium Krefeld, Germany |
| 25th of June 2005 | University-entrance diploma / Abitur |

University

| | |
|-----------------------|---|
| Oct. 2005 – Sep. 2007 | Studies of Biology: University of Saarland, Germany |
| 25th of Sep. 2007 | Intermediate examination |
| Oct. 2007 – Oct. 2010 | Studies of Neurobiology: Otto-von-Guericke-University Magdeburg, Germany |
| Oct. 2008 – Nov. 2009 | Assistant student at Leibniz Institute for Neurobiology, Magdeburg, Germany |
| Nov. 2009 – Oct. 2010 | Diploma student at Leibniz Institute for Neurobiology, Germany |
| 15. Oct. 2010 | Diploma Biology |

Graduate education

Oct. 2010 – Jan. 2011 Scientific assistant at Leibniz Institute for Neurobiology, Magdeburg, Germany

Since Sep. 2011 PhD student at Leibniz Institute for Neurobiology, Magdeburg, Germany

Member of the graduate school GRK 1167 „Cell-Cell-Communication in Neural and Immune Systems: Topological Organization of Signal Transduction“ of the DFG

Magdeburg, 21.7.15 _____

Publication

Juan Carlos Valenzuela, Christopher Heise, Gilbert Franken, Jeet Singh, **Barbara Schweitzer**, Constanze I. Seidenbecher and Renato Frischknecht; “Hyaluronan-based extracellular matrix under conditions of homeostatic plasticity”; Philosophical Transactions of the Royal Society B, 369(1654), 20130606, 2014

7 Literature

- Abraham WC, Bear MF (1996) Metaplasticity: the plasticity of synaptic plasticity. *Trends Neurosci* 19:126-130.
- Abramov E, Dolev I, Fogel H, Ciccotosto GD, Ruff E, Slutsky I (2009) Amyloid-beta as a positive endogenous regulator of release probability at hippocampal synapses. *Nat Neurosci* 12:1567-1576.
- Ahmad-Annuar A, Ciani L, Simeonidis I, Herreros J, Fredj NB, Rosso SB, Hall A, Brickley S, Salinas PC (2006) Signaling across the synapse: a role for Wnt and Dishevelled in presynaptic assembly and neurotransmitter release. *J Cell Biol* 174:127-139.
- Al-Hallaq RA, Conrads TP, Veenstra TD, Wenthold RJ (2007) NMDA di-heteromeric receptor populations and associated proteins in rat hippocampus. *J Neurosci* 27:8334-8343.
- Araki Y, Kawano T, Taru H, Saito Y, Wada S, Miyamoto K, Kobayashi H, Ishikawa HO, Ohsugi Y, Yamamoto T, Matsuno K, Kinjo M, Suzuki T (2007) The novel cargo Alcadein induces vesicle association of kinesin-1 motor components and activates axonal transport. *EMBO J* 26:1475-1486.
- Araki Y, Miyagi N, Kato N, Yoshida T, Wada S, Nishimura M, Komano H, Yamamoto T, De Strooper B, Yamamoto K, Suzuki T (2004) Coordinated metabolism of Alcadein and amyloid beta-protein precursor regulates FE65-dependent gene transactivation. *J Biol Chem* 279:24343-24354.
- Araki Y, Tomita S, Yamaguchi H, Miyagi N, Sumioka A, Kirino Y, Suzuki T (2003) Novel cadherin-related membrane proteins, Alcadeins, enhance the X11-like protein-mediated stabilization of amyloid beta-protein precursor metabolism. *J Biol Chem* 278:49448-49458.
- Bafico A, Gazit A, Pramila T, Finch PW, Yaniv A, Aaronson SA (1999) Interaction of frizzled related protein (FRP) with Wnt ligands and the frizzled receptor suggests alternative mechanisms for FRP inhibition of Wnt signaling. *J Biol Chem* 274:16180-16187.
- Barria A, Malinow R (2005) NMDA receptor subunit composition controls synaptic plasticity by regulating binding to CaMKII. *Neuron* 48:289-301.
- Beffert U, Weeber EJ, Durudas A, Qiu S, Masiulis I, Sweatt JD, Li WP, Adelman G, Frotscher M, Hammer RE, Herz J (2005) Modulation of synaptic plasticity and memory by Reelin involves differential splicing of the lipoprotein receptor Apoer2. *Neuron* 47:567-579.
- Beique JC, Lin DT, Kang MG, Aizawa H, Takamiya K, Huganir RL (2006) Synapse-specific regulation of AMPA receptor function by PSD-95. *Proc Natl Acad Sci U S A* 103:19535-19540.
- Bellone C, Mameli M, Luscher C (2011) In utero exposure to cocaine delays postnatal synaptic maturation of glutamatergic transmission in the VTA. *Nat Neurosci* 14:1439-1446.
- Bernard-Trifilo JA, Kramar EA, Torp R, Lin CY, Pineda EA, Lynch G, Gall CM (2005) Integrin signaling cascades are operational in adult hippocampal synapses and modulate NMDA receptor physiology. *J Neurochem* 93:834-849.
- Bhat RA, Stauffer B, Komm BS, Bodine PV (2007) Structure-function analysis of secreted frizzled-related protein-1 for its Wnt antagonist function. *J Cell Biochem* 102:1519-1528.
- Bienenstock EL, Cooper LN, Munro PW (1982) Theory for the development of neuron selectivity: orientation specificity and binocular interaction in visual cortex. *J Neurosci* 2:32-48.
- Bikkavilli RK, Malbon CC (2009) Mitogen-activated protein kinases and Wnt/beta-catenin signaling: Molecular conversations among signaling pathways. *Commun Integr Biol* 2:46-49.
- Blanpied TA, Scott DB, Ehlers MD (2002) Dynamics and regulation of clathrin coats at specialized endocytic zones of dendrites and spines. *Neuron* 36:435-449.
- Bouton ME, Westbrook RF, Corcoran KA, Maren S (2006) Contextual and temporal modulation of extinction: behavioral and biological mechanisms. *Biol Psychiatry* 60:352-360.
- Bradbury EJ, Moon LD, Popat RJ, King VR, Bennett GS, Patel PN, Fawcett JW, McMahon SB (2002) Chondroitinase ABC promotes functional recovery after spinal cord injury. *Nature* 416:636-640.

- Brakebusch C, Seidenbecher CI, Asztely F, Rauch U, Matthies H, Meyer H, Krug M, Bockers TM, Zhou X, Kreutz MR, Montag D, Gundelfinger ED, Fassler R (2002) Brevican-deficient mice display impaired hippocampal CA1 long-term potentiation but show no obvious deficits in learning and memory. *Mol Cell Biol* 22:7417-7427.
- Brakeman JS, Gu SH, Wang XB, Dolin G, Baraban JM (1999) Neuronal localization of the Adenomatous polyposis coli tumor suppressor protein. *Neuroscience* 91:661-672.
- Bukalo O, Schachner M, Dityatev A (2001) Modification of extracellular matrix by enzymatic removal of chondroitin sulfate and by lack of tenascin-R differentially affects several forms of synaptic plasticity in the hippocampus. *Neuroscience* 104:359-369.
- Bukalo O, Schachner M, Dityatev A (2007) Hippocampal metaplasticity induced by deficiency in the extracellular matrix glycoprotein tenascin-R. *J Neurosci* 27:6019-6028.
- Carlisle HJ, Kennedy MB (2005) Spine architecture and synaptic plasticity. *Trends Neurosci* 28:182-187.
- Carmignoto G, Vicini S (1992) Activity-dependent decrease in NMDA receptor responses during development of the visual cortex. *Science* 258:1007-1011.
- Celio MR, Blumcke I (1994) Perineuronal nets--a specialized form of extracellular matrix in the adult nervous system. *Brain Res Brain Res Rev* 19:128-145.
- Cerpa W, Farias GG, Godoy JA, Fuenzalida M, Bonansco C, Inestrosa NC (2010) Wnt-5a occludes Abeta oligomer-induced depression of glutamatergic transmission in hippocampal neurons. *Mol Neurodegener* 5:3.
- Cerpa W, Godoy JA, Alfaro I, Farias GG, Metcalfe MJ, Fuentealba R, Bonansco C, Inestrosa NC (2008) Wnt-7a modulates the synaptic vesicle cycle and synaptic transmission in hippocampal neurons. *J Biol Chem* 283:5918-5927.
- Chalifoux JR, Carter AG (2011) Glutamate spillover promotes the generation of NMDA spikes. *J Neurosci* 31:16435-16446.
- Chan CS, Weeber EJ, Zong L, Fuchs E, Sweatt JD, Davis RL (2006) Beta 1-integrins are required for hippocampal AMPA receptor-dependent synaptic transmission, synaptic plasticity, and working memory. *J Neurosci* 26:223-232.
- Chen BS, Gray JA, Sanz-Clemente A, Wei Z, Thomas EV, Nicoll RA, Roche KW (2012) SAP102 mediates synaptic clearance of NMDA receptors. *Cell Rep* 2:1120-1128.
- Chen WS, Bear MF (2007) Activity-dependent regulation of NR2B translation contributes to metaplasticity in mouse visual cortex. *Neuropharmacology* 52:200-214.
- Chong JM, Uren A, Rubin JS, Speicher DW (2002) Disulfide bond assignments of secreted Frizzled-related protein-1 provide insights about Frizzled homology and netrin modules. *J Biol Chem* 277:5134-5144.
- Chung HJ, Huang YH, Lau LF, Huganir RL (2004) Regulation of the NMDA receptor complex and trafficking by activity-dependent phosphorylation of the NR2B subunit PDZ ligand. *J Neurosci* 24:10248-10259.
- Clapp P, Gibson ES, Dell'acqua ML, Hoffman PL (2010) Phosphorylation regulates removal of synaptic N-methyl-D-aspartate receptors after withdrawal from chronic ethanol exposure. *J Pharmacol Exp Ther* 332:720-729.
- Cruciat CM, Niehrs C (2013) Secreted and transmembrane wnt inhibitors and activators. *Cold Spring Harb Perspect Biol* 5:a015081.
- Cull-Candy SG, Leszkiewicz DN (2004) Role of distinct NMDA receptor subtypes at central synapses. *Sci STKE* 2004:re16.
- D'Arcangelo G, Curran T (1998) Reeler: new tales on an old mutant mouse. *Bioessays* 20:235-244.
- Dalby NO, Mody I (2003) Activation of NMDA receptors in rat dentate gyrus granule cells by spontaneous and evoked transmitter release. *J Neurophysiol* 90:786-797.
- Dann CE, Hsieh JC, Rattner A, Sharma D, Nathans J, Leahy DJ (2001) Insights into Wnt binding and signalling from the structures of two Frizzled cysteine-rich domains. *Nature* 412:86-90.

- De A (2011) Wnt/Ca²⁺ signaling pathway: a brief overview. *Acta biochimica et biophysica Sinica* 43:745-756.
- de Vivo L, Landi S, Panniello M, Baroncelli L, Chierzi S, Mariotti L, Spolidoro M, Pizzorusso T, Maffei L, Ratto GM (2013) Extracellular matrix inhibits structural and functional plasticity of dendritic spines in the adult visual cortex. *Nat Commun* 4:1484.
- Deliano M, Scheich H, Ohl FW (2009) Auditory cortical activity after intracortical microstimulation and its role for sensory processing and learning. *J Neurosci* 29:15898-15909.
- Desai NS, Cudmore RH, Nelson SB, Turrigiano GG (2002) Critical periods for experience-dependent synaptic scaling in visual cortex. *Nat Neurosci* 5:783-789.
- Dijksterhuis JP, Petersen J, Schulte G (2014) WNT/Frizzled signalling: receptor-ligand selectivity with focus on FZD-G protein signalling and its physiological relevance: IUPHAR Review 3. *Br J Pharmacol* 171:1195-1209.
- Dityatev A, Seidenbecher CI, Schachner M (2010) Compartmentalization from the outside: the extracellular matrix and functional microdomains in the brain. *Trends Neurosci* 33:503-512.
- Dougherty JJ, Wu J, Nichols RA (2003) Beta-amyloid regulation of presynaptic nicotinic receptors in rat hippocampus and neocortex. *J Neurosci* 23:6740-6747.
- Dreier L, Burbea M, Kaplan JM (2005) LIN-23-mediated degradation of beta-catenin regulates the abundance of GLR-1 glutamate receptors in the ventral nerve cord of *C. elegans*. *Neuron* 46:51-64.
- Dzubay JA, Jahr CE (1996) Kinetics of NMDA channel opening. *J Neurosci* 16:4129-4134.
- Edwards DR, Handsley MM, Pennington CJ (2008) The ADAM metalloproteinases. *Mol Aspects Med* 29:258-289.
- Ehlers MD (2003) Activity level controls postsynaptic composition and signaling via the ubiquitin-proteasome system. *Nat Neurosci* 6:231-242.
- Erisir A, Harris JL (2003) Decline of the critical period of visual plasticity is concurrent with the reduction of NR2B subunit of the synaptic NMDA receptor in layer 4. *J Neurosci* 23:5208-5218.
- Erondu NE, Kennedy MB (1985) Regional distribution of type II Ca²⁺/calmodulin-dependent protein kinase in rat brain. *J Neurosci* 5:3270-3277.
- Erreger K, Dravid SM, Banke TG, Wyllie DJ, Traynelis SF (2005) Subunit-specific gating controls rat NR1/NR2A and NR1/NR2B NMDA channel kinetics and synaptic signalling profiles. *J Physiol* 563:345-358.
- Ethell DW, Kinloch R, Green DR (2002) Metalloproteinase shedding of Fas ligand regulates beta-amyloid neurotoxicity. *Curr Biol* 12:1595-1600.
- Fagiolini M, Hensch TK (2000) Inhibitory threshold for critical-period activation in primary visual cortex. *Nature* 404:183-186.
- Fagiolini M, Pizzorusso T, Berardi N, Domenici L, Maffei L (1994) Functional postnatal development of the rat primary visual cortex and the role of visual experience: dark rearing and monocular deprivation. *Vision Res* 34:709-720.
- Farias GG, Alfaro IE, Cerpa W, Grabowski CP, Godoy JA, Bonansco C, Inestrosa NC (2009) Wnt-5a/JNK signaling promotes the clustering of PSD-95 in hippocampal neurons. *J Biol Chem* 284:15857-15866.
- Farias GG, Valles AS, Colombres M, Godoy JA, Toledo EM, Lukas RJ, Barrantes FJ, Inestrosa NC (2007) Wnt-7a induces presynaptic colocalization of alpha 7-nicotinic acetylcholine receptors and adenomatous polyposis coli in hippocampal neurons. *J Neurosci* 27:5313-5325.
- Finch PW, He X, Kelley MJ, Uren A, Schaudies RP, Popescu NC, Rudikoff S, Aaronson SA, Varmus HE, Rubin JS (1997) Purification and molecular cloning of a secreted, Frizzled-related antagonist of Wnt action. *Proc Natl Acad Sci U S A* 94:6770-6775.
- Flint AC, Maisch US, Weishaupt JH, Kriegstein AR, Monyer H (1997) NR2A subunit expression shortens NMDA receptor synaptic currents in developing neocortex. *J Neurosci* 17:2469-2476.

- Foster KA, McLaughlin N, Edbauer D, Phillips M, Bolton A, Constantine-Paton M, Sheng M (2010) Distinct roles of NR2A and NR2B cytoplasmic tails in long-term potentiation. *J Neurosci* 30:2676-2685.
- Fox K, Sato H, Daw N (1989) The location and function of NMDA receptors in cat and kitten visual cortex. *J Neurosci* 9:2443-2454.
- Frenkel MY, Bear MF (2004) How monocular deprivation shifts ocular dominance in visual cortex of young mice. *Neuron* 44:917-923.
- Frischknecht R, Heine M, Perrais D, Seidenbecher CI, Choquet D, Gundelfinger ED (2009) Brain extracellular matrix affects AMPA receptor lateral mobility and short-term synaptic plasticity. *Nat Neurosci* 12:897-904.
- Fuerer C, Nusse R (2010) Lentiviral vectors to probe and manipulate the Wnt signaling pathway. *PLoS One* 5:e9370.
- Galli LM, Barnes T, Cheng T, Acosta L, Anglade A, Willert K, Nusse R, Burrus LW (2006) Differential inhibition of Wnt-3a by Sfrp-1, Sfrp-2, and Sfrp-3. *Dev Dyn* 235:681-690.
- Gambrill AC, Barria A (2011) NMDA receptor subunit composition controls synaptogenesis and synapse stabilization. *Proc Natl Acad Sci U S A* 108:5855-5860.
- Giamanco KA, Morawski M, Matthews RT (2010) Perineuronal net formation and structure in aggrecan knockout mice. *Neuroscience* 170:1314-1327.
- Gladding CM, Raymond LA (2011) Mechanisms underlying NMDA receptor synaptic/extrasynaptic distribution and function. *Molecular and cellular neurosciences* 48:308-320.
- Goel A, Jiang B, Xu LW, Song L, Kirkwood A, Lee HK (2006) Cross-modal regulation of synaptic AMPA receptors in primary sensory cortices by visual experience. *Nat Neurosci* 9:1001-1003.
- Gogolla N, Caroni P, Luthi A, Herry C (2009) Perineuronal nets protect fear memories from erasure. *Science* 325:1258-1261.
- Gray JA, Shi Y, Usui H, During MJ, Sakimura K, Nicoll RA (2011) Distinct modes of AMPA receptor suppression at developing synapses by GluN2A and GluN2B: single-cell NMDA receptor subunit deletion in vivo. *Neuron* 71:1085-1101.
- Gray R, Rajan AS, Radcliffe KA, Yakehiro M, Dani JA (1996) Hippocampal synaptic transmission enhanced by low concentrations of nicotine. *Nature* 383:713-716.
- Groc L, Choquet D, Stephenson FA, Verrier D, Manzoni OJ, Chavis P (2007) NMDA receptor surface trafficking and synaptic subunit composition are developmentally regulated by the extracellular matrix protein Reelin. *J Neurosci* 27:10165-10175.
- Guastella AJ, Lovibond PF, Dadds MR, Mitchell P, Richardson R (2007) A randomized controlled trial of the effect of D-cycloserine on extinction and fear conditioning in humans. *Behav Res Ther* 45:663-672.
- Guo Y, Huang S, de Pasquale R, McGehrin K, Lee HK, Zhao K, Kirkwood A (2012) Dark exposure extends the integration window for spike-timing-dependent plasticity. *J Neurosci* 32:15027-15035.
- Haass C, Kaether C, Thinakaran G, Sisodia S (2012) Trafficking and proteolytic processing of APP. *Cold Spring Harbor perspectives in medicine* 2:a006270.
- Happel MFK, Niekisch H, Castiblanco LL, Ohl FW, Deliano M, Frischknecht R (2014) Enhanced cognitive flexibility in reversal learning induced by removal of the extracellular matrix in auditory cortex. *PNAS*.
- Hardingham GE, Fukunaga Y, Bading H (2002) Extrasynaptic NMDARs oppose synaptic NMDARs by triggering CREB shut-off and cell death pathways. *Nat Neurosci* 5:405-414.
- Hata S, Fujishige S, Araki Y, Kato N, Araseki M, Nishimura M, Hartmann D, Saftig P, Fahrenholz F, Taniguchi M, Urakami K, Akatsu H, Martins RN, Yamamoto K, Maeda M, Yamamoto T, Nakaya T, Gandy S, Suzuki T (2009) Alcadin cleavages by amyloid beta-precursor protein (APP) alpha- and gamma-secretases generate small peptides, p3-Alcs, indicating Alzheimer disease-related gamma-secretase dysfunction. *J Biol Chem* 284:36024-36033.

- He HY, Hodos W, Quinlan EM (2006) Visual deprivation reactivates rapid ocular dominance plasticity in adult visual cortex. *J Neurosci* 26:2951-2955.
- Hedstrom KL, Xu X, Ogawa Y, Frischknecht R, Seidenbecher CI, Shrager P, Rasband MN (2007) Neurofascin assembles a specialized extracellular matrix at the axon initial segment. *J Cell Biol* 178:875-886.
- Hensch TK (2005) Critical period plasticity in local cortical circuits. *Nat Rev Neurosci* 6:877-888.
- Hensch TK, Fagiolini M, Mataga N, Stryker MP, Baekkeskov S, Kash SF (1998) Local GABA circuit control of experience-dependent plasticity in developing visual cortex. *Science* 282:1504-1508.
- Hinkle CL, Diestel S, Lieberman J, Maness PF (2006) Metalloprotease-induced ectodomain shedding of neural cell adhesion molecule (NCAM). *J Neurobiol* 66:1378-1395.
- Hintsch G, Zurlinden A, Meskenaite V, Steuble M, Fink-Widmer K, Kinter J, Sonderegger P (2002) The calyntenins--a family of postsynaptic membrane proteins with distinct neuronal expression patterns. *Molecular and cellular neurosciences* 21:393-409.
- Hoerndli FJ, Walser M, Frohli Hoier E, de Quervain D, Papassotiropoulos A, Hajnal A (2009) A conserved function of *C. elegans* CASY-1 calyntenin in associative learning. *PLoS One* 4:e4880.
- Hoffmann H, Gremme T, Hatt H, Gottmann K (2000) Synaptic activity-dependent developmental regulation of NMDA receptor subunit expression in cultured neocortical neurons. *J Neurochem* 75:1590-1599.
- Hynes RO (2002) Integrins: bidirectional, allosteric signaling machines. *Cell* 110:673-687.
- Iafrafi J, Orejarena MJ, Lassalle O, Bouamrane L, Gonzalez-Campo C, Chavis P (2014) Reelin, an extracellular matrix protein linked to early onset psychiatric diseases, drives postnatal development of the prefrontal cortex via GluN2B-NMDARs and the mTOR pathway. *Mol Psychiatry* 19:417-426.
- Ikeda DD, Duan Y, Matsuki M, Kunitomo H, Hutter H, Hedgecock EM, Iino Y (2008) CASY-1, an ortholog of calyntenins/alcadeins, is essential for learning in *Caenorhabditis elegans*. *Proc Natl Acad Sci U S A* 105:5260-5265.
- Inestrosa NC, Arenas E (2010) Emerging roles of Wnts in the adult nervous system. *Nat Rev Neurosci* 11:77-86.
- Iwai Y, Fagiolini M, Obata K, Hensch TK (2003) Rapid critical period induction by tonic inhibition in visual cortex. *J Neurosci* 23:6695-6702.
- Jacobsen LK, Picciotto MR, Heath CJ, Mencl WE, Gelernter J (2009) Allelic variation of calyntenin 2 (CLSTN2) modulates the impact of developmental tobacco smoke exposure on mnemonic processing in adolescents. *Biol Psychiatry* 65:671-679.
- John N, Krugel H, Frischknecht R, Smalla KH, Schultz C, Kreutz MR, Gundelfinger ED, Seidenbecher CI (2006) Brevican-containing perineuronal nets of extracellular matrix in dissociated hippocampal primary cultures. *Molecular and cellular neurosciences* 31:774-784.
- Johnson JW, Ascher P (1987) Glycine potentiates the NMDA response in cultured mouse brain neurons. *Nature* 325:529-531.
- Kaech S, Banker G (2006) Culturing hippocampal neurons. *Nat Protoc* 1:2406-2415.
- Kirkwood A, Rioult MC, Bear MF (1996) Experience-dependent modification of synaptic plasticity in visual cortex. *Nature* 381:526-528.
- Kirson ED, Yaari Y (1996) Synaptic NMDA receptors in developing mouse hippocampal neurones: functional properties and sensitivity to ifenprodil. *J Physiol* 497 (Pt 2):437-455.
- Kleinschmidt A, Bear MF, Singer W (1987) Blockade of "NMDA" receptors disrupts experience-dependent plasticity of kitten striate cortex. *Science* 238:355-358.
- Kochlamazashvili G, Henneberger C, Bukalo O, Dvoretzkova E, Senkov O, Lievens PM, Westenbroek R, Engel AK, Catterall WA, Rusakov DA, Schachner M, Dityatev A (2010) The extracellular matrix molecule hyaluronic acid regulates hippocampal synaptic plasticity by modulating postsynaptic L-type Ca(2+) channels. *Neuron* 67:116-128.

- Kohl MM, Shipton OA, Deacon RM, Rawlins JN, Deisseroth K, Paulsen O (2011) Hemisphere-specific optogenetic stimulation reveals left-right asymmetry of hippocampal plasticity. *Nat Neurosci* 14:1413-1415.
- Kohr G, Seeburg PH (1996) Subtype-specific regulation of recombinant NMDA receptor-channels by protein tyrosine kinases of the src family. *J Physiol* 492 (Pt 2):445-452.
- Konecna A, Frischknecht R, Kinter J, Ludwig A, Steuble M, Meskenaite V, Indermuhle M, Engel M, Cen C, Mateos JM, Streit P, Sonderegger P (2006) Calsyntenin-1 docks vesicular cargo to kinesin-1. *Mol Biol Cell* 17:3651-3663.
- Kopec CD, Li B, Wei W, Boehm J, Malinow R (2006) Glutamate receptor exocytosis and spine enlargement during chemically induced long-term potentiation. *J Neurosci* 26:2000-2009.
- Koppe G, Bruckner G, Brauer K, Hartig W, Bigl V (1997) Developmental patterns of proteoglycan-containing extracellular matrix in perineuronal nets and neuropil of the postnatal rat brain. *Cell Tissue Res* 288:33-41.
- Kornau HC, Schenker LT, Kennedy MB, Seeburg PH (1995) Domain interaction between NMDA receptor subunits and the postsynaptic density protein PSD-95. *Science* 269:1737-1740.
- Krupp JJ, Vissel B, Heinemann SF, Westbrook GL (1998) N-terminal domains in the NR2 subunit control desensitization of NMDA receptors. *Neuron* 20:317-327.
- Kurayoshi M, Yamamoto H, Izumi S, Kikuchi A (2007) Post-translational palmitoylation and glycosylation of Wnt-5a are necessary for its signalling. *Biochem J* 402:515-523.
- Kwok JC, Carulli D, Fawcett JW (2010) In vitro modeling of perineuronal nets: hyaluronan synthase and link protein are necessary for their formation and integrity. *J Neurochem* 114:1447-1459.
- Lander C, Kind P, Maleski M, Hockfield S (1997) A family of activity-dependent neuronal cell-surface chondroitin sulfate proteoglycans in cat visual cortex. *J Neurosci* 17:1928-1939.
- Lavezzari G, McCallum J, Lee R, Roche KW (2003) Differential binding of the AP-2 adaptor complex and PSD-95 to the C-terminus of the NMDA receptor subunit NR2B regulates surface expression. *Neuropharmacology* 45:729-737.
- Law AJ, Weickert CS, Webster MJ, Herman MM, Kleinman JE, Harrison PJ (2003) Expression of NMDA receptor NR1, NR2A and NR2B subunit mRNAs during development of the human hippocampal formation. *Eur J Neurosci* 18:1197-1205.
- Le Meur K, Galante M, Angulo MC, Audinat E (2007) Tonic activation of NMDA receptors by ambient glutamate of non-synaptic origin in the rat hippocampus. *J Physiol* 580:373-383.
- Lee MC, Yasuda R, Ehlers MD (2010) Metaplasticity at single glutamatergic synapses. *Neuron* 66:859-870.
- Lemons ML, Condic ML (2008) Integrin signaling is integral to regeneration. *Exp Neurol* 209:343-352.
- Lim HH, Lenarz T, Joseph G, Battmer RD, Samii A, Samii M, Patrick JF, Lenarz M (2007) Electrical stimulation of the midbrain for hearing restoration: insight into the functional organization of the human central auditory system. *J Neurosci* 27:13541-13551.
- Lin B, Arai AC, Lynch G, Gall CM (2003) Integrins regulate NMDA receptor-mediated synaptic currents. *J Neurophysiol* 89:2874-2878.
- Lin K, Wang S, Julius MA, Kitajewski J, Moos M, Jr., Luyten FP (1997) The cysteine-rich frizzled domain of Frzb-1 is required and sufficient for modulation of Wnt signaling. *Proc Natl Acad Sci U S A* 94:11196-11200.
- Liu L, Wong TP, Pozza MF, Lingenhoehl K, Wang Y, Sheng M, Auberson YP, Wang YT (2004) Role of NMDA receptor subtypes in governing the direction of hippocampal synaptic plasticity. *Science* 304:1021-1024.
- Liu Y, Wong TP, Aarts M, Rooyackers A, Liu L, Lai TW, Wu DC, Lu J, Tymianski M, Craig AM, Wang YT (2007) NMDA receptor subunits have differential roles in mediating excitotoxic neuronal death both in vitro and in vivo. *J Neurosci* 27:2846-2857.
- Ludwig A, Blume J, Diep TM, Yuan J, Mateos JM, Leuthauser K, Steuble M, Streit P, Sonderegger P (2009) Calsyntenins mediate TGN exit of APP in a kinesin-1-dependent manner. *Traffic* 10:572-589.

- Luo J, Wang Y, Yasuda RP, Dunah AW, Wolfe BB (1997) The majority of N-methyl-D-aspartate receptor complexes in adult rat cerebral cortex contain at least three different subunits (NR1/NR2A/NR2B). *Mol Pharmacol* 51:79-86.
- Lynch G, Larson J, Kelso S, Barrionuevo G, Schottler F (1983) Intracellular injections of EGTA block induction of hippocampal long-term potentiation. *Nature* 305:719-721.
- Malinow R, Schulman H, Tsien RW (1989) Inhibition of postsynaptic PKC or CaMKII blocks induction but not expression of LTP. *Science* 245:862-866.
- Mandelzys A, De Koninck P, Cooper E (1995) Agonist and toxin sensitivities of ACh-evoked currents on neurons expressing multiple nicotinic ACh receptor subunits. *J Neurophysiol* 74:1212-1221.
- Mao B, Wu W, Li Y, Hoppe D, Stannek P, Glinka A, Niehrs C (2001) LDL-receptor-related protein 6 is a receptor for Dickkopf proteins. *Nature* 411:321-325.
- Margolis RU, Margolis RK, Santella R, Atherton DM (1972) The hyaluronidase of brain. *J Neurochem* 19:2325-2332.
- Martel MA, Wyllie DJ, Hardingham GE (2009) In developing hippocampal neurons, NR2B-containing N-methyl-D-aspartate receptors (NMDARs) can mediate signaling to neuronal survival and synaptic potentiation, as well as neuronal death. *Neuroscience* 158:334-343.
- Matsuda S, Matsuzawa D, Nakazawa K, Sutoh C, Ohtsuka H, Ishii D, Tomizawa H, Iyo M, Shimizu E (2010) d-serine enhances extinction of auditory cued fear conditioning via ERK1/2 phosphorylation in mice. *Prog Neuropsychopharmacol Biol Psychiatry* 34:895-902.
- Matsumoto-Miyai K, Sokolowska E, Zurlinden A, Gee CE, Luscher D, Hettwer S, Wolfel J, Ladner AP, Ster J, Gerber U, Rulicke T, Kunz B, Sonderegger P (2009) Coincident pre- and postsynaptic activation induces dendritic filopodia via neurotrophin-dependent agrin cleavage. *Cell* 136:1161-1171.
- Matsuzaki M, Ellis-Davies GC, Nemoto T, Miyashita Y, Iino M, Kasai H (2001) Dendritic spine geometry is critical for AMPA receptor expression in hippocampal CA1 pyramidal neurons. *Nat Neurosci* 4:1086-1092.
- Matta JA, Ashby MC, Sanz-Clemente A, Roche KW, Isaac JT (2011) mGluR5 and NMDA receptors drive the experience- and activity-dependent NMDA receptor NR2B to NR2A subunit switch. *Neuron* 70:339-351.
- Mayer J, Hamel MG, Gottschall PE (2005) Evidence for proteolytic cleavage of brevican by the ADAMTSs in the dentate gyrus after excitotoxic lesion of the mouse entorhinal cortex. *BMC Neurosci* 6:52.
- Mayer ML, MacDermott AB, Westbrook GL, Smith SJ, Barker JL (1987) Agonist- and voltage-gated calcium entry in cultured mouse spinal cord neurons under voltage clamp measured using arsenazo III. *J Neurosci* 7:3230-3244.
- Mayer ML, Westbrook GL, Guthrie PB (1984) Voltage-dependent block by Mg²⁺ of NMDA responses in spinal cord neurones. *Nature* 309:261-263.
- McKeon RJ, Jurynek MJ, Buck CR (1999) The chondroitin sulfate proteoglycans neurocan and phosphacan are expressed by reactive astrocytes in the chronic CNS glial scar. *J Neurosci* 19:10778-10788.
- Michaluk P, Mikasova L, Groc L, Frischknecht R, Choquet D, Kaczmarek L (2009) Matrix metalloproteinase-9 controls NMDA receptor surface diffusion through integrin beta1 signaling. *J Neurosci* 29:6007-6012.
- Milev P, Maurel P, Chiba A, Mevissen M, Popp S, Yamaguchi Y, Margolis RK, Margolis RU (1998) Differential regulation of expression of hyaluronan-binding proteoglycans in developing brain: aggrecan, versican, neurocan, and brevican. *Biochem Biophys Res Commun* 247:207-212.
- Monyer H, Burnashev N, Laurie DJ, Sakmann B, Seeburg PH (1994) Developmental and regional expression in the rat brain and functional properties of four NMDA receptors. *Neuron* 12:529-540.
- Moon LD, Asher RA, Rhodes KE, Fawcett JW (2001) Regeneration of CNS axons back to their target following treatment of adult rat brain with chondroitinase ABC. *Nat Neurosci* 4:465-466.
- Mould AP, Humphries MJ (2004) Regulation of integrin function through conformational complexity: not simply a knee-jerk reaction? *Current opinion in cell biology* 16:544-551.

- Myers KM, Davis M (2007) Mechanisms of fear extinction. *Mol Psychiatry* 12:120-150.
- Nagy V, Bozdagi O, Matynia A, Balcerzyk M, Okulski P, Dzwonek J, Costa RM, Silva AJ, Kaczmarek L, Huntley GW (2006) Matrix metalloproteinase-9 is required for hippocampal late-phase long-term potentiation and memory. *J Neurosci* 26:1923-1934.
- Nakazawa T, Komai S, Tezuka T, Hisatsune C, Umemori H, Semba K, Mishina M, Manabe T, Yamamoto T (2001) Characterization of Fyn-mediated tyrosine phosphorylation sites on GluR epsilon 2 (NR2B) subunit of the N-methyl-D-aspartate receptor. *J Biol Chem* 276:693-699.
- Niederost BP, Zimmermann DR, Schwab ME, Bandtlow CE (1999) Bovine CNS myelin contains neurite growth-inhibitory activity associated with chondroitin sulfate proteoglycans. *J Neurosci* 19:8979-8989.
- Niethammer M, Kim E, Sheng M (1996) Interaction between the C terminus of NMDA receptor subunits and multiple members of the PSD-95 family of membrane-associated guanylate kinases. *J Neurosci* 16:2157-2163.
- Nowak L, Bregestovski P, Ascher P, Herbet A, Prochiantz A (1984) Magnesium gates glutamate-activated channels in mouse central neurones. *Nature* 307:462-465.
- Oliva CA, Vargas JY, Inestrosa NC (2013) Wnts in adult brain: from synaptic plasticity to cognitive deficiencies. *Front Cell Neurosci* 7:224.
- Orlando C, Ster J, Gerber U, Fawcett JW, Raineteau O (2012) Perisynaptic chondroitin sulfate proteoglycans restrict structural plasticity in an integrin-dependent manner. *J Neurosci* 32:18009-18017, 18017a.
- Otmakhov N, Griffith LC, Lisman JE (1997) Postsynaptic inhibitors of calcium/calmodulin-dependent protein kinase type II block induction but not maintenance of pairing-induced long-term potentiation. *J Neurosci* 17:5357-5365.
- Otto MW, Basden SL, Leyro TM, McHugh RK, Hofmann SG (2007) Clinical perspectives on the combination of D-cycloserine and cognitive-behavioral therapy for the treatment of anxiety disorders. *CNS Spectr* 12:51-56, 59-61.
- Paoletti P, Bellone C, Zhou Q (2013) NMDA receptor subunit diversity: impact on receptor properties, synaptic plasticity and disease. *Nat Rev Neurosci* 14:383-400.
- Papassotiropoulos A, Stephan DA, Huentelman MJ, Hoerndli FJ, Craig DW, Pearson JV, Huynh KD, Brunner F, Corneveaux J, Osborne D, Wollmer MA, Aerni A, Coluccia D, Hanggi J, Mondadori CR, Buchmann A, Reiman EM, Caselli RJ, Henke K, de Quervain DJ (2006) Common Kibra alleles are associated with human memory performance. *Science* 314:475-478.
- Papke RL, Bencherif M, Lippiello P (1996) An evaluation of neuronal nicotinic acetylcholine receptor activation by quaternary nitrogen compounds indicates that choline is selective for the alpha 7 subtype. *Neurosci Lett* 213:201-204.
- Peixoto RT, Kunz PA, Kwon H, Mabb AM, Sabatini BL, Philpot BD, Ehlers MD (2012) Transsynaptic signaling by activity-dependent cleavage of neuroligin-1. *Neuron* 76:396-409.
- Peng J, Kim MJ, Cheng D, Duong DM, Gygi SP, Sheng M (2004) Semiquantitative proteomic analysis of rat forebrain postsynaptic density fractions by mass spectrometry. *J Biol Chem* 279:21003-21011.
- Philpot BD, Espinosa JS, Bear MF (2003) Evidence for altered NMDA receptor function as a basis for metaplasticity in visual cortex. *J Neurosci* 23:5583-5588.
- Philpot BD, Sekhar AK, Shouval HZ, Bear MF (2001) Visual experience and deprivation bidirectionally modify the composition and function of NMDA receptors in visual cortex. *Neuron* 29:157-169.
- Pierschbacher MD, Ruoslahti E (1984) Cell attachment activity of fibronectin can be duplicated by small synthetic fragments of the molecule. *Nature* 309:30-33.
- Pizzorusso T, Medini P, Berardi N, Chierzi S, Fawcett JW, Maffei L (2002) Reactivation of ocular dominance plasticity in the adult visual cortex. *Science* 298:1248-1251.
- Popp S, Andersen JS, Maurel P, Margolis RU (2003) Localization of aggrecan and versican in the developing rat central nervous system. *Dev Dyn* 227:143-149.

- Porter S, Clark IM, Kevorkian L, Edwards DR (2005) The ADAMTS metalloproteinases. *Biochem J* 386:15-27.
- Preuschhof C, Heekeren HR, Li SC, Sander T, Lindenberger U, Backman L (2010) KIBRA and CLSTN2 polymorphisms exert interactive effects on human episodic memory. *Neuropsychologia* 48:402-408.
- Previtali SC, Archelos JJ, Hartung HP (1997) Modulation of the expression of integrins on glial cells during experimental autoimmune encephalomyelitis. A central role for TNF-alpha. *Am J Pathol* 151:1425-1435.
- Prybylowski K, Chang K, Sans N, Kan L, Vicini S, Wenthold RJ (2005) The synaptic localization of NR2B-containing NMDA receptors is controlled by interactions with PDZ proteins and AP-2. *Neuron* 47:845-857.
- Puente XS, Sanchez LM, Overall CM, Lopez-Otin C (2003) Human and mouse proteases: a comparative genomic approach. *Nat Rev Genet* 4:544-558.
- Qiu S, Zhao LF, Korwek KM, Weeber EJ (2006) Differential reelin-induced enhancement of NMDA and AMPA receptor activity in the adult hippocampus. *J Neurosci* 26:12943-12955.
- Quinlan EM, Olstein DH, Bear MF (1999a) Bidirectional, experience-dependent regulation of N-methyl-D-aspartate receptor subunit composition in the rat visual cortex during postnatal development. *Proc Natl Acad Sci U S A* 96:12876-12880.
- Quinlan EM, Philpot BD, Haganir RL, Bear MF (1999b) Rapid, experience-dependent expression of synaptic NMDA receptors in visual cortex in vivo. *Nat Neurosci* 2:352-357.
- Quirk GJ (2006) Extinction: new excitement for an old phenomenon. *Biol Psychiatry* 60:317-318.
- Rath A, Glibowicka M, Nadeau VG, Chen G, Deber CM (2009) Detergent binding explains anomalous SDS-PAGE migration of membrane proteins. *Proc Natl Acad Sci U S A* 106:1760-1765.
- Rattner A, Hsieh JC, Smallwood PM, Gilbert DJ, Copeland NG, Jenkins NA, Nathans J (1997) A family of secreted proteins contains homology to the cysteine-rich ligand-binding domain of frizzled receptors. *Proc Natl Acad Sci U S A* 94:2859-2863.
- Rauch U (2004) Extracellular matrix components associated with remodeling processes in brain. *Cell Mol Life Sci* 61:2031-2045.
- Rauner C, Kohr G (2011) Triheteromeric NR1/NR2A/NR2B receptors constitute the major N-methyl-D-aspartate receptor population in adult hippocampal synapses. *J Biol Chem* 286:7558-7566.
- Rehn M, Pihlajaniemi T, Hofmann K, Bucher P (1998) The frizzled motif: in how many different protein families does it occur? *Trends Biochem Sci* 23:415-417.
- Ring L, Neth P, Weber C, Steffens S, Faussner A (2014) beta-Catenin-dependent pathway activation by both promiscuous "canonical" WNT3a-, and specific "noncanonical" WNT4- and WNT5a-FZD receptor combinations with strong differences in LRP5 and LRP6 dependency. *Cell Signal* 26:260-267.
- Ring L, Perobner I, Karow M, Jochum M, Neth P, Faussner A (2011) Reporter gene HEK 293 cells and WNT/Frizzled fusion proteins as tools to study WNT signaling pathways. *Biol Chem* 392:1011-1020.
- Roche KW, Standley S, McCallum J, Dune Ly C, Ehlers MD, Wenthold RJ (2001) Molecular determinants of NMDA receptor internalization. *Nat Neurosci* 4:794-802.
- Rodriguez J, Esteve P, Weigl C, Ruiz JM, Fermin Y, Trousse F, Dwivedy A, Holt C, Bovolenta P (2005) SFRP1 regulates the growth of retinal ganglion cell axons through the Fz2 receptor. *Nat Neurosci* 8:1301-1309.
- Rubinfeld B, Souza B, Albert I, Muller O, Chamberlain SH, Masiarz FR, Munemitsu S, Polakis P (1993) Association of the APC gene product with beta-catenin. *Science* 262:1731-1734.
- Rusakov DA, Kullmann DM (1998) Extrasynaptic glutamate diffusion in the hippocampus: ultrastructural constraints, uptake, and receptor activation. *J Neurosci* 18:3158-3170.
- Saghatelyan AK, Dityatev A, Schmidt S, Schuster T, Bartsch U, Schachner M (2001) Reduced perisomatic inhibition, increased excitatory transmission, and impaired long-term potentiation in mice deficient

- for the extracellular matrix glycoprotein tenascin-R. *Molecular and cellular neurosciences* 17:226-240.
- Sakry D, Neitz A, Singh J, Frischknecht R, Marongiu D, Biname F, Perera SS, Endres K, Lutz B, Radyushkin K, Trotter J, Mittmann T (2014) Oligodendrocyte precursor cells modulate the neuronal network by activity-dependent ectodomain cleavage of glial NG2. *PLoS biology* 12:e1001993.
- Sankaranarayanan S, De Angelis D, Rothman JE, Ryan TA (2000) The use of pHluorins for optical measurements of presynaptic activity. *Biophys J* 79:2199-2208.
- Sanz-Clemente A, Matta JA, Isaac JT, Roche KW (2010) Casein kinase 2 regulates the NR2 subunit composition of synaptic NMDA receptors. *Neuron* 67:984-996.
- Sbai O, Ferhat L, Bernard A, Gueye Y, Ould-Yahoui A, Thiolloy S, Charrat E, Charton G, Tremblay E, Risso JJ, Chauvin JP, Arsanto JP, Rivera S, Khrestchatsky M (2008) Vesicular trafficking and secretion of matrix metalloproteinases-2, -9 and tissue inhibitor of metalloproteinases-1 in neuronal cells. *Molecular and cellular neurosciences* 39:549-568.
- Schulte G, Bryja V (2007) The Frizzled family of unconventional G-protein-coupled receptors. *Trends Pharmacol Sci* 28:518-525.
- Semenov MV, Habas R, Macdonald BT, He X (2007) SnapShot: Noncanonical Wnt Signaling Pathways. *Cell* 131:1378.
- Sharma RP, Chopra VL (1976) Effect of the Wingless (*wg1*) mutation on wing and haltere development in *Drosophila melanogaster*. *Dev Biol* 48:461-465.
- Sheng M, Cummings J, Roldan LA, Jan YN, Jan LY (1994) Changing subunit composition of heteromeric NMDA receptors during development of rat cortex. *Nature* 368:144-147.
- Shi Y, Mowery RA, Ashley J, Hentz M, Ramirez AJ, Bilgicer B, Slunt-Brown H, Borchelt DR, Shaw BF (2012) Abnormal SDS-PAGE migration of cytosolic proteins can identify domains and mechanisms that control surfactant binding. *Protein Sci* 21:1197-1209.
- Shipton OA, Paulsen O (2014) GluN2A and GluN2B subunit-containing NMDA receptors in hippocampal plasticity. *Philos Trans R Soc Lond B Biol Sci* 369:20130163.
- Sobczyk A, Scheuss V, Svoboda K (2005) NMDA receptor subunit-dependent $[Ca^{2+}]$ signaling in individual hippocampal dendritic spines. *J Neurosci* 25:6037-6046.
- Ster J, Steuble M, Orlando C, Diep TM, Akhmedov A, Raineteau O, Pernet V, Sonderegger P, Gerber U (2014) Calsyntenin-1 regulates targeting of dendritic NMDA receptors and dendritic spine maturation in CA1 hippocampal pyramidal cells during postnatal development. *J Neurosci* 34:8716-8727.
- Stern R, Jedrzejewski MJ (2006) Hyaluronidases: their genomics, structures, and mechanisms of action. *Chem Rev* 106:818-839.
- Steuble M, Diep TM, Schatzle P, Ludwig A, Tagaya M, Kunz B, Sonderegger P (2012) Calsyntenin-1 shelters APP from proteolytic processing during anterograde axonal transport. *Biol Open* 1:761-774.
- Strack S, Colbran RJ (1998) Autophosphorylation-dependent targeting of calcium/calmodulin-dependent protein kinase II by the NR2B subunit of the N-methyl-D-aspartate receptor. *J Biol Chem* 273:20689-20692.
- Sykova E, Nicholson C (2008) Diffusion in brain extracellular space. *Physiol Rev* 88:1277-1340.
- Takagi J, Petre BM, Walz T, Springer TA (2002) Global conformational rearrangements in integrin extracellular domains in outside-in and inside-out signaling. *Cell* 110:599-511.
- Tan CL, Kwok JC, Patani R, French-Constant C, Chandran S, Fawcett JW (2011) Integrin activation promotes axon growth on inhibitory chondroitin sulfate proteoglycans by enhancing integrin signaling. *J Neurosci* 31:6289-6295.
- Toth AB, Terauchi A, Zhang LY, Johnson-Venkatesh EM, Larsen DJ, Sutton MA, Umemori H (2013) Synapse maturation by activity-dependent ectodomain shedding of SIRPalpha. *Nat Neurosci* 16:1417-1425.

- Tovar KR, McGinley MJ, Westbrook GL (2013) Triheteromeric NMDA receptors at hippocampal synapses. *J Neurosci* 33:9150-9160.
- Tovar KR, Westbrook GL (1999) The incorporation of NMDA receptors with a distinct subunit composition at nascent hippocampal synapses in vitro. *J Neurosci* 19:4180-4188.
- Townsend M, Yoshii A, Mishina M, Constantine-Paton M (2003) Developmental loss of miniature N-methyl-D-aspartate receptor currents in NR2A knockout mice. *Proc Natl Acad Sci U S A* 100:1340-1345.
- Traynelis SF, Wollmuth LP, McBain CJ, Menniti FS, Vance KM, Ogden KK, Hansen KB, Yuan H, Myers SJ, Dingledine R (2010) Glutamate receptor ion channels: structure, regulation, and function. *Pharmacol Rev* 62:405-496.
- Turrigiano GG, Leslie KR, Desai NS, Rutherford LC, Nelson SB (1998) Activity-dependent scaling of quantal amplitude in neocortical neurons. *Nature* 391:892-896.
- Ueda I, Shinoda F, Kamaya H (1994) Temperature-dependent effects of high pressure on the bioluminescence of firefly luciferase. *Biophys J* 66:2107-2110.
- Uren A, Reichsman F, Anest V, Taylor WG, Muraiso K, Bottaro DP, Cumberledge S, Rubin JS (2000) Secreted frizzled-related protein-1 binds directly to Wingless and is a biphasic modulator of Wnt signaling. *J Biol Chem* 275:4374-4382.
- Vagnoni A, Perkinton MS, Gray EH, Francis PT, Noble W, Miller CC (2012) Calsyntenin-1 mediates axonal transport of the amyloid precursor protein and regulates Abeta production. *Hum Mol Genet* 21:2845-2854.
- Valenzuela JC, Heise C, Franken G, Singh J, Schweitzer B, Seidenbecher CI, Frischknecht R (2014) Hyaluronan-based extracellular matrix under conditions of homeostatic plasticity. *Philos Trans R Soc Lond B Biol Sci* 369:20130606.
- Varela-Nallar L, Grabowski CP, Alfaro IE, Alvarez AR, Inestrosa NC (2009) Role of the Wnt receptor Frizzled-1 in presynaptic differentiation and function. *Neural Dev* 4:41.
- Vastagh C, Gardoni F, Bagetta V, Stanic J, Zianni E, Giampa C, Picconi B, Calabresi P, Di Luca M (2012) N-methyl-D-aspartate (NMDA) receptor composition modulates dendritic spine morphology in striatal medium spiny neurons. *J Biol Chem* 287:18103-18114.
- Veeman MT, Slusarski DC, Kaykas A, Louie SH, Moon RT (2003) Zebrafish prickles, a modulator of noncanonical Wnt/Fz signaling, regulates gastrulation movements. *Curr Biol* 13:680-685.
- Verhey KJ, Lizotte DL, Abramson T, Barenboim L, Schnapp BJ, Rapoport TA (1998) Light chain-dependent regulation of Kinesin's interaction with microtubules. *J Cell Biol* 143:1053-1066.
- Vernino S, Amador M, Luetje CW, Patrick J, Dani JA (1992) Calcium modulation and high calcium permeability of neuronal nicotinic acetylcholine receptors. *Neuron* 8:127-134.
- Vicini S, Wang JF, Li JH, Zhu WJ, Wang YH, Luo JH, Wolfe BB, Grayson DR (1998) Functional and pharmacological differences between recombinant N-methyl-D-aspartate receptors. *J Neurophysiol* 79:555-566.
- Vogt L, Schrimpf SP, Meskenaite V, Frischknecht R, Kinter J, Leone DP, Ziegler U, Sonderegger P (2001) Calsyntenin-1, a proteolytically processed postsynaptic membrane protein with a cytoplasmic calcium-binding domain. *Molecular and cellular neurosciences* 17:151-166.
- von Engelhardt J, Coserea I, Pawlak V, Fuchs EC, Kohr G, Seeburg PH, Monyer H (2007) Excitotoxicity in vitro by NR2A- and NR2B-containing NMDA receptors. *Neuropharmacology* 53:10-17.
- von Marschall Z, Fisher LW (2010) Secreted Frizzled-related protein-2 (sFRP2) augments canonical Wnt3a-induced signaling. *Biochem Biophys Res Commun* 400:299-304.
- Wang HY, Lee DH, Davis CB, Shank RP (2000) Amyloid peptide Abeta(1-42) binds selectively and with picomolar affinity to alpha7 nicotinic acetylcholine receptors. *J Neurochem* 75:1155-1161.
- Wang S, Krinks M, Lin K, Luyten FP, Moos M, Jr. (1997) Frzb, a secreted protein expressed in the Spemann organizer, binds and inhibits Wnt-8. *Cell* 88:757-766.

- Wang XB, Bozdagi O, Nikitczuk JS, Zhai ZW, Zhou Q, Huntley GW (2008) Extracellular proteolysis by matrix metalloproteinase-9 drives dendritic spine enlargement and long-term potentiation coordinately. *Proc Natl Acad Sci U S A* 105:19520-19525.
- Wang XQ, Sun P, Paller AS (2003) Ganglioside GM3 inhibits matrix metalloproteinase-9 activation and disrupts its association with integrin. *J Biol Chem* 278:25591-25599.
- Watson PM, Humphries MJ, Relton J, Rothwell NJ, Verkhratsky A, Gibson RM (2007) Integrin-binding RGD peptides induce rapid intracellular calcium increases and MAPK signaling in cortical neurons. *Molecular and cellular neurosciences* 34:147-154.
- Weber M, Hart J, Richardson R (2007) Effects of D-cycloserine on extinction of learned fear to an olfactory cue. *Neurobiol Learn Mem* 87:476-482.
- Wu Y, Chen L, Zheng PS, Yang BB (2002) beta 1-Integrin-mediated glioma cell adhesion and free radical-induced apoptosis are regulated by binding to a C-terminal domain of PG-M/versican. *J Biol Chem* 277:12294-12301.
- Xavier CP, Melikova M, Chuman Y, Uren A, Baljinnam B, Rubin JS (2014) Secreted Frizzled-related protein potentiation versus inhibition of Wnt3a/beta-catenin signaling. *Cell Signal* 26:94-101.
- Xu J, Xiao N, Xia J (2010) Thrombospondin 1 accelerates synaptogenesis in hippocampal neurons through neuroligin 1. *Nat Neurosci* 13:22-24.
- Xu Z, Chen RQ, Gu QH, Yan JZ, Wang SH, Liu SY, Lu W (2009) Metaplastic regulation of long-term potentiation/long-term depression threshold by activity-dependent changes of NR2A/NR2B ratio. *J Neurosci* 29:8764-8773.
- Yamagata T, Saito H, Habuchi O, Suzuki S (1968) Purification and properties of bacterial chondroitinases and chondrosulfatases. *J Biol Chem* 243:1523-1535.
- Yamaguchi Y (2000) Lecticans: organizers of the brain extracellular matrix. *Cell Mol Life Sci* 57:276-289.
- Yang K, Trepanier C, Sidhu B, Xie YF, Li H, Lei G, Salter MW, Orser BA, Nakazawa T, Yamamoto T, Jackson MF, Macdonald JF (2012) Metaplasticity gated through differential regulation of GluN2A versus GluN2B receptors by Src family kinases. *EMBO J* 31:805-816.
- Yong VW (2005) Metalloproteinases: mediators of pathology and regeneration in the CNS. *Nat Rev Neurosci* 6:931-944.
- Yuan W, Matthews RT, Sandy JD, Gottschall PE (2002) Association between protease-specific proteolytic cleavage of brevican and synaptic loss in the dentate gyrus of kainate-treated rats. *Neuroscience* 114:1091-1101.
- Zhang S, Edelmann L, Liu J, Crandall JE, Morabito MA (2008a) Cdk5 regulates the phosphorylation of tyrosine 1472 NR2B and the surface expression of NMDA receptors. *J Neurosci* 28:415-424.
- Zhang XH, Wu LJ, Gong B, Ren M, Li BM, Zhuo M (2008b) Induction- and conditioning-protocol dependent involvement of NR2B-containing NMDA receptors in synaptic potentiation and contextual fear memory in the hippocampal CA1 region of rats. *Mol Brain* 1:9.
- Zhou XH, Brakebusch C, Matthies H, Oohashi T, Hirsch E, Moser M, Krug M, Seidenbecher CI, Boeckers TM, Rauch U, Buettner R, Gundelfinger ED, Fassler R (2001) Neurocan is dispensable for brain development. *Mol Cell Biol* 21:5970-5978.